

ATS 15097

(NASA-CR-123717) DESIGN AND FABRICATION OF  
PROTOTYPE SYSTEM FOR EARLY WARNING OF  
IMPENDING BEARING FAILURE J.J. Broderick,  
et al (Mechanical Technology, Inc.) Jan.  
1972 97 p

N72-28501

Unclas  
35688

MTI-71TR1

DESIGN AND FABRICATION OF PROTOTYPE  
SYSTEM FOR EARLY WARNING OF  
IMPENDING BEARING FAILURE

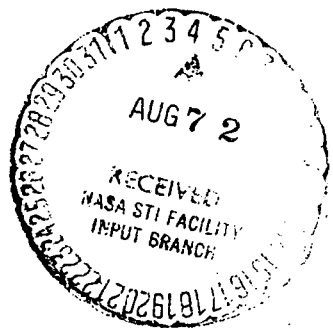
DESIGN REPORT

by

J. J. Broderick  
R. F. Burchill  
H. L. Clark

January, 1972

Reproduced by  
NATIONAL TECHNICAL  
INFORMATION SERVICE  
U S Department of Commerce  
Springfield VA 22151



... research and development division

110982

Handwritten initials in a circle

Handwritten initials in a circle

CR-123717

N72-28501

MTI-71TRI

DESIGN AND FABRICATION OF PROTOTYPE  
SYSTEM FOR EARLY WARNING OF  
IMPENDING BEARING FAILURE

DESIGN REPORT

by

J. J. Broderick  
R. F. Burchill  
H. L. Clark

January, 1972

prepared for

George C. Marshall Space Flight Center  
National Aeronautics and Space Administration  
Marshall Space Flight Center  
Huntsville, Alabama 35812

Prepared under Contract NAS8-25706

by

Mechanical Technology Incorporated  
968 Albany-Shaker Road  
Latham, New York 12110

REPRODUCED BY  
NATIONAL TECHNICAL  
INFORMATION SERVICE  
U.S. DEPARTMENT OF COMMERCE  
SPRINGFIELD, VA. 22161

111



N O T I C E

THIS DOCUMENT HAS BEEN REPRODUCED FROM THE BEST COPY FURNISHED US BY THE SPONSORING AGENCY. ALTHOUGH IT IS RECOGNIZED THAT CERTAIN PORTIONS ARE ILLEGIBLE, IT IS BEING RELEASED IN THE INTEREST OF MAKING AVAILABLE AS MUCH INFORMATION AS POSSIBLE.

## SUMMARY

This report covers a series of ball bearing performance tests that were run on several identical ball bearings under a variety of load, speed, temperature and lubrication conditions.

Bearing temperature, torque, vibration, noise, strain, cage speed, etc., were monitored to establish those measurements most suitable as indicators of ball bearing health.

The tests were conducted on an installed facility originally provided as a Hybrid Boost Bearing Test Vehicle on Contract N00019-68-C-0269. (Reference 6). The tests were run from October through December, 1970. A total of sixty-six (66) data points were taken during the conductance of thirty-three (33) different tests.

Development of the prototype diagnostic system, which was the program objective, required the bearing performance data described above. Tape records were made under steady-state conditions of a variety of speeds and loads. Sample sections were selected from the taped data for narrowband spectral analysis with a Real Time Analyzer.

An artificial flow was created across the inner race surface of one bearing using an acid etch technique to produce the "scratch." Tape records obtained before and after established a "characteristic" frequency response that identifies the presence of the flow.

The signals found most useful as indicators of performance degradation were ultrasonic outputs.

The test findings are discussed fully in Section III, and the application of test results to the construction of a Bearing Fault Detector are included in Section IV.

## FOREWORD

The work described in this report has been performed by Mechanical Technology Incorporated, Latham, New York, under Contract NAS8-25706 awarded by the George C. Marshall Space Flight Center, National Aeronautics and Space Administration, Marshall Space Flight Center, Alabama.

The diagnostic procedures evolved from this effort are intended for use by the Space Administration to monitor the operation of two (2) ball bearings used to support the spin axis of a large control moment gyro (CMG) wheel.

This report describes the tests that were conducted to establish those measurements most suitable as indicators of bearing health. Test data obtained was analyzed and utilized in providing input signals to the prototype diagnostic system that evolved.

TABLE OF CONTENTS

<u>SECTION</u>	<u>PAGE</u>
SUMMARY -----	i
FOREWORD -----	ii
I. INTRODUCTION -----	1
II. TEST PROGRAM -----	4
A. Test Facility -----	4
B. Instrumentation -----	7
C. Test Procedure -----	10
III. TEST RESULTS AND CONCLUSIONS -----	13
IV. PROTOTYPE DIAGNOSTIC SYSTEM -----	24
V. REFERENCES -----	31
APPENDIX A. TEST BEARING SPINDLE ASSEMBLY -----	A-1
APPENDIX B. BEARING PARAMETERS -----	B-1
APPENDIX C. PERTINENT TEST INFORMATION -----	C-1
APPENDIX D. COMPUTED TEST BEARING INFORMATION -----	D-1
APPENDIX E. TEST FACILITY DETAILS -----	E-1
a. Test Facility -----	E-2
b. Instrumentation -----	E-3
c. Test Rig Assembly Procedure -----	E-4
d. Test Set-up Procedure -----	E-6
APPENDIX F. TEST DATA -----	F-1
APPENDIX G. TEST EQUIPMENT -----	G-1

## SECTION I

### INTRODUCTION

Rolling contact fatigue tests (Reference 1) on 52100 steel balls have demonstrated that a thicker elastohydrodynamic (EHD) film resulting from either higher rolling speeds or increased lubricant viscosity will substantially extend ball bearing life. The improvement is attributed to reduced surface stresses due to a reduction of asperity contacts and redistribution of load by way of elastohydrodynamic pressures.

When lubrication becomes marginal surface distress will occur, indicated initially by a burnished appearance. This may be followed by metal transfer and wear followed by fatigue spalling.

Bearings on the verge of failure generate ultrasonic frequencies of measurable amplitude before audible or mechanical signals can be detected. This fact suggests that ultrasonic detection equipment may provide the most useful signal for monitoring incipient bearing failure. The ultrasonic signal will appear prior to a temperature rise or increase in driving torque.

The MTI test rig mounts several ultrasonic sensors for signal pickup from the test bearing. A Hewlett-Packard Delcon 4950A ultrasonic translator with probe in contact with ball bearing outer race was placed in the plane of ball path, vertically above bearing. See Figure C-3. This sensor is designed to monitor frequencies in the 36-44 K Hz range.

A Wilcoxon accelerometer, model 90, was procured for installation on the bearing housing to monitor ultrasonic outputs up to 80 K Hz. This sensor was mounted adjacent to the Delcon unit mentioned above and in the plane of the ball track.

Two Bruel & Kjaer model 4313 accelerometers were also mounted on the bearing housing to monitor "low frequency" responses in the axial and radial directions. These accelerometers have mounted natural resonances near 40 K Hz. and have flat response curves to 15 K Hz.

Lubricant viscosity and flow rate, shaft speed and bearing loading are all controlled in the test rig. By careful adjustment of these factors, the onset of marginal lubrication can be established, using the ultrasonic detection means. Where the condition of marginal or inadequate lubrication is permitted to continue, other warning signs will appear such as temperature rise, increased torque, increased audible noise and increased vibration.

The wear life of a rolling element bearing is dependent on environmental conditions. Excessive radial clearance will develop as a result of wear. A particular bearing application will determine the permissible wear limits that can be tolerated (Reference 2). Where a sensor can provide readout under conditions of marginal lubrication, it would be possible to log the accumulative total of wear life hours.

A method for computing the adequacy of the lubricant film for a given set of speed, load and lubricating oil conditions has been developed by SKF Industries (Reference 3). A sample calculation of the Barden 107H bearing installation covered by this report is included in Appendix D. Reference 4 also discusses this computational method and points out that where the computed application factor lies between 1 and 3, possible surface wear and short life can be anticipated.

#### Test Stand Limitations

Referring to Figure C-3, Test Rig Assembly, Partial Section A-A shows the torque arm arrangement. Figure C-3 also illustrates how the radial load is applied at the bottom of the bearing housing through the right angle pulley-cable system. Any application of radial load places a heavy restriction on the freedom of the torque measuring system. Therefore, to utilize the torque measuring system in this series of tests, radial load was replaced by an equivalent axial load. To establish the equivalent values, an available computer program, (Reference 5), was utilized. A severe overload resulting in a computed fatigue life of seventy-five hours can be created by applying a 1000 lb.-radial load in combination with a 50 lb. thrust load.

Approximately the same fatigue life, seventy-three hours, results from a 1000 lb. thrust load and a 15 lb. radial load. The 15 lb. radial load is actually the housing weight. It should be noted that the seventy-three hour life means that 90 percent of the bearings subjected to this loading will survive for at least seventy-three hours or, conversely, 10 percent will fail in that period.

#### Bearing Load Schedule

The bearing load-fatigue life relationship is given in Table I, Appendix B. Table V-1 in Appendix B gives the computed fatigue life values, based on the A. B. Jones Computational Method, Reference 5.

Table III in Appendix B presents a complete summary of all operational testing. Taped records from these runs when analyzed in our real time analyzer provided the diagnostic information needed to establish criteria for the prototype diagnostic system described in Section IV.

## SECTION II

### TEST PROGRAM

#### A. TEST FACILITY

The test facility in which the bearing tests were conducted and prototype diagnostic system was evaluated was West Cell #62 and is shown in Figure C-1. This facility consists of a test rig, auxiliary systems, such as loading and lubrication systems, and instrumentation. A detailed description of this test facility follows: (See Appendix E for equipment details).

#### Test Rig

A system schematic of the entire test rig is shown in Figure C-2. An assembly drawing of the test rig, including the loading devices, is shown in Figure C-3. The test-rig drive consists of an M-G set and an electrically-coupled, variable-speed, DC dynamometer. The shaft of the dynamometer is coupled to the input of the gear box with a Thomas Coupling. The gear box step-up ratio is 6.34:1. The output of the gear-box is coupled, in turn, to the shaft of a test spindle with a high speed Sier-Bath gear coupling (52).

The spindle (47) carries the thrust load applied during tests on a pair of tandem mounted spindle bearings, located at the drive end. The test end of spindle is also supported on a pair of tandem mounted ball bearings. These bearings carry radial load only in addition to a nominal amount of preload applied to the bearing system by a preload spring (70).

The ball bearing component of the test system is rotatably supported on the protruding front end of the spindle shaft. The inner race of the bearing is clamped in place between the oil seal plate (17) and locknut (60).

The housing for the test bearing consists of an outer bearing housing (18) and drive end seal plate (19).

The bearing housing is provided with torque arms (36) which contain ball inserts to reduce effects of housing misalignment on torque measurement. Two

beam supports (32) are installed on either side of the torque arm to serve as mounting supports for the strain-gaged beams.

### Auxiliary Systems

The auxiliary systems used apply mainly to the loading and lubrication areas. A detailed description of each system is given below.

#### Bearing Loading System

Thrust load is applied through an air cylinder (44) and load button (4) to a load ram (6) supported on a linear ball bushing (45) and pedestal (5). A Dillon load cell carried on a thrust spider transfers the compressive load to the test bearing. The air cylinder has a 2.5-inch bore yielding the following relationship between pressure and thrust load:

$$F_x = 4.9 p_s - 50$$

where  $p_s$  is the supply pressure to the pneumatic actuator in psig. The constant 50 represents a pull-back spring force present in the actuator, which keeps the actuator in retracted position when no pressure is applied.

Radial loading is applied at the underside of the bearing housing through a system consisting of: an eyebolt (67), which is mounted in the bearing housing, and an aircraft steel cable (66), which connects the eyebolt with a pneumatic actuator (43) through a pulley (30,55) arrangement. The actuator load characteristics can be expressed in the following form:

$$F_z = 8.3 p_s - 60 \quad (3.25 \text{ bore cylinder})$$

The actuating pressure in both cases is taken from a nitrogen bottle with a regulated supply pressure.

#### Lubricating System

The test set up provides two lubrication systems - the primary lube system and auxiliary spindle ball bearing system. Each one of these systems is briefly described as follows:

### Main Lubrication and Scavenge System

The basic schematic of this system is shown in Figure C-4. The system consists of a twenty gallon oil tank and a main lubricant pump driven by a 3 hp motor. The input line to the pump is submerged in the oil tank and contains a strainer at the inlet to prevent coarse contaminants or objects from entering the pump. At the pump discharge end the line branches off into two sections. One of these goes to the pressure control by-pass valve, and the other continues through an oil heater to a three-way valve. The oil heater is provided with a temperature control. When the three-way valve is in one position, all of the oil passes through the heater directly into the tank. This valve position is used to pre-heat the oil prior to the start of the test. Once the oil is heated up, the three-way valve is turned to its alternate position, closing off the by-pass to the tank and opening the line leading to the test stand. Oil then passes through two ten micron filters, arranged in parallel. Oil entering the test bearing passes through a flow control micrometer valve and fixed orifice of selected size. Oil pressure is controlled by an adjustable by-pass valve. Discharge from the test bearing housing is accomplished through the use of a positive displacement scavenge pump. The output of this pump is directed into a heat exchanger where the excess heat picked up in the stand is removed and the cooled oil is returned to the oil tank. This system has the capability of operation at temperatures up to 300 F. The lubricant employed in this series of tests was MIL-L-7808 synthetic polyester turbine oil.

### Spindle Lubrication System

Lubrication of the high speed spindle ball bearings is accomplished through the use of an air-oil mist lubrication system. This system was selected because of its simplicity as well as the low overall power loss resulting from air-oil mist lubrication. One Norgren lubricator delivering three drops per second at 40 psig is employed through a central feeding hole located between the spindle bearings.

B. INSTRUMENTATION

The test-rig instrumentation was selected to provide accurate readings of the critical bearing factors which were previously arrived at on the basis of calculations and diagnostic usefulness. These factors are:

1. Loading
2. Temperature
3. Ball bearing deflection under load
4. Vibration and noise
5. Oil flow to bearing components
6. Power loss

The specific instrumentation employed to obtain the necessary data and the reading accuracy is discussed in the following sections.

Loading

The bearing load arrangement employed to provide axial and radial loads to the test bearing during operation is described in detail on Page 10. To establish the thrust load magnitude a calibrated load cell was used. Bourdon-type pressure gages were employed for pressure measurements at the radial load cylinder. Gage accuracy was  $\pm 1.0$  psi resulting in a load reading accuracy of  $\pm 8.3$  lbs. for the radial loading system. Since the applied axial load varied between 50 lbs. and 1000 lbs., the overall axial load reading accuracy varied between  $\pm 1/2$  lb. for the low load, and  $\pm 5$  lbs. for the high load. No radial loading was applied other than housing weight. Refer to Table 2 for dynamic capacity of bearing under equivalent radial and thrust loads.

Temperature

Temperature measurements were obtained with copper constantan thermocouples. The outputs were printed out on a multipoint temperature recorder. Individual thermocouples were placed in the following positions as designated below:

<u>Positions</u>	<u>TC designation</u>
Spindle bearing	1 and 11
Spindle bearing	2 and 12
Ball bearing outer race, upper	3 and 13

<u>Positions</u>	<u>TC designation continued</u>
Ball bearing outer race, lower	4 and 14
Scavenge #1	5 and 15
Scavenge #2	6 and 16
Ball bearing oil inlet	9

Note that some of the thermocouples have dual designations. This indicates that the specific thermocouple occupied two points on the temperature recorder. This was done to cut the time between consecutive printouts of the same thermocouple. Readout accuracy on all thermocouples is  $\pm 1^{\circ}\text{F}$ .

Each probe was separately precalibrated in an oil bath over a temperature range of 70 to 250<sup>o</sup>F. bearing inner race temperature.

#### Ball Bearing Deflection

To provide a means of monitoring outer race cyclic strain, four (4) strain gages were cemented to the ball bearing outer race on the side facing the applied thrust load. The gages were placed 90 degrees apart, two in the horizontal and two in the vertical plane.

A second strain sensing system was evaluated using a PZT crystal cemented to the face of the bearing outer race beside the strain gages.

#### Vibration and Noise

Several types of sensors were applied to monitor the sonic and ultrasonic spectra. As illustrated on the cross section detail drawing and in the photographs, a Delcon 4950A ultrasonic translator was mounted vertically above the test bearing and in contact with the bearing outer race. This unit is selected to monitor the 36 - 44 K Hz range only.

A Wilcoxon Model 90 piezoelectric accelerometer was cemented to the housing adjacent to the Delcon unit. This unit has a mounted resonant frequency of 120 K Hz and a reasonably flat response curve to 80 K Hz.

On the front face of the housing, also in the plane of the spindle shaft, we mounted a Bruel & Kjaer Model 4313 accelerometer, using cement as the mounting method. This unit has a mounted resonant frequency of 40 K Hz with a flat response curve to 15 K Hz. The calibration curves for two of these units are included in the Appendix.

To monitor the audible noise spectrum and noise density or level, the Bruel & Kjaer Model 2203 Sound Level Meter was employed. This equipment was mounted as shown in the accompanying photograph of the test setup.

A Bently non-contacting shaft position indicating probe was mounted in the housing to monitor shaft speed. This unit, Model 302L-30-3.5 was positioned about .050 inches from the rotating shaft. Built-in shaft runout produced a once-per-revolution sinusoidal voltage output. By taping the Bently signal in combination with the other accelerometer outputs, the speed trace can be related to the higher frequency inputs.

#### Oil Flow

Oil flow was regulated with a Schrader Micro Valve which was precalibrated for use in MIL-L-7808 oil at temperatures ranging up to 150 F. Ball bearing oil supply flow was also controlled by pressure regulation in the 10 - 50 psi range. Reading accuracy is estimated to be  $\pm 5$  percent at the low flow limit and improving as the flow increases.

#### Power Loss

Power loss was measured through the use of torque arms built into the floating bearing housing. The full arrangement is shown in Figure C-3, Section A-A. The two torque arms (36) protruding from the housing contain balls (102) which transmit the torque load through a point contact onto a deflection beam that is instrumented with strain gages (35). This beam is allowed to deflect a limited amount before it engages a solid stop (33). The true value of the bearing torque measurements is difficult to determine inasmuch as bearing torque is affected to some extent by windage, oil churning and oil flow rates. In the design of this test vehicle, precautions have been taken to minimize oil accumulation and

churning effects. The extent to which this was actually accomplished is difficult to ascertain at this stage. The oil scavenge lines employed on the housing also offer some restraint and thus affect torque measurements. These restraints have, however, been accounted for in the initial torque calibration procedure.

To obtain meaningful torque readings, the test bearing was loaded axially. Table I provides the load schedule which establishes equivalent thrust loads to replace radial loads for a given dynamic capacity and fatigue life.

### C. TEST PROCEDURE

With the test in fully assembled state and the instrumentation calibrated and checked out, the following test sequence was adopted:

1. Ball Bearing Normal Signature Tests
2. Variable Thrust Load Bearing Tests
3. Bearing Lubricant Flow Tests
4. Induced Fault Bearing Tests

Much of the above specified testing involved a number of separate runs to establish bearing performance characteristics. Details are presented below.

#### Ball Bearing Normal Signature Tests

The test procedure consisted of the following:

1. With oil inlet maintained at 110<sup>o</sup>F and 0.1 gal. per minute flow, the test bearing was brought to 8000 rpm. Axial load was maintained at 50 lbs. Bearing radial load was 15 lbs. and was due entirely to housing and line weight.
2. After sufficient operation to provide thermal equilibrium (minimum 20 minutes operation), a complete set of sensor outputs was recorded.
3. Speed is reduced to 6000 rpm and after equilibrium is reached, another complete set of sensor outputs was recorded.

### Variable Thrust Load Bearing Tests

To evaluate the effect of load upon various sensor outputs each bearing was operated at several different thrust values. The initial plan was to run tests at 50 lb. thrust, 250 lb. thrust and 500 lb. thrust, but during testing the maximum thrust load was increased to 1000 lbs. Data was recorded only after thermal equilibrium was obtained.

### Bearing Lubricant Flow Tests

To evaluate the effect of lubricant flow rate upon bearing performance, it was intended to operate with several different orifice diameters. It was found that complete elimination of oil flow did not produce measurable differences over operation with copious supply rates (0.1 GPM) so only two conditions were evaluated.

### Induced Fault Bearing Tests

It has been shown (Reference 7) that the presence of discrete frequency components at the repetition rate of contact of the individual bearing balls and inner and outer race is an indication of bearing damage. By assuming that no slip or skid are present, the following rolling contact relationships hold:

$$\text{Frequency, Outer Race Defect } f_e = \frac{n}{2} f_r \left( 1 - \frac{BD}{PD} \cos \beta \right) \text{ (cps)}$$

$$\text{Frequency, Inner Race Defect } f_i = \frac{n}{2} f_r \left( 1 + \frac{BD}{PD} \cos \beta \right) \text{ (cps)}$$

$$\text{Frequency, Ball Defect } f_b = \frac{PD}{BD} f_r \left[ 1 - \left( \frac{BD}{PD} \right)^2 \cos^2 \beta \right] \text{ (cps)}$$

where  $f_r$  = Relative Speed between inner and outer race (rev/sec)

BD = Ball Dia.

PD = Pitch Dia.

$\beta$  = Contact Angle

n = Number of Balls

For this series 107 H Test Ball Bearing, the following frequencies were computed:

FAULT	8000 RPM	6000 RPM	PER REV
Inner race Defect	1156 Hz	867	8.7
Outer Race Defect	840 Hz	630	6.3
Ball Defect	793 Hz	595	6.0

It was intended to induce bearing faults by two methods: by operating at high loads without oil to induce fatigue faults, and by simulating fatigue damage by artificially producing a typical fault.

As fatigue at the inner race is the most likely point for this type of damage to occur, it was decided to induce a fault at this point. A line was etched in the inner race 0.012 inches wide and 0.0012 inches deep (see Fig. F-6) to insure contact with the defect at any thrust load. This fault was induced after the bearing normal signatures were recorded.

### SECTION III

#### TEST RESULTS AND CONCLUSIONS

In the preceding section, test equipment, loading methods, lubrication and instrumentation have been discussed. Also, test procedures, conditions of load, speed, lubrication and bearing quality were outlined. Figure C-12 in Appendix C lists the test procedure that was followed in conducting the five basic tests of this program. Table III in Appendix B presents a summary of all operational testing that was undertaken. It will be noted that thirty-three (33) tests were run between October 15 and December 1.

Some variation of speed, load, oil flow or bearing quality characterized each test. Table IV in Appendix B groups the test and data point numbers with the respective bearing serial number on which the test was run.

Three individual bearings were operated to complete the procedure outlined in Section II. Bearing S/N 1 was used to establish basic installation and test procedures and to provide general operating experience. Test data from this bearing were carefully reviewed but results were suspect in that assembly and disassembly loads were excessive. Later assembly activities had the benefits of experience and additional fixturing.

Bearing S/N 2 provided good baseline signatures from all sensors and was used to define the effects of load upon bearing performance. Oil flow variations were evaluated, and the bearing was operated for a considerable period at 1000 pound thrust load without external oil supply in an attempt to produce bearing damage. This bearing was finally operated after being solvent washed to remove all lubricant and it was destroyed after two minutes of running at 50 pounds thrust and 8000 rpm.

Bearing S/N 3 was evaluated for base line signatures and found to compare well with data from Bearing S/N 2. After complete analyses, the bearing was removed and disassembled and a simulated fault was induced by acid etch. The race was

masked with paraffin and a single relief was made across the ball path with a scribe. A 20 percent solution of Nitric acid at room temperature was used to produce the defect shown on Figure G-6. This fault simulates the typical first fatigue spall obtained by extended operation except that it extends across the ball track. This insures that the fault will be in the ball path for any load condition.

The complete load and speed cycle was rerun to define sensor outputs under fault-included conditions.

#### Review of Bearing Instrumentation Performance

Three individual bearings were tested with a variety of sensors to define the signatures of each bearing performance parameter. The basic goal of this program was to define a monitoring system which would detect the initial signs of bearing failure and permit repair or replacement to be accomplished at a convenient time. A variety of sensor types were evaluated.

The choice of a suitable bearing condition sensor included the following criteria:

1. The sensor should produce positive indications of bearing fault.
2. The fault indications ideally would be unaffected by bearing operating conditions (load, temperature, speed).
3. The fault indicator output should vary with the state of bearing deterioration to permit end-of-life predictions to be made.
4. The sensor installation should not restrict normal operation of the bearing being protected.

A basic assumption is that a rolling element bearing will operate for a major portion of its life with very nominal operating deterioration. At a point, however, the rate of deterioration will increase and the effective useful life will be limited. In a typical application, the onset of the first fatigue spall signals that the bearing has operated 90 to 95 percent of its effective life and that additional fatigue indications will occur at some exponentially increasing rate.

### Bearing Loading

The dynamic output of the Dillon Load Cell used to define bearing thrust load was tape recorded to evaluate variations between new and damaged bearings. The electronics of the signal conditioning device had response to 1000 Hz but no response above two times rotation was seen. It was concluded that bearing mounting variations could be evaluated with this type of sensing system but that it was not applicable to fault detection.

### Bearing Temperature

Test bearing outer race thermocouples were monitored throughout the test series for evidence of thermal difficulties but the range of loads, speeds, and oil flow conditions evaluated did not produce variations which could be related to bearing operating condition. Testing of the S/N 2 bearing without oil flow at 1000 lb.thrust load and 8000 rpm gave peak outer race temperature of 168<sup>o</sup>F at equilibrium. During this test the Amot temperature indicator for 174<sup>o</sup>F on the inner race was released while the outer race temperature was 167<sup>o</sup>F. This differential temperature of seven Fahrenheit degrees is very moderate. It was concluded that bearing temperature conditions could not be controlled accurately enough to produce reliable indications of bearing physical condition.

### Bearing Deflection

It was thought that a deteriorated bearing might produce unique race strain patterns which would be detectable, so two systems were used to measure these indications: conventional miniature strain gages and directly applied piezo-electric crystals which have a charge sensitivity dependent upon strain.

The strain gages used were of the foil type manufactured by Micro-Measurements. These were installed circumferentially on the face of the outer race to sense hoop stresses developed within the race. Bridge completion was accomplished by an Ellis BAM-1 amplifier. The amplifier was AC coupled to the tape recorder so only the dynamic components of strain were measured. Frequency response of this system was greater than 20 K Hz but significant output did not occur above 2000 Hz. Discrete frequency components at outer race ball passing frequency occurred for all bearing test conditions. The ability to detect ball pass could be

valuable for bearing slip or skid determination but this monitoring system did not appear to be of use in this program.

The second bearing deflection monitoring system used a Clevite Corp. PZT-4 piezoelectric crystal bonded directly to the outer race in the same plane as the strain gages. This material has the property of producing a state of charge which is dependent upon the strain which is imposed upon the crystal. A Kistler Model 848 Charge Amplifier is used to produce a voltage level proportional to charge which can be tape recorded.

Output from this strain sensing system produced almost identical results to those produced by the strain gage. The predominant frequency present in its frequency analysis was ball passing frequency but there were some small components at once and twice rotation which were not present in the strain gage setup. It is felt that these were due to acceleration of the bearing housing. It should be noted that this material is most typically used for accelerometers where a seismic mass is supported by the crystal. In that application extreme pains are taken to isolate the PZT material from any case strain or mounting loads. The conclusions about this bearing monitoring system are the same as for the strain gage system: if ball pass measurement were needed, this would be a way of getting it, but the basic condition of the bearing is not defined by its output.

#### Vibration and Noise

A variety of monitors was used to evaluate sonic and ultrasonic vibration and noise produced by the test bearings.

Ultrasonic Translator - A Hewlett-Packard Delcon 4950-A Ultrasonic Translator was installed with its sensor contacting the outer race in line with the ball track through a housing clearance hole. Other investigators (Ref. 8) have successfully used this instrument to evaluate bearing performance so an attempt was made to evaluate its mechanism of fault detection. The instrument filters the output from its sensor and measures response in the 36 K Hz to 44 K Hz range. This information is "folded" and translated to the zero to 4000 Hz range and indicated on a logarithmic scale (0 to 100 dB). This "folding" process mixes

the data from 36 K Hz to 40 K Hz with the data from 40 K Hz to 44 K Hz so it is not possible to locate specific frequency components in the translated spectrum, but frequency analyses were performed on the output data to determine the character of the sensor response.

Spectrum analysis of output data indicated that the translated output was much like "white noise" with broad random content. No specific discrete components were present. The overall level of noise did increase when the induced fault was included in the test of bearing No. 3 such that the meter indication increased from 47 dB up to 71 dB, an increase by a factor of 16 in level. Comparisons between new bearings gave a spread of 18 dB or a factor of 8 in level so this points out that the best application of this device is for periodic monitoring of an installed system to evaluate deterioration with time. It is also felt that any hand probing device such as this one requires considerable operator skill to get dependable results.

Wilcoxon Accelerometer - A Wilcoxon Model 90 accelerometer was housing mounted in the vertical plane of the bearing to measure radial acceleration responses. This accelerometer was chosen for its broad frequency response characteristics which permit investigation of ultrasonic outputs. Advertised response is for output flat to 40 K Hz and for a mounted resonance at 120 K Hz. This sensor provided maximum definition of test bearing condition with significant output differences for the variation in performance evaluated and its response will be discussed fully in the Analysis section of this report.

Bruel and Kjaer Model 4313 Accelerometer - Two of these accelerometers were used to evaluate performance in the frequency range to 15,000 Hz: one for radial acceleration and the second for axial acceleration. These sensors were useful for defining performance over the usual machinery analysis frequency range and are rugged and straightforward to use. Calibration curves are included in Appendix C, Figure C-13. Each suffers by having its mounted resonance in the area of 35 K Hz which was at times excited by frequency components in this range. Resonant response is 6 to 40 times greater in amplitude than would occur for non-resonant inputs so normal range data tends to be lost in noise. Neither sensor location provided significant analysis capability beyond once and twice rotation and ball pass frequency.

### Sound

A Bruel and Kjaer Precision Sound Level Meter Model 2203 was placed approximately six inches from the test bearing to provide sound spectrum data. The sound pressure level produced by the test facility and lubrication was unfortunately at such a high level that no significant change in output occurred with all the test variables attempted. Typically, good sound information cannot be obtained unless the background level is more than 10 dB below the level present with the test part in operation.

### Shaft Orbit

Shaft radial orbit was measured using a Bently Nevada eddy current displacement sensor and detector to relate shaft position to operating events. The area viewed by the sensor had a mechanical runout of 0.003 inches which gave a sinusoidal reference signal for position and also for speed indication. The output of this sensor did not change with variations in bearing operation (other than speed).

### Oil Flow

It was intended to measure bearing performance under varying oil flow conditions to determine if any other parameter than temperature would be an effective monitor. It was found that there was no measurable output (other than bearing temperature) which could detect the presence or lack of oil flow, even under extremes of loading. Consequently, test data presented is for an oil inlet temperature of 110<sup>o</sup>F and a flow rate of 0.1 gal per minute. No testing was done to evaluate flooded oil flow conditions.

### Power Loss

Steady-state torque measurements were limited by DC drift problems so detailed power loss data were not available for the bearing test conditions evaluated. However, dynamic torque outputs were successfully tape recorded and scanned for content which might contribute to definition of bearing operation condition. It was found that once-per-revolution and twice-per-revolution components were present but no higher frequency component responses were produced. It was concluded that this sensing technique did not produce pertinent condition information.

### Analysis of Test Data

Experimental data from the various sensors used was recorded on a Lockheed Electronics 7 Channel tape recorder. Tape recorder speed was set at 30 inches per second to provide frequency response from 200 Hz to 100 K Hz on the Direct Record Channel and DC to 10 K Hz response on five FM Record Channels. Voice commentary was also recorded. Playback of test data was done at 7 1/2 inches per second to compress the data into a frequency range compatible with a Spectral Dynamics 301A Real Time Analyzer (0 to 20 K Hz) which was used for most of the signature analysis work. This unit provides narrow band analysis capability virtually instantaneously (50 m seconds after the data is fed into the analyzer). For a portion of the analysis a Spectral Dynamics Model 302B Time Averager was available to reduce the spurious components of the data. A photo of the analysis center used for data reduction is included as Figure G-7.

During testing of the No. 3 bearing after the pit was induced, it was noted that individual bearing balls gave a discrete oscilloscope response from the Wilcoxon accelerometer output as each passed the etched damage location. The oscilloscope was being triggered by the Bently Nevada displacement probe output at once per shaft revolution and 8.7 "bursts" occurred per shaft rotation.

Figure F-1 in Appendix F includes an oscilloscope photo of the accelerometer output data which shows the response for 8000 rpm and 50 pounds thrust load. The same figure shows the real time analysis output of the accelerometer over a frequency range from 240 Hz to 80,000 Hz. Comparison of this figure with the same test condition run before the fault was included (Fig. F-2) shows the change in character of the raw data and in content of the spectrum. The ball passing frequency so evident in the raw data of the damaged bearing does not appear in the low frequency spectrum analysis of the accelerometer output shown as Fig. F-3.

Further examination indicated that these ball passing pulses were actually modulation of signals present at 28 K Hz and that the real time spectrum analyzer could not detect this modulation as it shows up only as a change in amplitude of the 28 K Hz "carrier." Because the presence of the inner race defect was so evident in the oscilloscope display it was felt that additional signal conditioning would produce valuable fault-detection information.

A Spectral Dynamics Model SD 103 Dynamic Input Sine Converter was used to condition these accelerometer output signals to permit further analysis. This unit is normally applied to convert pulse information to a sine wave of fixed amplitude which is phased to the input signal. When a complex signal is applied to it, the Sine Converter tries to produce sine waves for each input pulse so a spectrum analysis of its output contains significant frequencies. The gain setting of the Sine Converter was adjusted to show discrete components in the 700 to 1400 Hz range. With this analysis method, a spectrum analysis as shown on Fig. F-4 was produced. This shows the presence of modulating frequencies at ball pass of the inner race defect. The Sine Converter output for the undamaged bearing test did not show any inner race ball pass frequency component (Fig. F-5).

It was surmised that bearing fault information was being carried on high frequency accelerometer outputs much like an AM communications signal. It was also surmised that a system capable of detecting the amplitude modulation could provide useful information to define the nature of a bearing fault and could, with additional study, guide the decision to restrict operation of a failing bearing.

The source of the 28 K Hz signal "carrier" was of prime interest in evaluating the overall system performance. A check of the race and ball resonance for this bearing gave the following values: (see Computations, Appendix D-4)

	1st Critical
Inner Race (free)	6.1 k Hz
Outer Race (free)	2.8 k Hz
Ball	555 k Hz

Treating the inner race as a free ring is quite far from reality as it is an interference fit on the shaft, and in fact it seems that it should be treated as a solid cylinder. The outer race, however, has a clearance fit in its housing so the calculated resonance probably is quite good. There was no recognized response in the 2800 Hz area which could be attributed to outer race resonance. Resonance of the ball itself is far above the range of experimental analysis used.

It is concluded that the 28 K Hz response must be related to the mass of a ball on its supporting contacts.

The effects of varying test parameters upon this resonant response are shown on Figs. F-6 through F-20. Note that overall amplitudes from unconditioned data photos for damaged bearing tests are much greater than the summation of analyzed spectra levels. This occurs because the input data has a characteristic resonant "ring" shape for each impact which begins as a very high spike and decays logarithmically. The analyzer is designed to process data which occur regularly so it produces an amplitude related to the average of the input response over a time period. Because the point of beginning of an individual spectrum analysis is not phased to the input data, Ensemble Averaging over a large number of spectrum ensembles produces statistically better results. This technique involves the memory storage of the sum of a number of subsequent spectra which are thus divided by the number stored. In these data plots, either 32 or 64 spectra are "time averaged" to produce representative data.

Increasing thrust load produced increasing responses of 28 K Hz and at 55 K Hz for the induced pit condition as shown by Figs. F-6 and F-7 for 8000 rpm. Reference to the spectrum traces for the undamaged bearing at the same loads (Figs. F-10 and F-11) shows that the 55 K Hz response is very sensitive to load while the 28 K Hz area is hardly affected. This indicates that the 28 K Hz response is a unique output which is greatly affected by bearing damage but only weakly responsive to load and then only when damage is present. It is shown in the spectra analyses for the low frequency range to 2000 Hz (Fig. F-8, F-9, F-12, F-13 and F-14) that the inner race fault frequency of 1156 Hz does not appear as a significant signal under any test conditions.

A review of the same test load cycle for 6000 rpm operation with the induced inner race fault is available from Figs. F-15, F-16 and F-17. These spectra plots shown an even lesser response of the 28 K Hz resonance to variations in load. The 25 percent reduction in bearing speed did not cause any change in the frequency of the 28 K Hz response which further enforces the premise that it is an inherent response of this bearing. Again the spectrum for the low frequency range (Fig. F-18) shows that the damage indication is too slight to appear in the direct accelerometer output. Figures F-19 and F-20 show the 50 pound thrust load accelerometer characteristics for the undamaged test of this bearing at 6000 rpm.

In summary, it is concluded that response to the inner-race defect is as follows: Each ball impacts on the inner race "pit," causing the ball to resonate. Since the bearing load is primarily a thrust load, each ball impact is quite similar in amplitude to its neighbors. AFBMA Class 7 bearings have close ball diameter control so the resonant frequency value for each ball is very nearly the same. The resonating of the balls is transmitted to the outer race and to the bearing housing through the film of oil between balls and race and between race and housing bore. A housing accelerometer can then sense the vibration of the balls with peak response occurring at each impact.

Further experimental evidence for this thesis can be obtained from the oscilloscope photo shown on Fig. F-1. Note that at approximately 45 rotational degrees past the minimum amplitude point of the shaft runout trace, there is a maximum amplitude pulse. At that time the inner race pit, a ball, and the radial Wilcoxon accelerometer were directly in line. Approximately 90 degrees later the accelerometer output reaches a minimum when the pit is impacting a ball in a plane perpendicular to the accelerometer centerline. At a point another 90 degrees later there is a second, minor peak as the pit is on the opposite side of the shaft from the accelerometer but in line with it. There is a second minimum at the other out-of-plane impact and a maximum as the pit, ball and accelerometer again fall in line. Note that there are only 9 of the 15 balls involved in this cycle. The next revolution involves a different set of 9 balls in slightly different locations yet the response is essentially the same, so individual ball variations do not seem to enter in.

It is concluded that impacts from an outer race defect would also excite the resonance demonstrated by these tests but would occur at the frequency of ball pass for a single outer race location. It is expected that the modulation would not show the amplitude variation with inner race position but would instead be related to the location of the pit with respect to the accelerometer. This would mean that amplitudes might vary slowly as the outer race creeps in its mounting bore, and establishment of limits of vibration level would be more difficult.

By the same reasoning a ball fault would also cause resonant ringing at the discrete frequency of ball rotation, but it would have even greater possibility of

variation in output. Balls in a ball bearing characteristically find a particular plane of rotation for each operating condition of load or speed and it would be possible that a fault would not contact either race for extended periods of operation. As faults accumulated, however, the statistical opportunities of contact increase and the deterioration of the bearing would become apparent.

It is also concluded that multiple damage indications would have no effect on the ability to define bearing condition by this technique. The raw data may take on a more random appearance as more defect impacts occur, but narrow band frequency analysis should resolve the repetition rates of the individual fault locations.

Other responses shown on accelerometer spectrum plots at 32 K. Hz and 55K Hz have not been recognized or related to specific component ringing. The response at 55 K Hz response varies strongly with thrust load so it could be used as a measure of system operating conditions. It is conceivable that impending problems would show up as an increasing thrust load (such as higher temperature due to lubricant starvation) and the change in level of the 55 K. component would signify this.

All sensor outputs were scanned to find additional indicators of bearing fault but none produced definition as clear as from the Wilcoxon accelerometer.

## SECTION IV

### PROTOTYPE DIAGNOSTIC SYSTEM

The experimental determination of a bearing system resonance which was related to an induced bearing defect provides criteria which can be used for the detection and evaluation of bearing faults. The availability of two discrete indications permits the construction of a logic circuit which will give a fault indication only when both are present.

The overall signal level produced at 28 K Hz provides the first indicator of a bearing fault. The thirty-to-one variation between levels produced for the single fault and for the bearing when new, permits good resolution of early damage. As this phenomenon is not speed or load dependent, this criteria applies to any installation of this bearing size.

The second criteria used is that modulation occurs at discrete frequencies depending upon the bearing speed and upon which component incurs the initial damage indication. An inner race fault will produce ball contacts 8.7 times per shaft revolution, and from a statistical basis will be the most likely initiation point for fatigue faults. An outer race ball track defect will produce 6.3 contacts per shaft revolution and it is expected that overall amplitudes will vary depending upon the relationship of defect and sensor location. A normal bearing installation will permit the outer race to creep slowly and acceleration levels will be a peak when the defect is in the plane of the accelerometer and will be somewhat lower when the defect is 90 degrees out of plane from the sensor.

A ball defect will produce modulation at 6.0 times per shaft revolution but has the possibility of being quite erratic. If the initial ball defect should be out of plane from the ball spin axis occurring when monitoring is done, this fault indication will not be present.

The electronic circuit developed is shown in block form on Fig. IV-1. Housing vibration from the bearing under test is converted to a charge signal by a securely

attached high frequency response accelerometer. The charge is detected by a charge amplifier and a voltage proportional to housing acceleration is produced. This voltage is amplified and presented to the input of the Bearing Fault Detector. Only the information at the 28 K Hz resonance is of use so the input data is filtered to exclude all but the carrier and its sidebands. The shape of this filter is shown by the plot on Fig. IV-2. The band pass filter produces a maximum gain of 150 to the test point indicated as 28 K Hz out.

At this point, the signal has sufficient amplitude so that a simple diode detector can be used. The detected signal is fed to the adjustable low frequency Envelope Band Pass Filter and also to a low pass filter (integrator) to provide a DC output identified as point A. This DC level is proportional to the direct response at 28 K Hz.

The detected signal fed to the Envelope Band Pass Filter is available at the instrument tap identified as Envelope Detected Output and can be viewed on an oscilloscope and also be analyzed by a spectrum analyzer. This signal contains information relating to the time-varying change in level of the 28 K Hz resonance. The Envelope Band Pass Filter is designed as an adjustable filter with a constant Q of 50. The center frequency can be adjusted by a front panel control over the frequency range 700 to 1460 Hz (10 turn pot identified as Frequency Control). The maximum gain for this filter is approximately 50. An output after the filter is shown on Fig. IV-1 as Filtered Detected Output and can be monitored by an AC volt meter. This output is also at such a level that it can be diode detected and integrated to provide a DC output identified at Point B.

The Frequency Control pot is set based upon shaft speed to pass inner race defect, outer race defect, or ball defect frequency components.

The DC output of each detector circuit is fed to a comparator which has an adjustable trip level. For a fault indication to occur the levels of both signals must be sufficient to exceed the trip points. The output of each comparator is applied to one input of a two input logic "AND" gate. This gate will produce an output if, and only if, both inputs are present. The output of the "AND" gate is connected to a power amplifier to operate the damage indicator lamp.

A photograph of the Bearing Fault Detector is included as Fig. IV-3.

Internal defect limits settings for the Fault Detector were based upon output responses from a small induced fault which simulates the first fatigue spall in a bearing of this speed and load. It must be noted that response at the sensor from a particular bearing defect depends upon the transmission path and the housing configuration and mass. A damaged bearing indication is shown by the lighting of the Fault Indicator Lamp when the response at 28 K Hz is sufficiently high and also the level within the Envelope Band Pass Filter range is above the trip point.

Output spectra plots made from tape recorded accelerometer data played through the Bearing Fault Detector are shown in Appendix F as Figures F-21 through F-26. These spectra are from the Envelope Detected Output tap and represent the following conditions:

- Fig. F-21 8000 rpm 50 lb Thrust Load - New Bearing
- Fig. F-22 8000 rpm 50 lb Thrust Load - Bearing with an inner race defect. One division in the amplitude scale represents 50 times the output of one division on Fig. F-21. Note the response at inner race ball pass frequency of 1156 Hz.
- Fig. F-23 6000 rpm 50 lb Thrust Load - New Bearing
- Fig. F-24 6000 rpm 50 lb Bearing with an inner race defect. One division in the amplitude scale represents 100 times the output of one division on Fig. F-23. Inner race ball pass for 6000 rpm is 867 Hz and that response is well defined.
- Fig. F-25 8000 rpm 250 lb Thrust Load - Bearing with inner race defect.
- Fig. F-26 8000 rpm 1000 lb Thrust Load - Bearing with inner race defect.

Note the sidebands present around the fault indication frequency spike. These occur at plus and minus rotation frequency and are the result of ball impact variations due to the location of the defect with respect to the sensor location.

In the damaged bearing tests the Bearing Fault Detector clearly indicates the presence of damage at the inner race. The level of damage is minor so that other indicators such as torque, noise, temperature, and direct audio range frequency vibration would not have detected the presence. It is proposed that this device be used to evaluate the performance of new installations to guarantee that ball and race damage has not occurred prior to or during assembly, and also to monitor the rate of deterioration of an operating system. With data available to define the rate-of-change of bearing condition, precise limits of deterioration can be set to maximize unit safety and life.

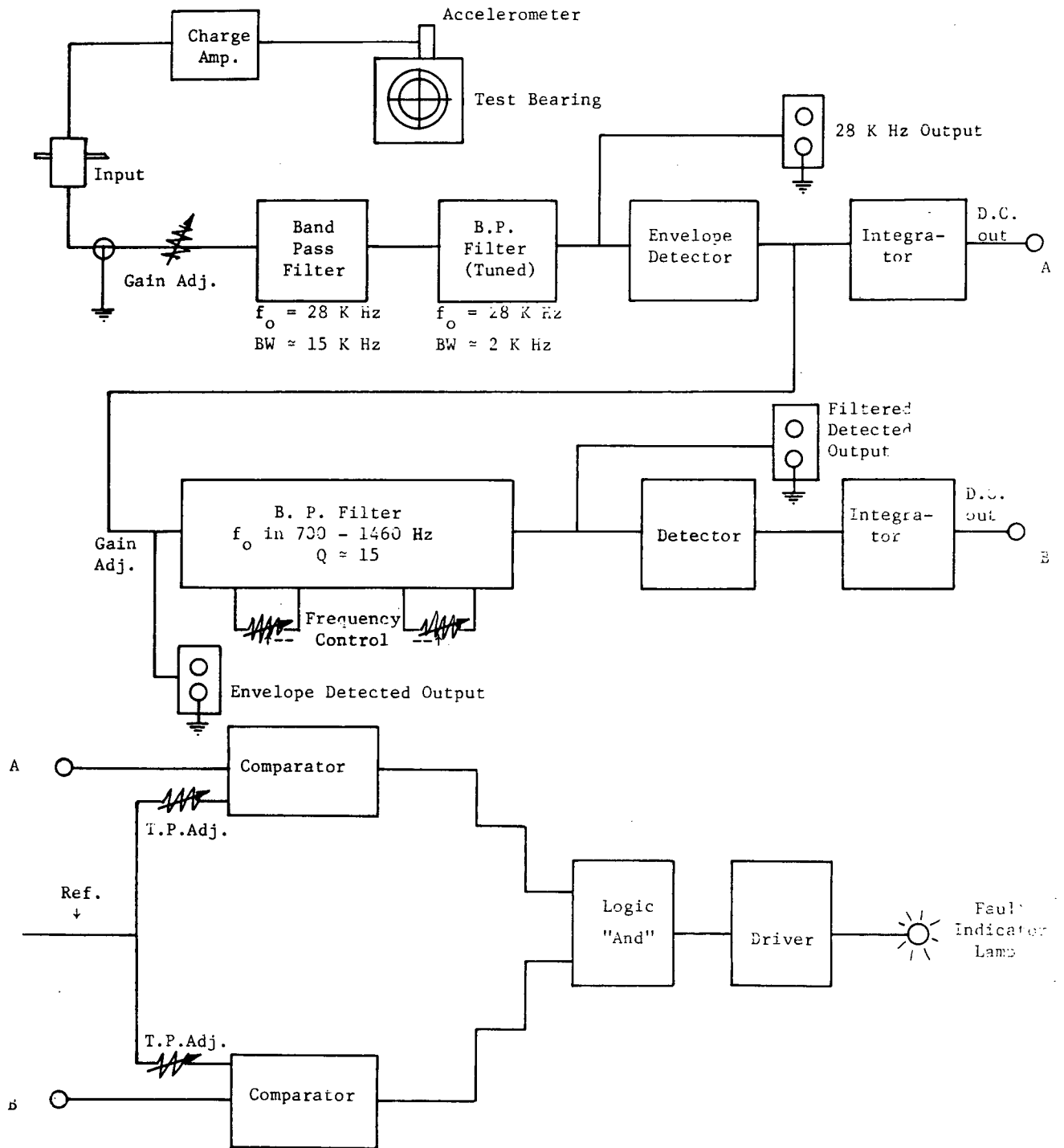


Fig. IV-1 Schematic of Bearing Fault Detector

TEST LOCATION Bench Test      TAPE NO. \_\_\_\_\_      JOB \_\_\_\_\_      DATE 2/9/71

TEST CONDITIONS Fault Detector Filter Shape

INPUT: \_\_\_\_\_

ANALYZER: \_\_\_\_\_

TRANSUCER Oscillator      RANGE V,RMS \_\_\_\_\_

CALIBRATOR 0.40 V peak-to-peak      FREQUENCY HZ \_\_\_\_\_

AMPLIFIER \_\_\_\_\_      GAIN 21.2V/0.4V = 53      TIME AVERAGE \_\_\_\_\_

TAPE CHANNEL NO. \_\_\_\_\_       FM       DIR

RECORDED: \_\_\_\_\_

GAIN \_\_\_\_\_

X-UNITS 0 - 50,000 Hz

Y-UNITS 5.0 V AC/inch

BY R. F. Burchill

Output Voltage  
Peak-to-peak

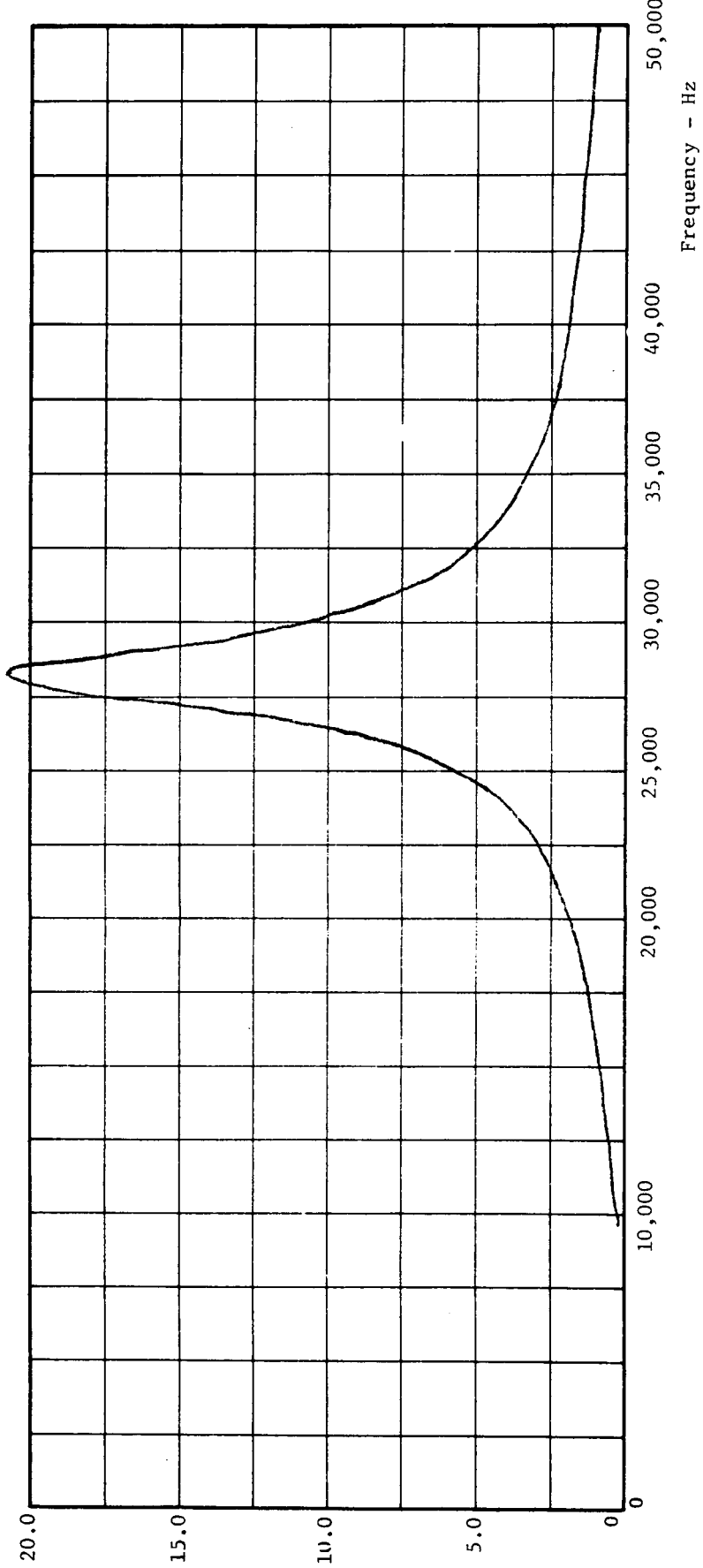


Fig. IV-2 28K Hz Filter Shape, Bearing Fault Detector, Sine Wave Input Test



Fig. IV-3 Bearing Fault Detector

SECTION V

REFERENCES

1. Valori, R. R., Sibley, L. B., and Tallian, T. W., "Elastohydrodynamic Film Effects on the Load-Life Behavior of Rolling Contacts" ASME Paper 65-LUBS-11.
2. Eschmann, Paul, "Rolling Bearing Wear Life," ASME Paper 67-WA/LUB-27.
3. Harris, T. A., Staff Engineer, SKF Industries, Inc., "A New Way to Evaluate Bearing Lubrication," Product Engineering, April 12, 1965.
4. Rumbarger, J. H. and Dunfee, J., "Current Requirements and Advances in Rolling Element Bearing Technology for Machine Tool Applications," ASME Paper 68-DE-56.
5. Jones, A. B., Consulting Engineer, Newington, Conn., "Rolling-Element Bearing Analysis Program."
6. Winn, L. W., "Development and Test of Long-Life Hybrid Boost Thrust Bearings for Small, High-Speed Jet Engine Applications," MTI Report 69TR17, June, 1969.
7. Frarey, J. L. and Zabriski, C. J., "The Acoustic Analyzer as a Diagnostic Tool for Turbine Engine," Annals of Reliability and Maintainability, Vol. 4 (July, 1965), p. 759.
8. Holloway, L. W., Nichols Construction Corp. and Kellum, G. B., Dow Chemical Co., "Ultrasonic Energy in Analyzing the Condition of Anti-Friction Bearings," presented to the 27th National Conference of The Society for Nondestructive Testing, Inc., Cleveland, Ohio, October 16-19, 1967.
9. Griffel, William "Vibration Frequency Charts," Design News, Vol. 18, No. 7, April 3, 1964.
10. Love, A.E.H. "A Treatise on the Mathematical Theory of Elasticity," Fourth Edition, Cambridge at The University Press.

APPENDIX A

TEST BEARING SPINDLE ASSEMBLY

FOLDOUT FRAME 2

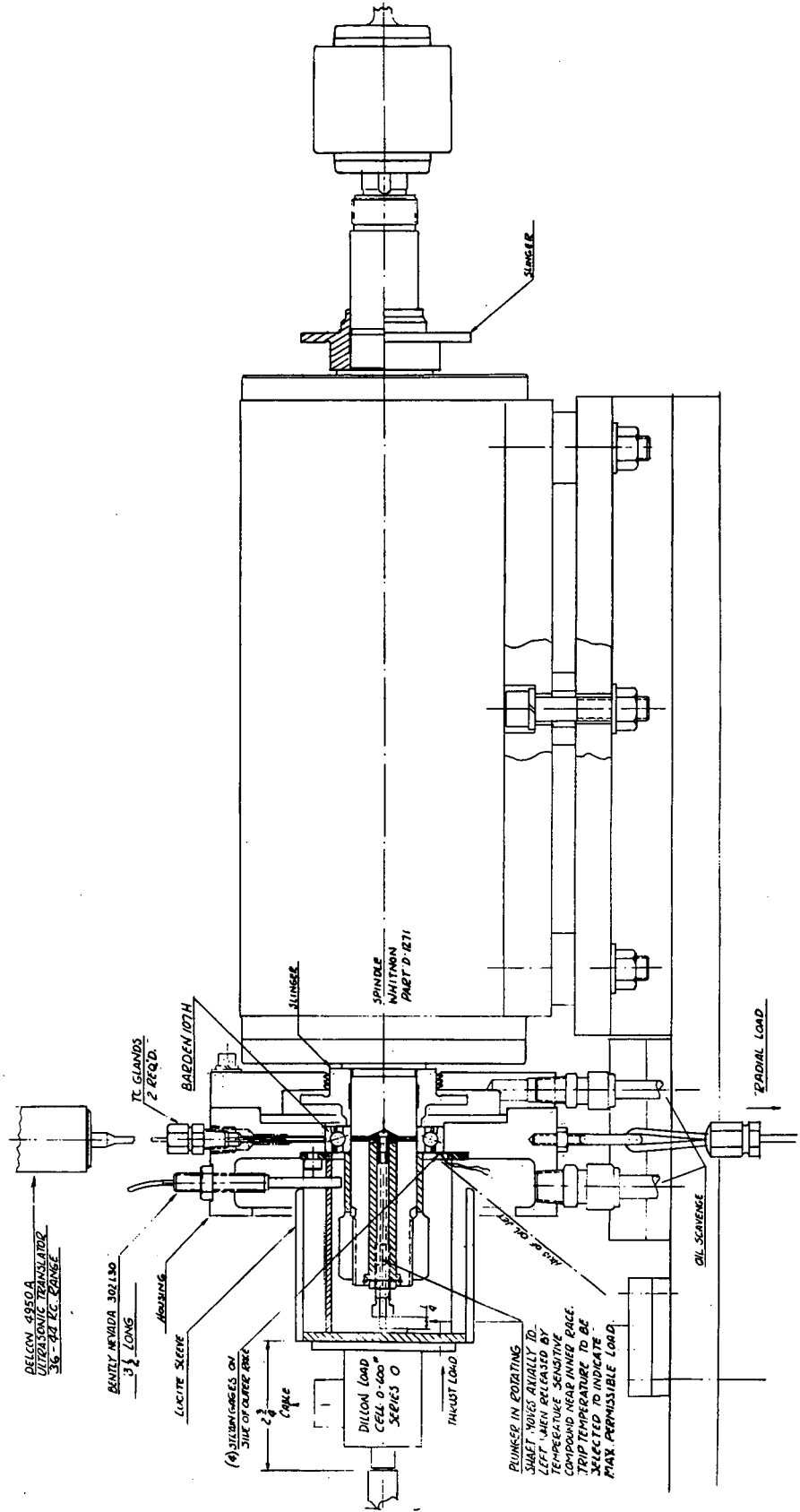


Fig. A-1 Test Bearing Spindle Assembly

FOLDOUT FRAME 1

APPENDIX B

BEARING PARAMETERS

TABLE B-1

BEARING LOAD SCHEDULE

Barden Ball Bearing 107 H Code 5 + 6  
 Initial Contact Angle 15 degrees ± 2 degrees  
 $ZD^2 = 1.46$   $R_S = 6.0$  lbs. (assumed unbalance @ 8000 RPM)

Calculation No.	Thrust Load T, lbs.	Factor Y	Radial Load $R_h$ , lbs.	Formula No. 1 $P = R_h + 1.2R_S$ Note 2	Formula No. 2 $P = x(R_h + 1.2R_S) + YT$ Note 2	Formula No. 3 $L = \frac{C}{R_A} \frac{S}{P}$ Note 3	Design Life, Hours	Average Life, Hours	AFBMA Life, Hours Note 4
1	50	1.25	500	507	280	1.07	700	3500	604
2	50	1.25	1000	1007	519	.538	< 100	400	75.5
3	500	1.06	15 Note 5	22	540	1.00	500	2500	---
4	1000	1.01	15 Note 5	22	1007	.538	< 100	400	72.9

- Notes:
1. From Chart C Barden Cat. No. G-3 pp 62
  2. Formula from " " pp 61
  3. Formula 3 from " " pp 62
  4. AFBMA Life computed by A. B. Jones Analytical Method.
  5. 15 lb. Radial load is weight of housing.

TABLE B-2

BEARING DATA:	Barden 107 H (0-9) ABEC 7
Outside diameter (62 mm)	2.4409 $\begin{matrix} -0.0002 \\ +0.0000 \end{matrix}$ inches
Bore diameter (35 mm)	1.3780 $\begin{matrix} -0.0002 \\ +0.0000 \end{matrix}$ inches
Pitch diameter	1.910 inches
Width of inner and outer race (14 mm)	.5512 $\begin{matrix} -0.001 \\ +0.000 \end{matrix}$ inches
Outer race radius of curvature	0.53 (53% of ball dia.)
Inner race radius of curvature	0.515 (51.5% of ball dia.)
Number of balls	15
Ball diameter	.3125 inches
Material (balls & races)	SAE 52100 steel
Cage material	Phenolic
Initial contact angle	$15^{\circ} \pm 2^{\circ}$ @ 10 lb. axial load
Radial Play	.0008 - .0012 inches
Value $ZD^2$	1.46
Static radial load rating	2640 lbs.
Static thrust load rating	7240 lbs.
Dynamic radial load rating	540 lbs. @ 8000 RPM
Basic dynamic load rating	3390 lbs.

TABLE B-3  
BALL BEARING TEST SUMMARY SHEET

DATE	TIME	TEST	DATA POINT NO.	TAPE NO.	RPM	THRUST LOAD, LBS.	REMARKS
10/15/70	1445	1	1	-	8000	50	No. 1 Brg.
10/16/70	1410	2	2	60	8000	50	
"	1457		3	60	8000	50	
"	1532	3	4	60	8000	250	
"	1600		5	60	8000	250	
"	1610	4	6	60	8100	500	
"	1635		7	60	8120	500	
10/26/70	1326	5	8	62	8000	50	
"	1345		9	62	8000	50	
"	1410		10	62	8000	50	
"	1413	6	11	62	8000	250	
"	1425		12	62	8030	250	
"	1500		13	62	7850	250	
"	1500	7	14	62	7850	500	
"			15	62	7950	500	
"	1523		16	62	8000	500	
"	1523	8	17	62	7950	1000	See Graph - Wilcoxon Accelerometer
"	1540		18	62	8000	1000	
"	1632	9	19	63	7950	1000	Oil Jet Cut Off
"	1651		20	63	7850	1000	" " " "
11/6/70	1350	10	21	66	8000	50	No. 2 Brg.
"	1450		22	66	8000	50	(with strain gaged O.R.)
"	1500		23	66	8000	50	
"	1500	11	24	66	8000	250	
"	1522		25	66	8000	250	
"	1530		26	66	8000	250	
"	1530	12	27	66	8000	1000	Oil off at 1600
"	1724	13	28	66	8000	1000	No Oil Flow
"	1742		29	66	8000	1000	" " " "
"	1755	14	30	66	8000	50	" " " "

TABLE B-3 (continued)

DATE	TIME	TEST	DATA POINT NO.	TAPE NO.	RPM	THRUST LOAD, LBS.	REMARKS
11/9/70	0903	15	31	67	8000	50	
"	0950		32	67	8000	50	
"	1015		33	67	8000	50	
"	1015	16	34	67	8000	250	
"	1045		35	67	8000	250	
"	1053		36	67	8000	250	
"	1053	17	37	67	8000	1000	
"	1109		38	67	8000	1000	
"	1140		39	67	8000	1000	
11/19/70	-	18	-	-	8000	50	Washed lubricant from brg with solvent. Ren 2 min. and failed. (Outer race temp. 220 F)
11/20/70	1355	19	40	68	8000	50	Failed Brg. Brg. No. 3
"	1420		41	68	8000	50	
"	1435		42	68	8000	50	
"	1435	20	43	68	8000	250	
"	1445		44	68	8000	250	
"	1455		45	68	8000	250	
"	1455	21	46	68	8000	1000	
"	1505		47	68	8000	1000	
"	1515		48	68	8000	1000	
"	1515	22	49	68	8000	50	Repeat Test 19
"	1530		50	68	8000	50	" "
"	1540		51	68	8000	50	" "
"	1540	23	52	68	6000	50	
"	1550		53	68	6000	50	
"	1600		54	68	6000	50	
"	1600	24	55	69	6000	250	
"	1612		56	69	6000	250	
"	1612	25	57	69	6000	1000	
"	1630		58	69	6000	1000	

TABLE B-3 (continued)

DATE	TIME	TEST NO.	DATA POINT NO.	TAPE NO.	RPM	THRUST LOAD, LBS.	REMARKS
12/1/70	1430	26	59	69	6000	50	No. 3 Brg.
"	1456	27	60	69	8000	50	
"	1513	28	61	64	8000	250	
"	1535	29	62	73	6000	250	
"	1553	30	63	73	6000	1000	
"	1613	31	64	73	8000	1000	
"	1630	32	65	73	8000	50	
"	1650	33	66	73	6000	50	

TABLE B-4

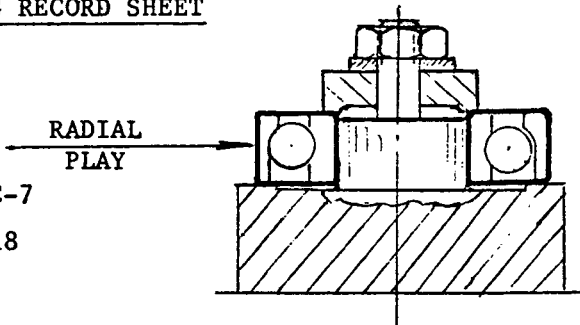
BALL BEARING RECORD SHEET

NASA Contract NAS 8-25706

MTI Project 241-40077

Barden Angular Contact Brg. 107H, ABEC-7

Ten Bearings Purchased - MTI PO 20-2818



Bearing Ser. No.	Test Nos. and Data Point Nos.	Radial Play		Brg. Wt. Grams		Total Wt. Loss	Total Hours
		Before	After	Before	After		
1	Tests 1-9 Data Points 1-20	.0012		147.8			
2	Tests 10-17 Data Points 21-39	.00115		147.70			
3	Tests 18-28 Data Points 40-66	.00110		147.60			
4		.00115		147.80			
5		.00120		147.60			
6		.00110		147.55			
7		.00150		147.85			
8		.00135		147.65			
9		.00125		147.60			
10		.00130		147.50			

No. Etched on Outer Race After 107H

Bearing O.D. - Housing Fit .0000/.0002 L

Bearing I.D. - Shaft Fit .0000/.0004 T

TABLE B-5

COMPUTER ANALYSIS SUMMARY - FATIGUE LIFE VS. LOAD

BEARING LOAD	FATIGUE LIFE IN HOURS				AFBMA	FRICTION TORQUE In-Lbs.
	OUTER	INNER	BRG. Note 1			
1000# Thrust 15# Radial	189	142	86.7	72.86	2.5 Note 2	
50# Thrust 15# Radial	1182	840	526	458	0.98	
50# Thrust 500# Radial	1515	820.8	568	604	.313	
50# Thrust 1000# Radial	220	111	78.8	75.5	.868	

Barden Bearing 107H

No. Balls 15  
Ball Diameter 5/16"  
Pitch Diameter 1.91"

Note 1) 90% Survival

2) Coef. Friction = .075



TABLE B-7  
 COMPUTER ANALYSIS SUMMARY - SPIN AND ROLL VELOCITY VS. LOAD

BEARING	LOAD, LBS.		SPIN VELOCITY		ROLL VELOCITY		SPIN/ROLL RATIO	SPIN TORQUE	TORQUE X SPIN/ROLL RATIO	STRESS X SPIN/ROLL RATIO
	THRUST	RADIAL	OUTER	INNER	OUTER	INNER				
Barden 107 H 15 Balls	1000	15	3256	0	20782	28110	.1567:1	.2548	$4 \times 10^{-2}$	31200
"	50	15	2976	0	20719	28175	.1436:1	.1163	$1.67 \times 10^{-2}$	19030
"	50	500	791.9	0	20481	28451	.0386:1	.2465	$.95 \times 10^{-2}$	7610
"	50	1000	373.3	0	20475	28468	.0182:1	.588	$1.07 \times 10^{-2}$	4460

APPENDIX C

PERTINENT TEST INFORMATION

1  
1  
3

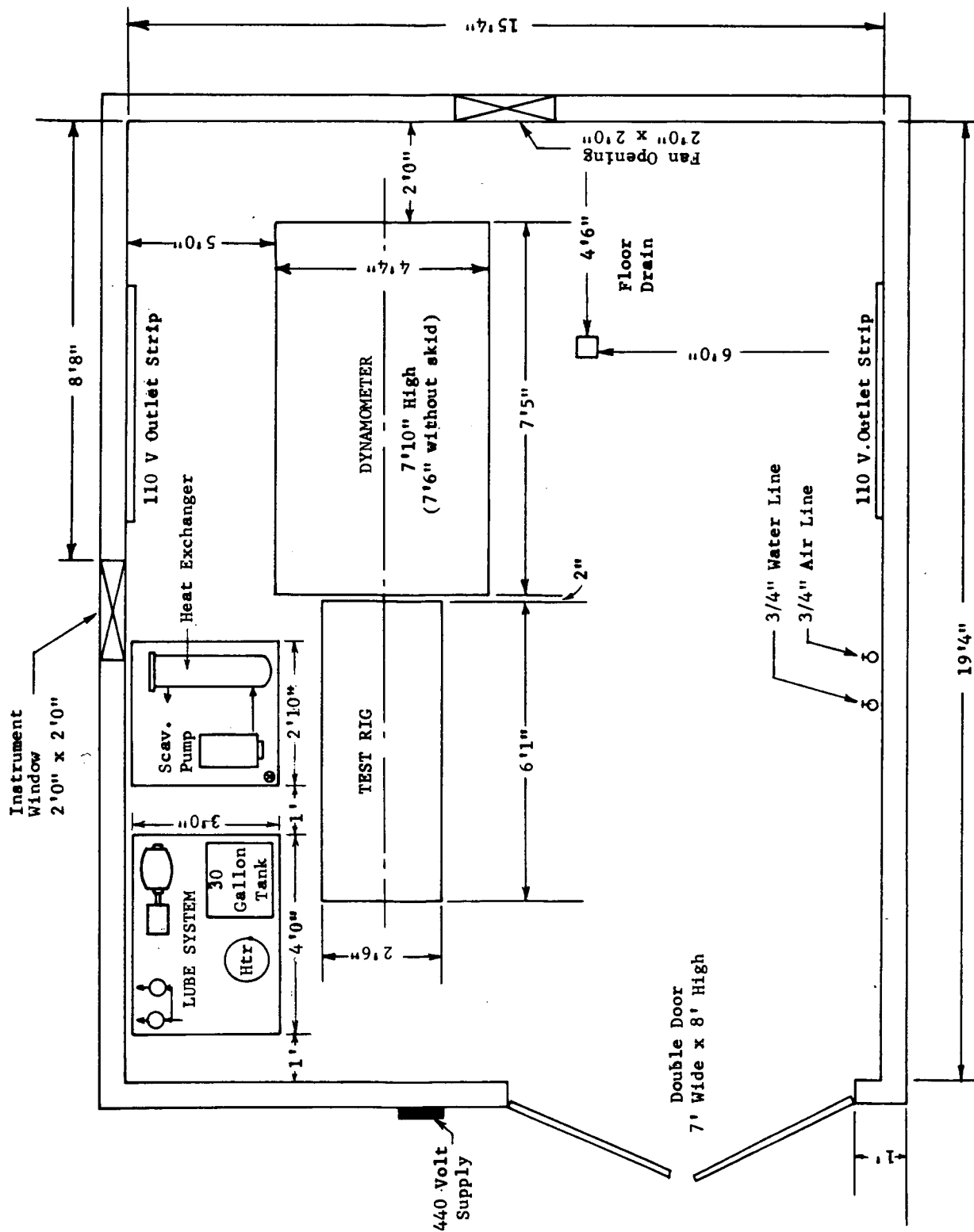


Fig. C-1 Test Cell Floorplan

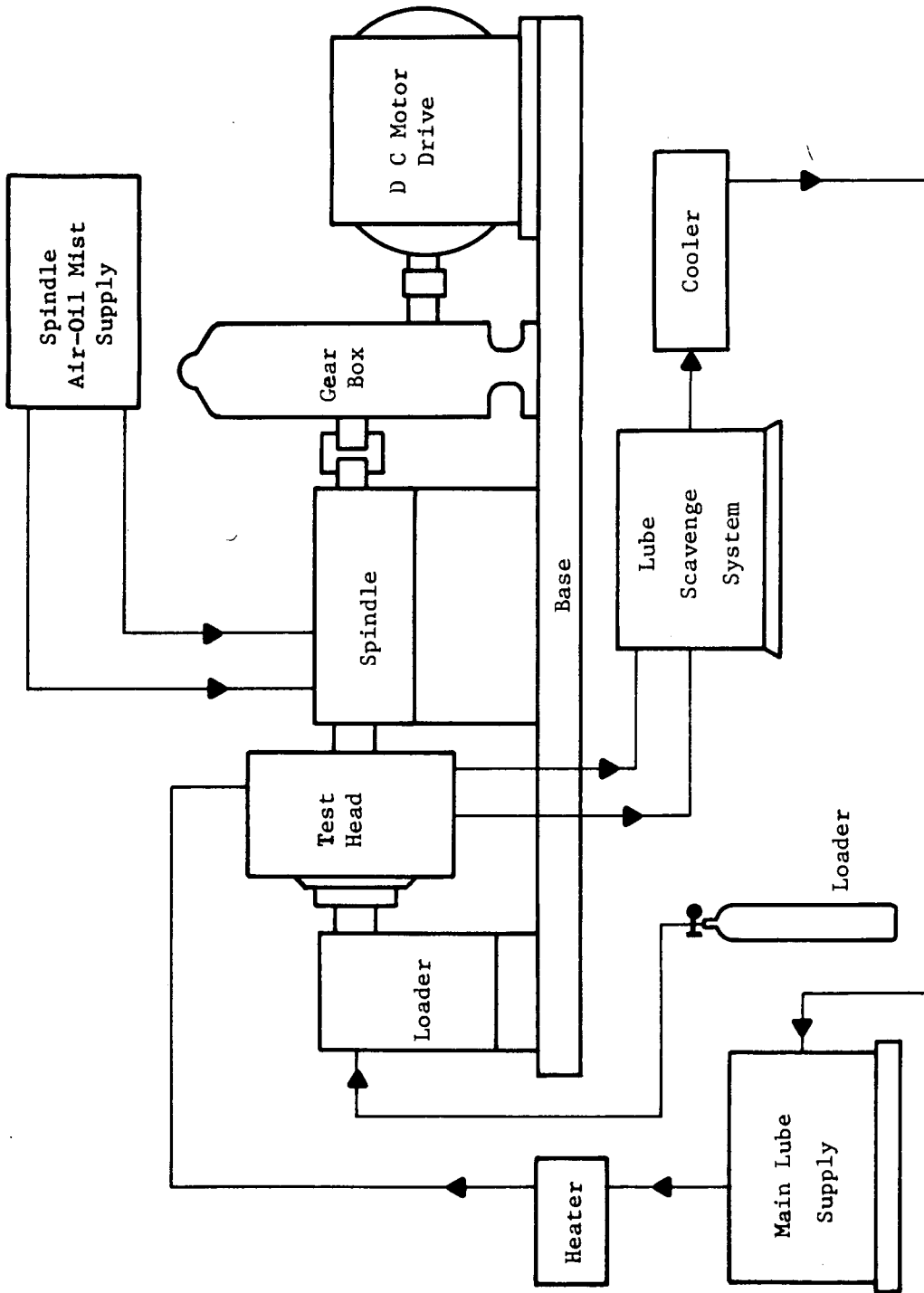


Fig. C-2 Test System Schematic



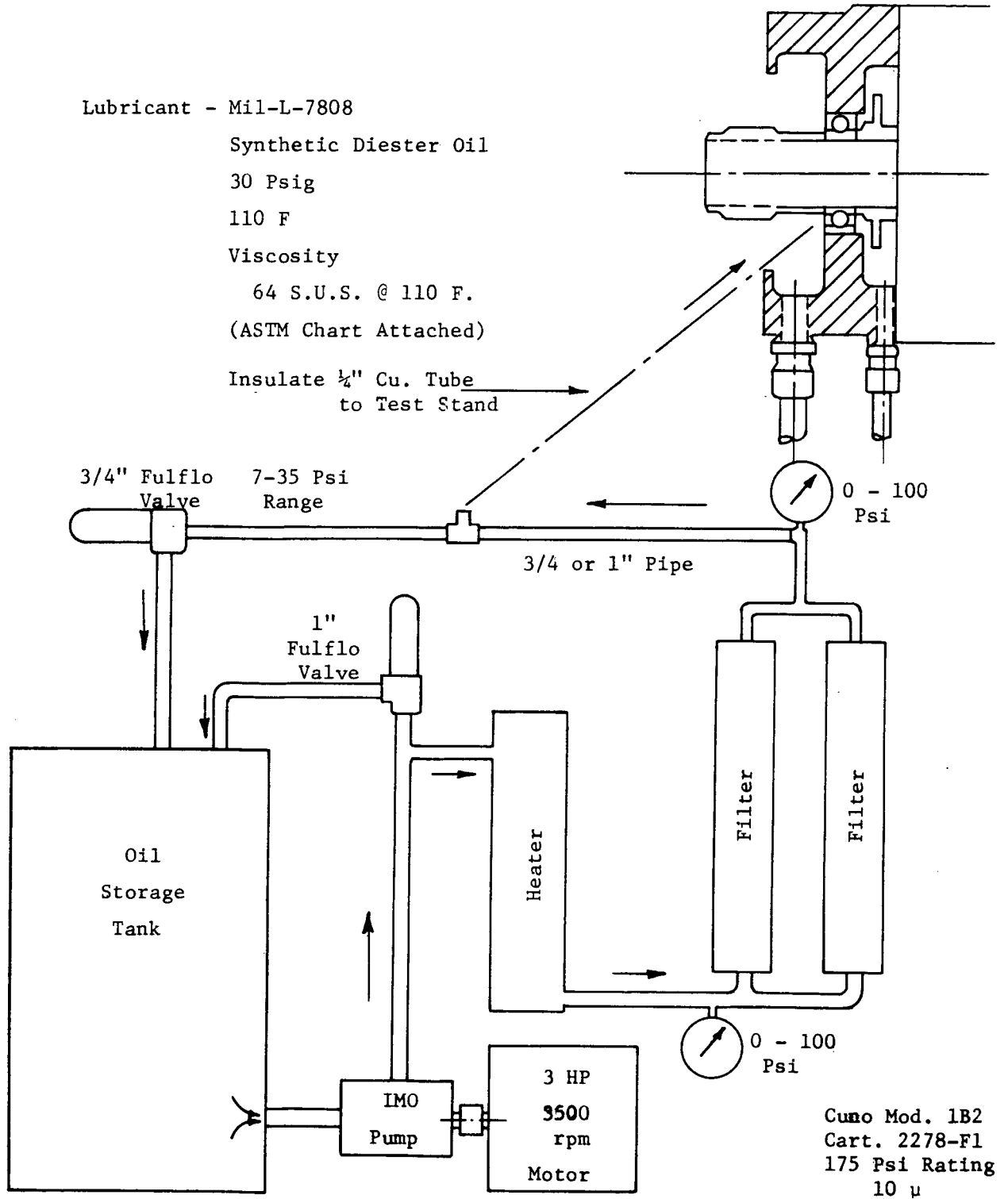
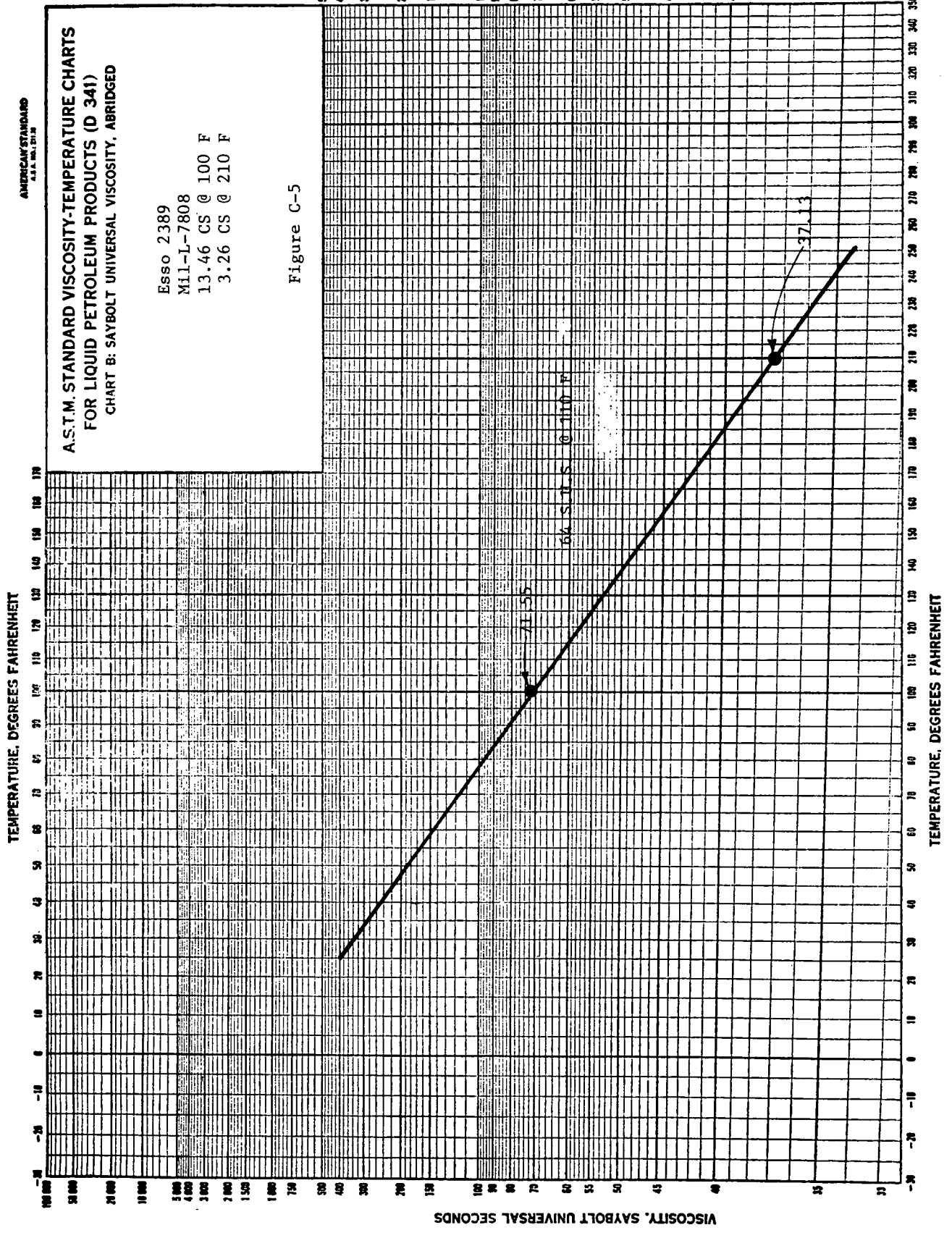


Fig. C-4 Lube Oil Supply

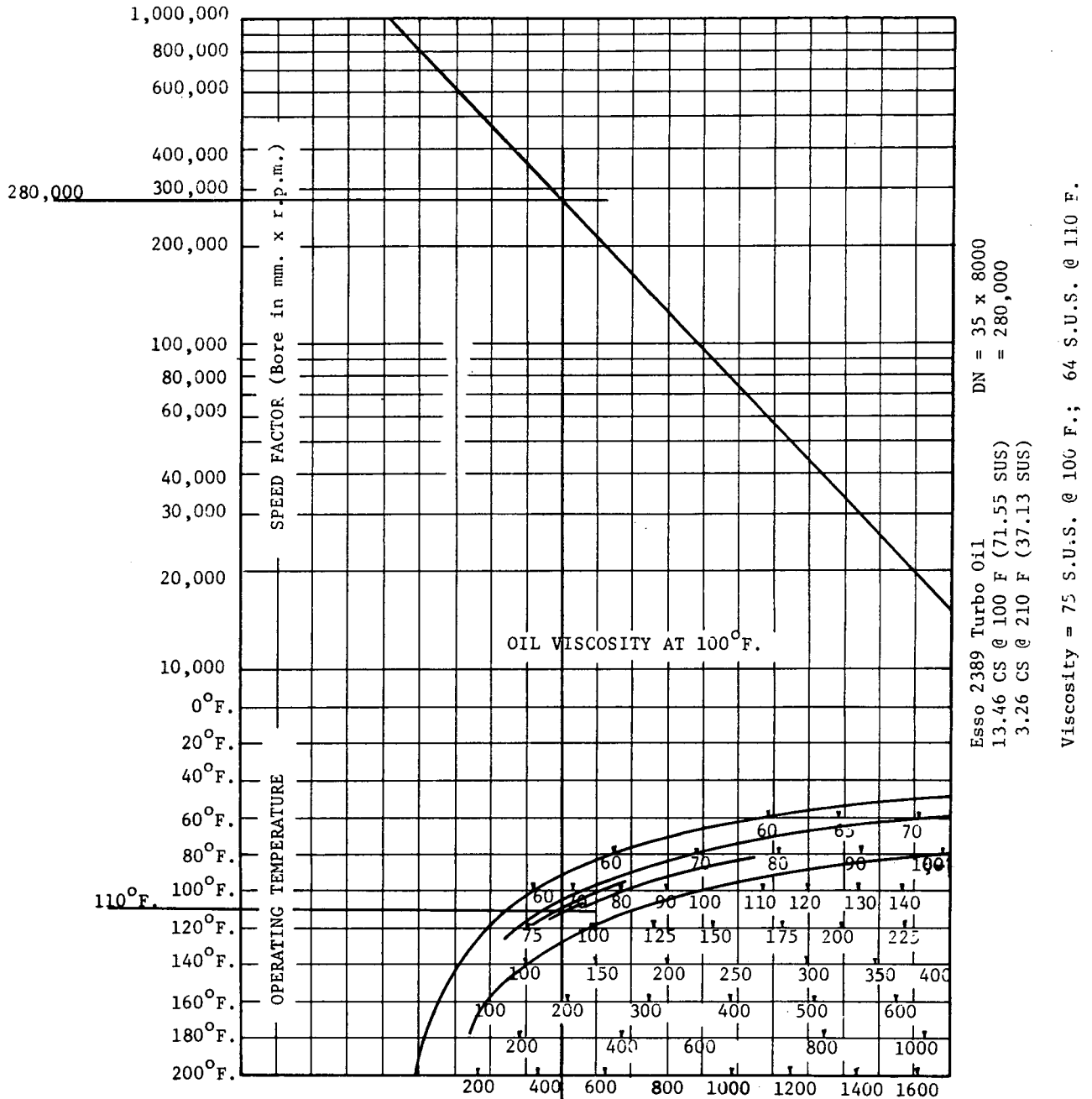


VISCOSITY, SAYBOLT UNIVERSAL SECONDS

TEMPERATURE, DEGREES FAHRENHEIT

TEMPERATURE, DEGREES FAHRENHEIT

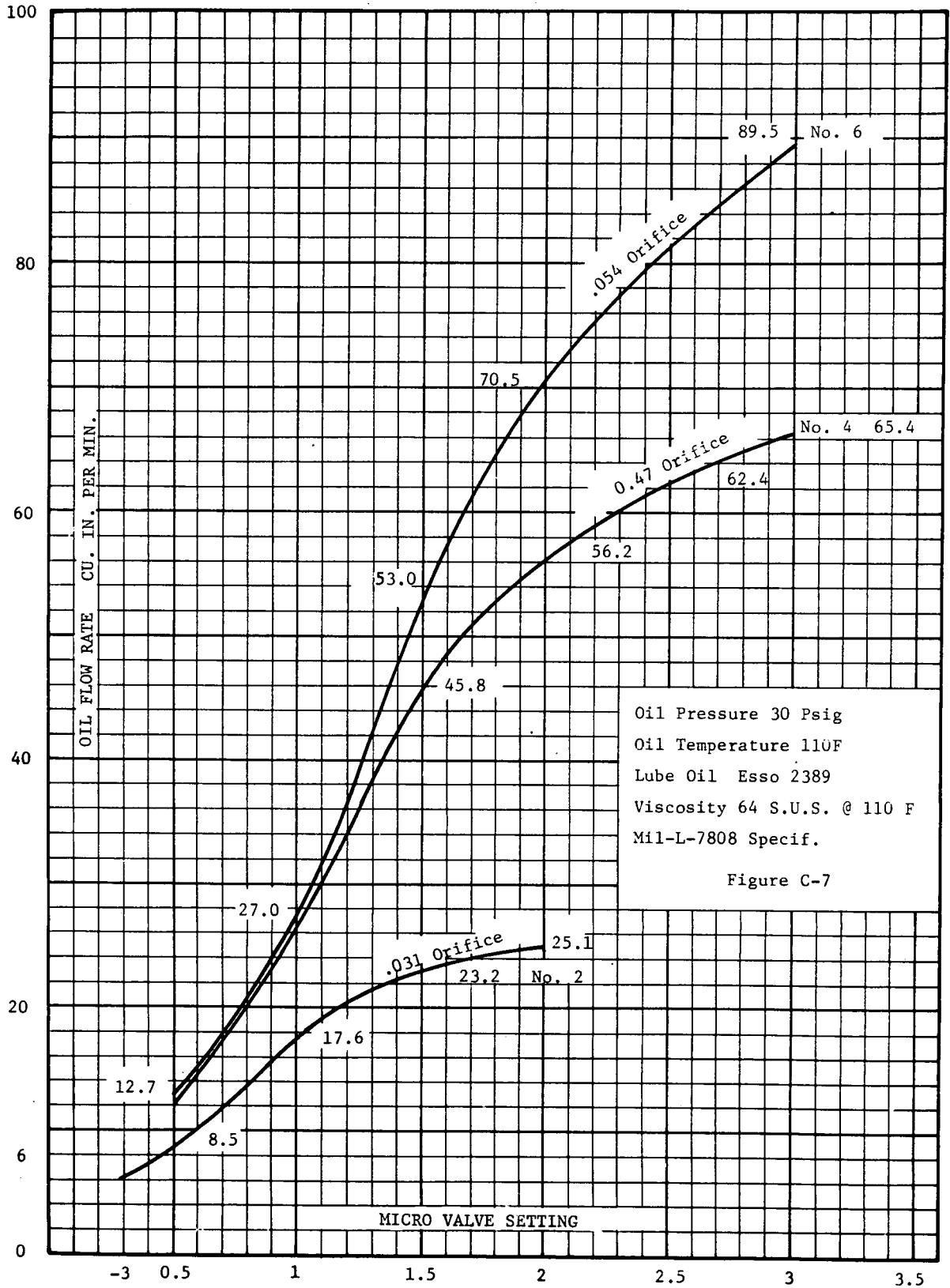
VISCOSITY, SAYBOLT UNIVERSAL SECONDS



The chart Figure 6 indicates the viscosity of oil most suitable for various size bearings running at various speeds and operating temperatures.

EXAMPLE: To determine the proper viscosity oil for a 20 mm. bore bearing operating at 10,000 rpm, and 160°F., multiply 20x10,000, which gives a Speed Factor of 200,000. Reading across from 200,000 to the diagonal line and then down to the line marked 160°F., it will be found that an oil having a Saybolt viscosity of 250 seconds at 100°F., is recommended.

Fig. C-6 Determining Correct Oil Viscosity



NAS 8 - 25705



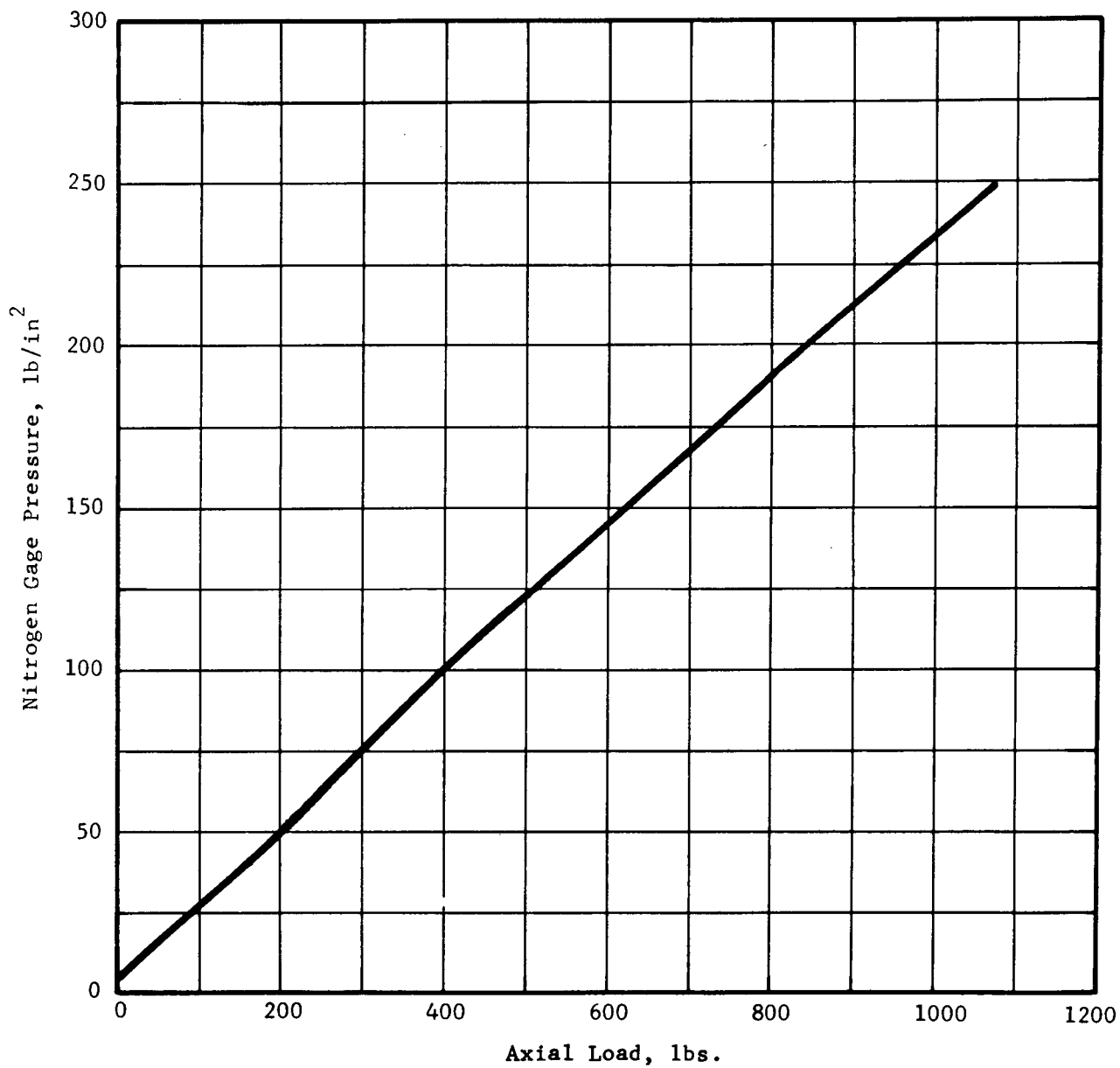


Fig. C-9 NASA Bearing Test. Calibration Curve for Model J62 Cylinder,  $2\frac{1}{2}$ -inch Bore, 1000 psi Rating

02

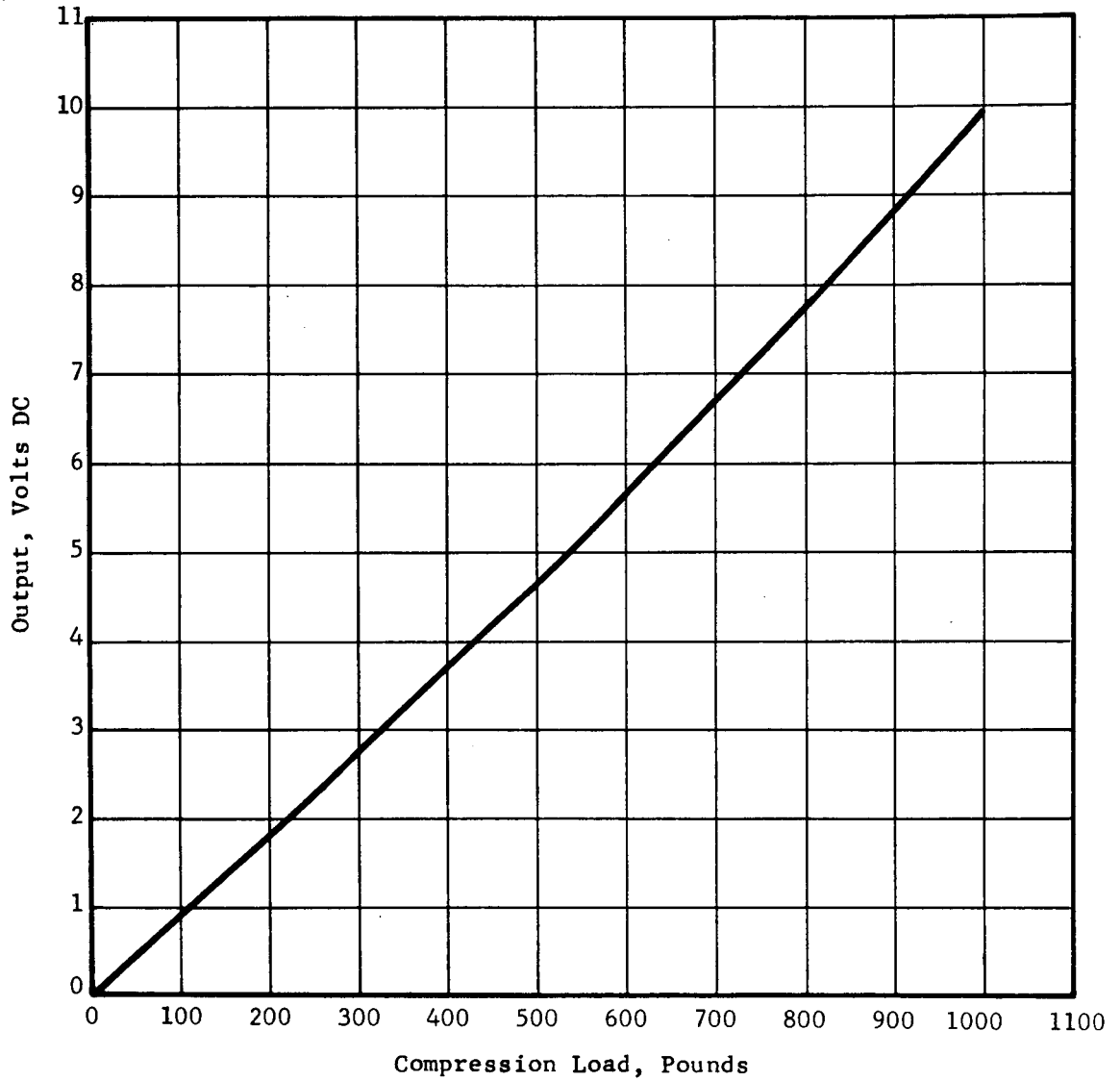


Fig. C-10 NASA Bearing Test. Calibration Curve for Dillon Load Cell, Series 0, Serial No. 3661

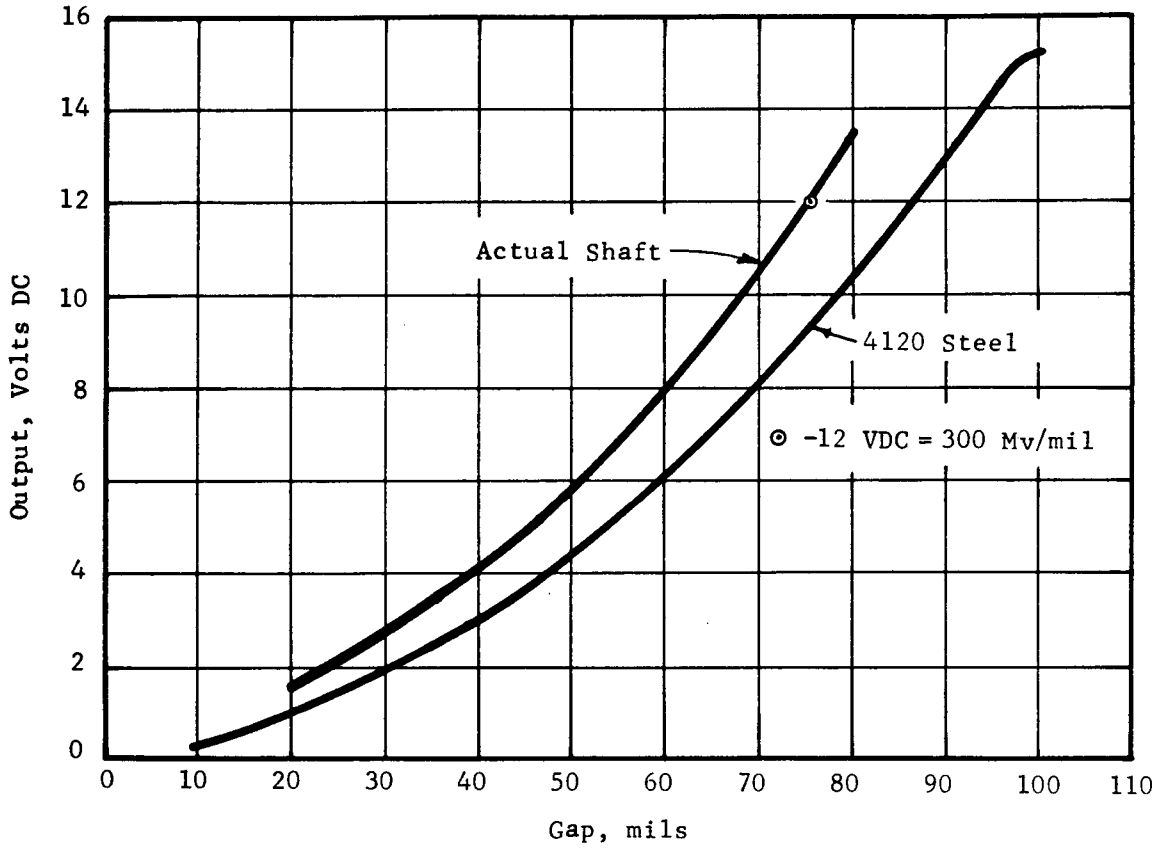


Fig. C-11 NASA Bearing Test. Calibration Curve for Bently Probe, Series 3000, Model 302L-30-3.5

FIGURE C-12

TEST PROCEDURE

- Test I Normal Signature 8000 RPM
- a. Using normal oil flow,\* 500 lb. axial preload and radial load removed. (See Calculation 3, Table I)
- Record:
1. Outer race temperature
  2. Torque
  3. Vertical, horizontal and axial housing vibration - B&K Accelerometer (acceleration to 20K Hz range)
  4. Acoustic signature - B&K Sound Level Meter
  5. Ultrasonic signature - Wilcoxon Mod. 90 Accelerometer
  6. Inner race temperature (less than - ) Amot Mod. 4102M
  7. Outer race strain signature
  8. Cage speed
- Repeat Test I on three bearings
- Test II High Load Test
- a. Same as Test I except 1000 lb. thrust load and radial load removed. (See Calculation 4, Table I)
- Test III Dry Bearing
- a. Reduce oil flow at 8000 RPM until outer race temperature reaches 350° maximum and record per Test I
  - b. Repeat at reduced speeds; i.e., 6000, 4000, 2000 RPM
  - c. Repeat on three bearings
- Test IV Flooded Bearing
- a. Determine influence of increased oil flow on parameters listed in Test I
- Test V Bearing with Raceway Defect
- a. Produce flaw by acid etching
  - b. Determine influence of defective bearing on items (4) and (5) of Test I.

-----  
\* To be established at Startup.

Brüel & Kjær

**Calibration Chart for Accelerometer Type 4333**



Serial no. 154286

Brüel & Kjær  
Copenhagen

Reference Sensitivity at 50 c/s at 23 °C  
and including

Cable Capacity of 104 pF

Voltage Sensitivity 16.9 mV/g\*

Charge Sensitivity 13.7 pC/g

Capacity (Including cable) 810 pF

Maximum Transverse Sensitivity at 30 c/s 2.6 %

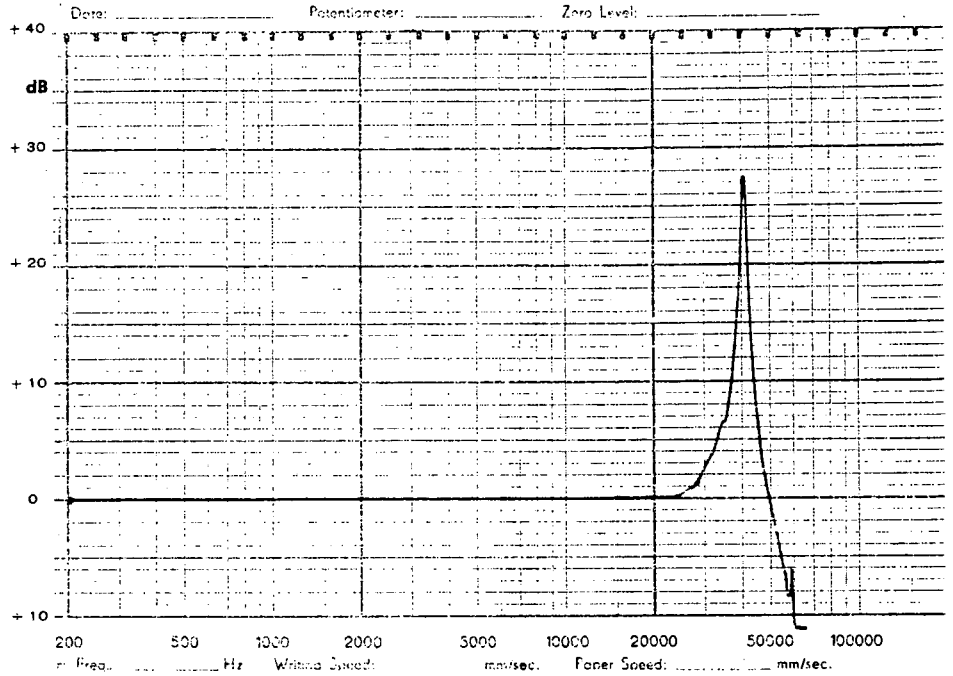
Undamped Natural Frequency 580 kc/s  
For Resonant Frequency mounted on steel exciter of 180 grams and for Frequency Response relative to Reference Sensitivity, see attached individual Frequency Response Curve.

Polarity is positive on the center of the connector for an acceleration directed from the mounting surface into the body of the accelerometer.

Resistance minimum 20000 Megohms at room temperature

Date 25-3-66 Signature E.F.

$$1g = 980.6 \text{ cm sec}^{-2}, \quad \frac{mV}{g} = \frac{mV_{rms}}{g_{rms}} = \frac{mV_{pk}}{g_{pk}}$$



Brüel & Kjær

**Calibration Chart for Accelerometer Type 4333**



Serial no. 149475

Brüel & Kjær  
Copenhagen

Reference Sensitivity at 50 c/s at 23 °C  
and including

Cable Capacity of 104 pF

Voltage Sensitivity 16.8 mV/g\*

Charge Sensitivity 13.7 pC/g

Capacity (Including cable) 822 pF

Maximum Transverse Sensitivity at 30 c/s 3.5 %

Undamped Natural Frequency 580 kc/s  
For Resonant Frequency mounted on steel exciter of 180 grams and for Frequency Response relative to Reference Sensitivity, see attached individual Frequency Response Curve.

Polarity is positive on the center of the connector for an acceleration directed from the mounting surface into the body of the accelerometer.

Resistance minimum 20000 Megohms at room temperature

Date 29-3-66 Signature E.F.

$$1g = 980.6 \text{ cm sec}^{-2}, \quad \frac{mV}{g} = \frac{mV_{rms}}{g_{rms}} = \frac{mV_{pk}}{g_{pk}}$$

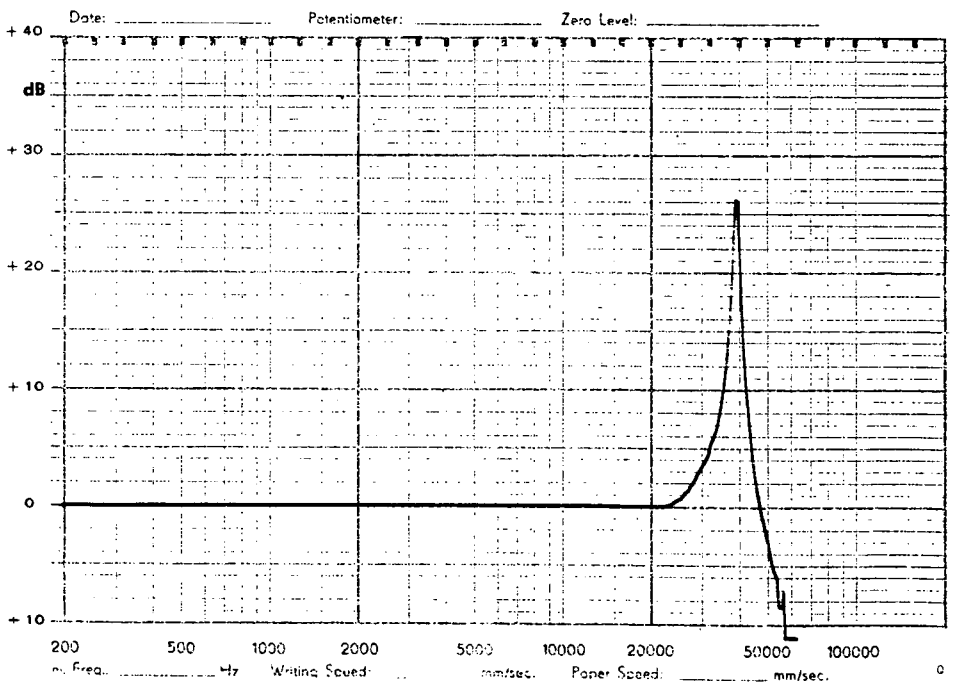


Fig. C-13 Accelerometer Calibration

APPENDIX D

COMPUTED TEST BEARING PARAMETERS

Figure D-1

BEARING DYNAMIC CAPACITY

Method from Barden Catalog G-3.

Barden Angular Contact Bearing 107 H.  
15 degree Contact Angle  $\pm$  2 degrees

From Table 8, page 65

107 H bearing, 15 balls  
5/16 ball dia.  
 $ZD^2 = 1.46$

To determine radial load due to unbalance:

Assume rotating weight at bearing = 30 lbs.  
Assume amplitude vibration 10001 radial displacement

$$\begin{aligned} \text{Force @ 8000 RPM} \\ &= .000028416 W_r N^2 \\ &= .000028416 \times 30 \times (8000)^2 \\ R_s &= 6 \text{ lbs.} \end{aligned}$$

Formula 1. page 61

$$\begin{aligned} P &= R_H + 1.2 R_s \\ &= 15 + 1.2 \times 6 = 22 \text{ lbs.} \end{aligned}$$

when  $R_H = 15$  lbs.

Formula 2. page 61

$$\begin{aligned} P &= X (R_H + 1.2 R_s) + YT \\ P &= .43 (22) + 1.06 \times 500 \\ &= 540 \end{aligned}$$

when  $T = 500$

$$\frac{T}{ZD^2} = \frac{500}{1.46} = 343$$

from Chart C, page 62

$$\begin{aligned} Y &= 1.06 \\ X &= .43 \end{aligned}$$

Formula 3. page 62

$$L_{RA} = \frac{C_s}{P}$$

$$\begin{aligned} L_{RA} &= \frac{540}{540} \\ &= 1 \end{aligned}$$

$L_{RA}$  = life ratio

$C_s$  = dynamic load rating, lbs.  
= 540 lbs.  
(page 31, 8000 RPM)  
 $P$  = equivalent radial load,  
Formula 2.  
= 540 lbs.

## Figure D-1 (continued)

From Chart 6, page 63

when  $L_{RA} = 1$ ,

Design Life = 500 hours

Average Life = 2500 hours

See Table I for calculated life values for other load conditions.

## Figure D-2

DESIGN MEMORANDUM

Subject: Lubrication  
Project Name: 241-40077

Date: October 8, 1970  
Sheet: One

Using Method by T. A. Harris, SKF. IND. PROD. ENGRG. April 12, 1965,  
Reference 3

Table I Angular Contact Bearing  
Barden 107 H  
Bearing Type E - 70C

Figure 2 H-Factor for 35 MM Bore  
= 70,000

Lubricant MIL-L-7808 Synthetic Diester Oil  
Viscosity 75 SUS @ 100 F

Figure 3 Viscosity Factor  
 $(\mu_o \propto)^{0.7} = 7 \times 10^{-8}$

Figure 5 Net Speed  
N = 8000 RPM  
 $N^{0.7} = 540$

$P_o$  Equivalent Radial Load = 540 lbs.  
From page 31 - Barden Cat. G-3

Figure 6  $P_o^{-.09} = .57$

$$\begin{aligned} \Lambda &= H [\mu_o \propto N]^{.7} P_o^{-.09} \\ &= 7 \times 10^4 \times 7 \times 10^{-8} \times 5.4 \times 10^2 \times .57 \\ &= 7 \times 7 \times 5.4 \times .57 \times 10^{-2} \\ &= 1.51 \end{aligned}$$

From Figure 7 35 percent Film

Figure D-3

BEARING COMPONENT RESONANT FREQUENCIES

To evaluate resonant frequencies of components of the test bearing, the following equations were used:

Race Resonances from Reference 9\* the natural frequencies for a thin circular member without end restraint

$$f = \frac{Ct}{r^2} \times 10^5 \text{ Hz} \quad \text{where: } f = \text{natural frequency, Hz}$$

t = plate thickness  
r = mean ring radius  
C = frequency constant

The frequency constant C depends upon the number of full waves around the periphery and is equal to:

Waves	Freq. Constant
2	0.25
3	0.70
4	1.40
5	2.20
6	3.20

These relationships hold for steel, aluminum and magnesium.

For this 107 bearing, the following dimensions are pertinent:

Outer race thickness = .13	Mean radius = 1.08 in.
Inner race thickness = .14	Mean radius = 0.76 in.

This gives the following resonances:

	1st Mode	2nd Mode
Outer Race	2780	7800
Inner Race	6070	17000

Ball Resonance from Reference 10\*, p. 286, the spheroidal resonant response of the ball is given by

$$f_b = \frac{0.424}{r_b} \sqrt{\frac{E}{\rho}}$$

\* See Section V, page 31.

Figure D-3 (continued)

where:  $r_b$  = ball radius-in.  
 $E$  = Youngs Modulus lb/in  
 $P$  = density of ball,  
 $\frac{\text{lb}_f \text{ sec}^2}{\text{in}^4}$

and in this mode the ball is distorted into an ellipsoid of revolution.  
 This assumes the material is incompressible for the 107 bearing, ball dia. =  
 5/16 inch., and

$$f_b = \frac{0.424}{5/32} \sqrt{\frac{30 \times 10^6}{.283/386}}$$

$$= 555 \text{ k Hz}$$

APPENDIX E

TEST FACILITY DETAILS

FACILITY DETAILSa. TEST FACILITY - TEST CELL ROOM 62

DRIVE MOTOR	Reliance D.C. Motor Type T - Shunt Wound 100 HP 4000 - 7500 rpm 460 volts 180 - 188 amps Frame 92TXY 12 Y Serial No. 1LT-17084-T3
SPEED INCREASER	Sundstrand Sundyne LMG Gearbox 50 HP Gear Ratio 6.43:1 Thrust Load 400# Max. Radial Load 1000# Max. Serial No. 1911-G Torque 75 ft-lb max.
COUPLING, MOTOR-TO-GEAR	Thomas Coupling Div. Rex Chain Belt, Inc. Flexible Disc - (Spacer Type) Size 163 DBZ-C
COUPLINGS GEAR-TO-SPINDLE	(a) Shear Coupling MTI Part 208B42  (b) Sier-Bath .9365/.9370 bore Max Speed 25,000 rpm 50 HP @ 25,000 rpm

SPINDLE, BASE MOUNTED	Whitnon Mfg. Co. D-1271 Max. speed 25,000 rpm Oil Mist Lube
SPINDLE LUBRICATOR	Norgren Micro-fog Oil System
TEST BEARING MOUNTING	MTI Design Sketch
TEST BEARING LUBE & SCAVENGE SYSTEM	Superior Design Corp. Design No. 1341 Oil Nozzle and Micro-Valve
LOAD CYLINDERS:	
RADIAL LOAD	Miller Air Cylinder Model A61 3 1/4" bore, 2" stroke Piston Rod, 1" Standard
AXIAL LOAD	Miller Air Cylinder Model J62 2 1/2" bore, 1" stroke Piston Rod, 5/8" Standard

b. INSTRUMENTATION

- (1) RPM Counter and Shaft Position Sensor
- (1) Thrust Load Cell
- (2) Thermocouples for test bearing OD
- (1) Ultrasonic sensor (36 - 44 KC range)
- (12) Strain Gages for bearing outer race
- (2) Strain Gages for torque measurement
- (3) Accelerometers (axial, horizontal, vertical)
- (1) Strobe light for cage speed readout
- (1) Microphone for acoustic pickup (B & K Sound Level Meter)
- (1) Lockheed 7 Channel Recorder/Amplifiers
- (1) Inner Race Temperature Detector

c. TEST RIG ASSEMBLY PROCEDURE

1. Install nut at coupling end of shaft. 1.375-18 NEF nut. Nut can be used for holding shaft when tightening nut at opposite end. Nut can also be used for removal of coupling.
2. Install coupling half by heating to 250F. Coupling requires (2) square keys for balance.
3. Locate spindle assembly on test stand and install shims under flange at (4) bolt down locations to obtain shaft alignment with driver within .001 inches per inch for both parallelism and squareness. Use alignment chart for recording shim thickness and runout. Drill and ream for (2) dowels when aligned. Driver to be rotated with bearings pressurized when indicating spindle alignment.
4. Assemble Sier-Bath coupling sleeve, "o" rings and retaining rings after specified alignment has been obtained and flange has been dowelled.
5. Connect (2) air-oil atomizer lubricator feed lines at top of spindle from Norgren system. Also connect thermocouple leads to readout.
6. Operate spindle at 8000 RPM for about 30 minutes to assure smoothness of operation and stability of spindle bearing temperatures.
7. Following initial test run, install test bearing with outer race markings outboard. Heat bearing to 200F for assembly on shaft.
8. Assemble shaft nut tight against bearing inner race by holding Sier-Bath coupling with belt wrench. Place dykem mark at end of nut and end of shaft so that any loosening of nut will be evident. Also mark phenolic ball retainer with dykem so that retainer rpm can be counted with stroboscope.
9. Install inner race temperature sensor in shaft bore with retaining ring. Fill chamber with duct seal so that bearing inner race temperature will be sensed.
10. Assemble flat plate on test bearing housing to form shoulder at bearing bore. Heat housing in oven to 200F and assemble on test bearing outer race.
11. After housing has cooled, replace flat plate with spider assembly which will act as bearing shoulder for thrust application.

## Test Rig Assembly Procedure, continued

12. Assemble split seal plate on rear face of bearing housing.
13. Assemble scavenge fittings, (2) thermocouples, Bently probe, ultrasonic translator, and (2) torque arms on housing. Also assemble small eyebolt at bottom of housing for radial load application.
14. Assemble flexible hose connections for (2) scavenge lines and connect to scavenge system.
15. Install (2) torque arm pedestals with balls and strain gages.
16. Install lube oil jet and regulating valve at underside of spider with nozzle aimed upward at ball bearing. Nozzle size and valve setting to be established by test.
17. Install lucite oil guard and Dillon load cell on spider. Connect load cell cable to readout to register applied thrust load. A minimum thrust load of 50 pounds should always be applied to angular contact bearing when rotating.
18. Install pulley and cable system at underside of housing for applying radial load to test bearing.

Test rig is now ready for use.

d. TEST SET-UP PROCEDURE

1. Install test bearing on shaft with outer race markings and strain gages facing shaft end. Warm bearing in oven to 200°F if necessary.
2. Assemble adapter sleeve\* and shaft nut and torque to 200 ft-lbs. (1 5/8 hex. nut). Hold Shaft against rotation at opposite end of spindle. Avoid applying bending load to shaft extension.
3. Preassemble all fittings and torque arms in housing and then assemble housing on outer race of test bearing. Strain gage locations on outer race to be in vertical and horizontal planes. Assemble (2) halves of Seal Plate, part 208C07 with scavenge tube connector in lower half. All 1/4 - 20 tapped holes on 4 3/4 B.C. to be plugged.
4. Assemble Amot Temperature Detector 4102 M - 174°F in holder and install in shaft end with retaining ring. Fill cavity with duct seal.
5. Install Spider assembly with (4) 1/4 - 20 socket head capscrews. Position spider to clear strain gages and to form shoulder for test bearing outer race. Be sure that spider contacts outer race uniformly at four places.
6. Attach Dillon load cell on end face of spider with cable connector vertically upward. Lucite sleeve can be placed over spider before cable is attached to load cell.
7. Install Bently probe and calibrate clearance gap with shaft sleeve.
8. Install Schrader micro valve and Alemite nozzle fitting #380791-6. Connect to constant pressure oil supply system set at 30 psig and 110°F. Spray nozzle to be located as shown on sketch. (45° upward at 6 o'clock position)
9. Apply 50 pound axial preload through Dillon load cell and calibrate readout. Check spindle assembly for free rotation by turning manually. Operate spindle to 8000 RPM and check vibration.
10. Install (2) housing thermocouples and ultrasonic translator. Conax fitting MPG-125 reworked to -156 is provided for translator mounting.

-----  
\* Adapter sleeve to be scribed for speed pickup.

APPENDIX F

TEST DATA

TEST LOCATION B-3 TAPE NO. 69 JOB \_\_\_\_\_ DATE 3/3/71

TEST CONDITIONS 8000 rpm 50 lb. Thrust Pitted

INPUT: ANALYZER: \_\_\_\_\_

TRANSDUCER Wilcoxon Accel. RANGE-V.RMS 0.316

CALIBRATOR \_\_\_\_\_ FREQUENCY-HZ 0-20 K x 4

AMPLIFIER 10 MV/G x 20 GAIN x 1 TIME AVERAGE 64

TAPE CHANNEL NO. 2  FM  DIR BY RFB

REORDERER: \_\_\_\_\_

GAIN 0.1 V/in

X-UNITS 0.80 K Hz

Y-UNITS Peak G's

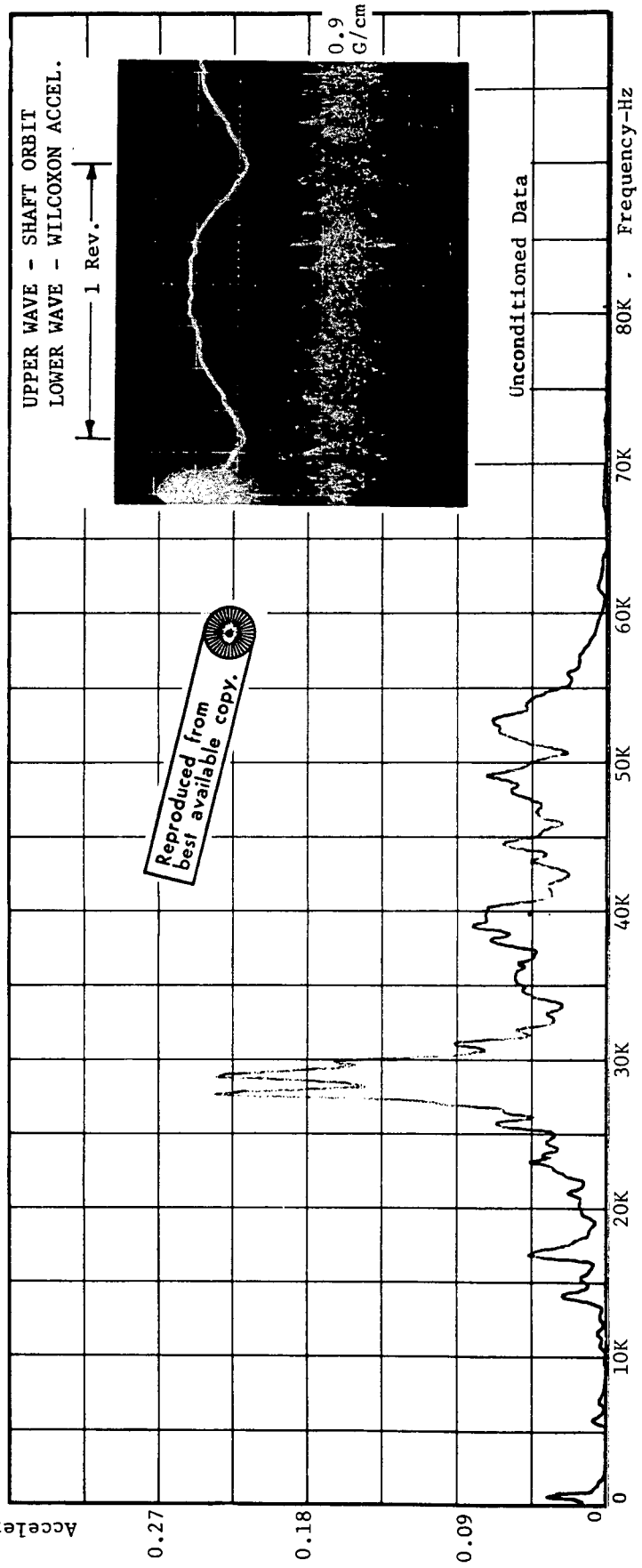


Fig. F-1 Radial Acceleration Spectrum, 50 lb. Thrust, 8000 rpm, Pitted

TEST LOCATION A-3 TAPE NO. 68 JOB            DATE 3/3/71

TEST CONDITIONS 8000 rpm 50 lb. Thrust Undamaged

INPUT: Wilcoxon Accel.

TRANSducer Wilcoxon Accel. ANALYZER: RANGE-V,RMS 0.316 RECORDER: GAIN 0.1 V/in

CALIBRATOR 10 MV/G x 100 FREQUENCY-HZ 0.20 K x 4 X-UNITS 0.80 K Hz

AMPLIFIER 10 MV/G x 100 GAIN x 1 Y-UNITS Peak G's

TAPE CHANNEL NO. 2  FM  DIR TIME AVERAGE 64 BY S RFB

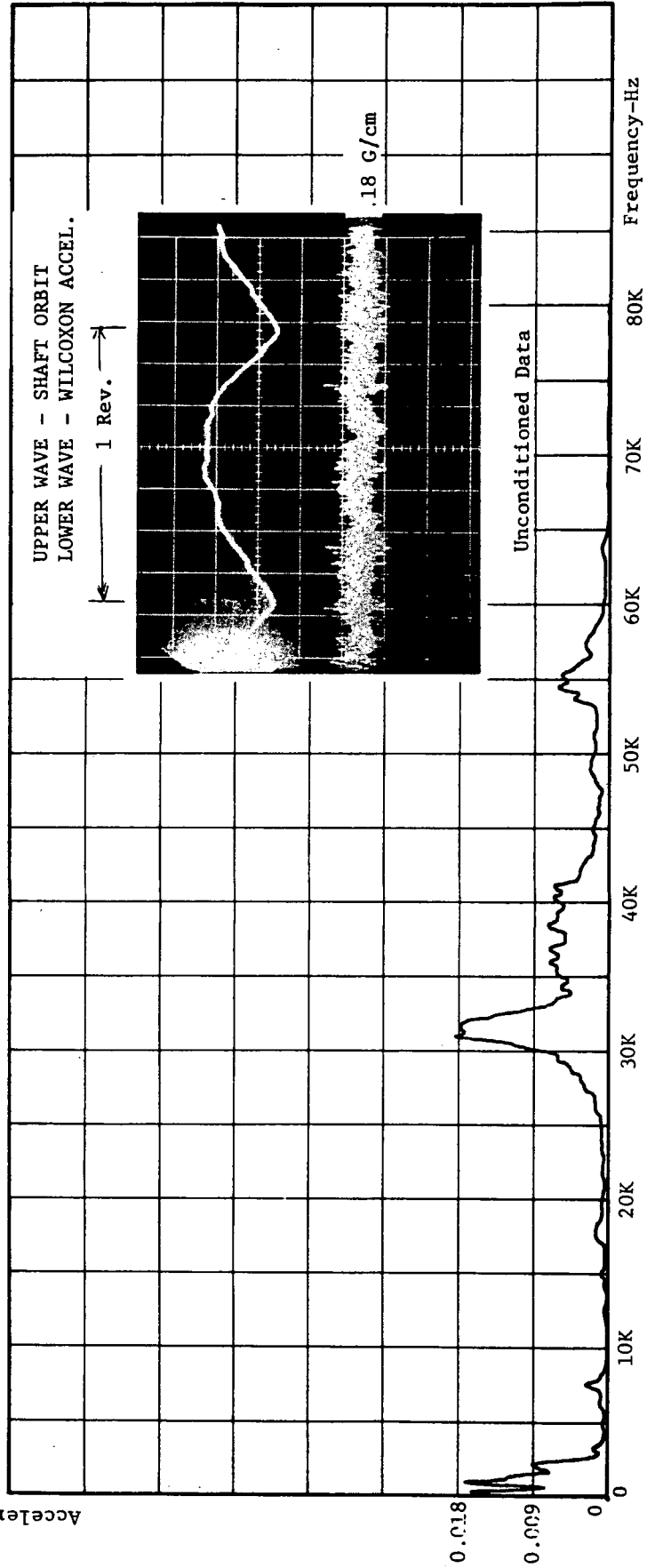


Fig. F-2 Radial Acceleration Spectrum, 50 lb. Thrust, 8000 rpm, Undamaged

TEST LOCATION B-2 TAPE NO. 69 JOB \_\_\_\_\_ DATE 10/11/71  
 TEST CONDITIONS 8000 rpm 50 lb. Thrust Damaged  
 INPUT: ANALYZER: RECORDER:  
 TRANSDUCER Wilcoxon Accel. RANGE-V,RMS 0.1 GAIN 0.5 V/in  
 CALIBRATOR \_\_\_\_\_ FREQUENCY-HZ 0 - 2 K X-UNITS 0 - 2 K Hz  
 AMPLIFIER 10 x 20 GAIN x 10 Y-UNITS \_\_\_\_\_  
 TAPE CHANNEL NO. 5  FM  DIR  RFB BY \_\_\_\_\_  
 TIME AVERAGE 32

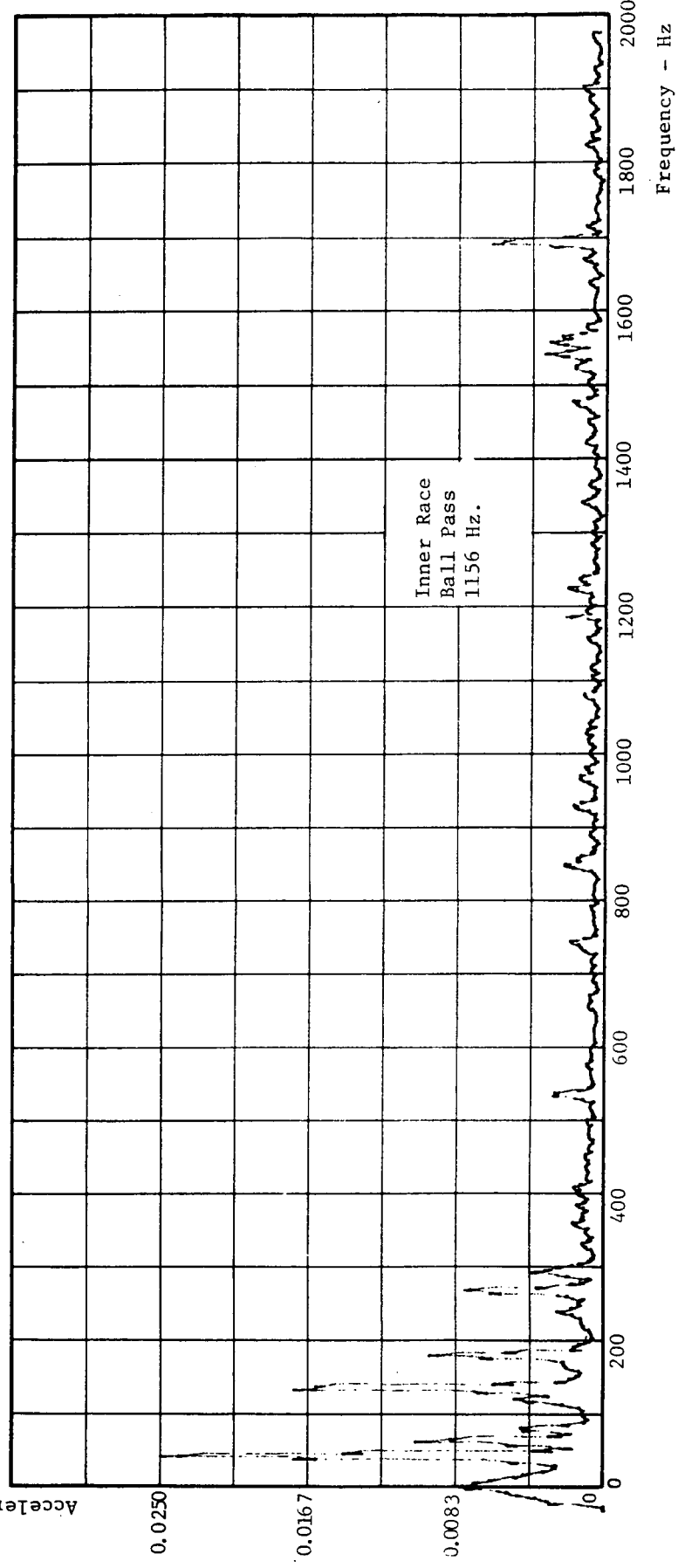


Fig. F-3 Radial Acceleration Spectrum, 50 lb. Thrust, 8000 rpm, Pitted

TEST LOCATION B-3 TAPE NO. 69 JOB \_\_\_\_\_ DATE 12/17/70  
 TEST CONDITIONS 8000 rpm 5016 Damaged  
 INPUT: \_\_\_\_\_  
 TRANSducer Wilcoxon/ Sine Conv. ANALYZER: \_\_\_\_\_  
 CALIBRATOR \_\_\_\_\_ RANGE-V,RMS 3.16 V REORDER: \_\_\_\_\_  
 AMPLIFIER \_\_\_\_\_ FREQUENCY-HZ 0 - 500 x 4 GAIN 0.5 V/in  
 TAPE CHANNEL NO. 2  FM  DIR TIME AVERAGE \_\_\_\_\_ X-UNITS 0 - 2000/Hz Y-UNITS \_\_\_\_\_  
 BY \_\_\_\_\_

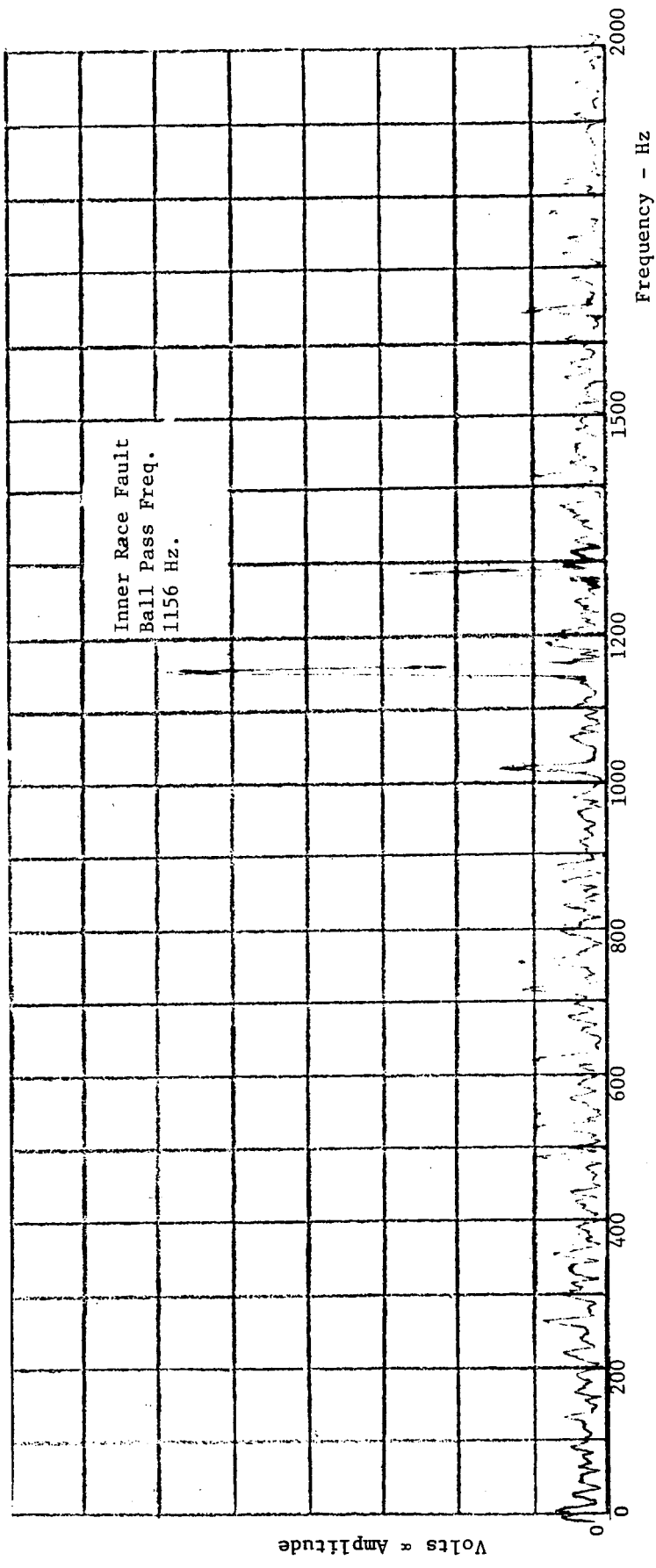


Fig. F-4 Radial Acceleration, Sine Converter Spectrum, 50 lb. Thrust, 8000 rpm, Pitted

TEST LOCATION D-3 TAPE NO. 68 JOB          DATE 12/17/70

TEST CONDITIONS 8000 rpm 50 lb.

INPUT:         

TRANSducer Wilcoxon/Sine Conv.

CALIBRATOR         

AMPLIFIER         

TAPE CHANNEL NO. 2  FM  DIR         

ANALYZER: RANGE-V.RMS 3.16 V RECORDER: GAIN 0.5 V/in

FREQUENCY-HZ 0 - 500 x 4 X-UNITS 0 - 2000 Hz

GAIN          Y-UNITS         

TIME AVERAGE          BY         

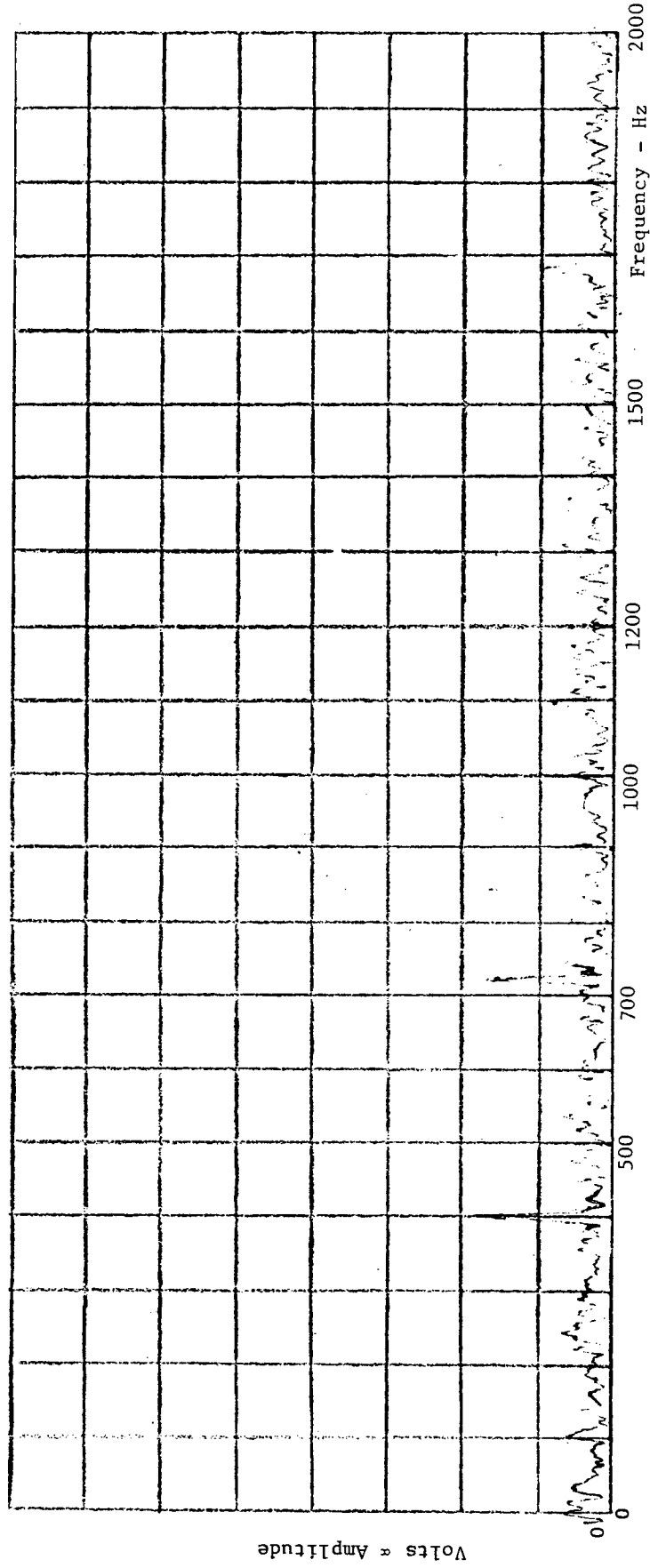


Fig. F-5 Radial Acceleration, Sine Converter Spectrum, 50 lb. Thrust, 8000 rpm, Undamaged

TEST LOCATION C-3 TAPE NO. 69 JOB          DATE 3/3/71  
 TEST CONDITIONS 8000 rpm 250 lb. Thrust Pitted  
 INPUT: ANALYZER:          RANGE V. RMS 0.316  
 TRANSDUCER Wilcoxon Accel. FREQUENCY-HZ 0 - 20 K x 4  
 CALIBRATOR          GAIN x 1 Y-UNITS Peak G's  
 AMPLIFIER 10 MV/G x 20 TIME AVERAGE 64 BY RFB  
 TAPE CHANNEL NO. 2  FM  DIR

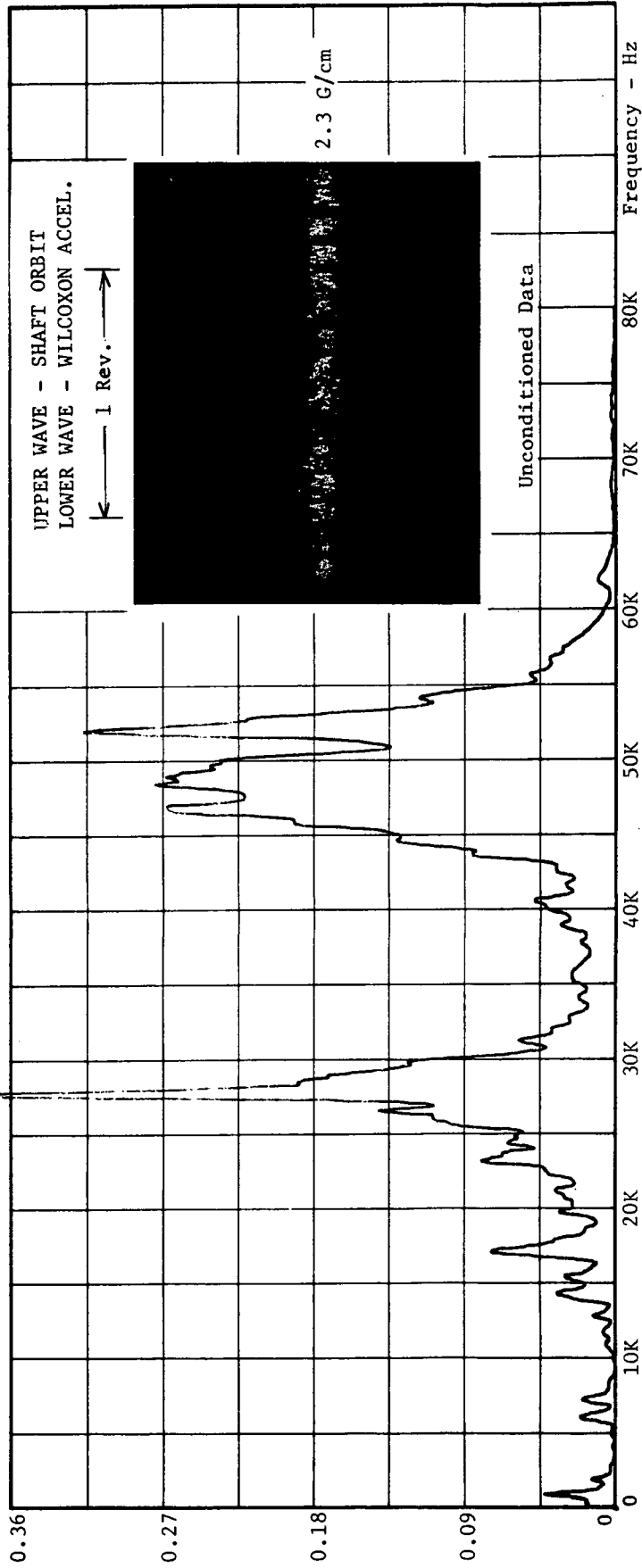


Fig. F-6 Radial Acceleration Spectrum, 250 lb. Thrust, 8000 rpm, Pitted

TEST LOCATION F-3 TAPE NO. 73 JOB 73 DATE 3/3/71

TEST CONDITIONS 8000 rpm 1000 lb. Thrust Pitted

INPUT: ANALYZER: RECORDER:  
 TRANSducer Wilcoxon Accel. RANGE-V, RMS 0.316 GAIN 0.1 V/in  
 CALIBRATOR 10 MV/G x 10 FREQUENCY-HZ 0 - 20 K x 4 X-UNITS 0 - 80 K Hz  
 AMPLIFIER 10 MV/G x 10 GAIN 64 Y-UNITS Peak G's  
 TAPE CHANNEL NO. 2  FM  DIR BY RFB

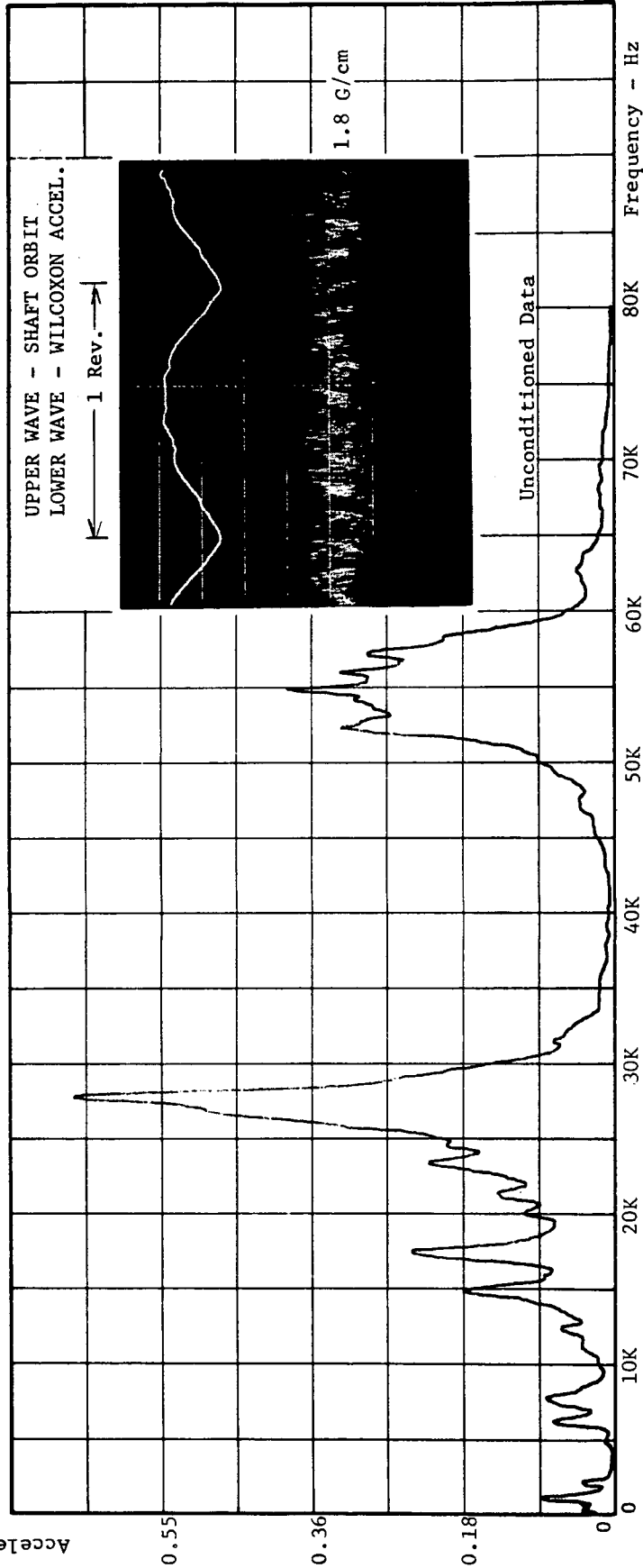


Fig. F-7 Radial Acceleration Spectrum, 1000 lb. Thrust, 8000 rpm, Pitted

TEST LOCATION C-2 TAPE NO. 69 JOB \_\_\_\_\_ DATE 10/11/71  
 TEST CONDITIONS 8000 rpm 250 lb. Thrust Damaged  
 INPUT: \_\_\_\_\_  
 TRANSDUCER Wilcoxon Accel. ANALYZER: \_\_\_\_\_  
 CALIBRATOR \_\_\_\_\_ RANGE-V,RMS 0.1 RECORDER: \_\_\_\_\_  
 AMPLIFIER 10 x 20 FREQUENCY-HZ 0 - 2 K GAIN 0.5 V/12  
 TAPE CHANNEL NO. 5  FM  DIR  TIME AVERAGE 32 X-UNITS 0 - 2 K Hz  
 Y-UNITS \_\_\_\_\_ BY RFB

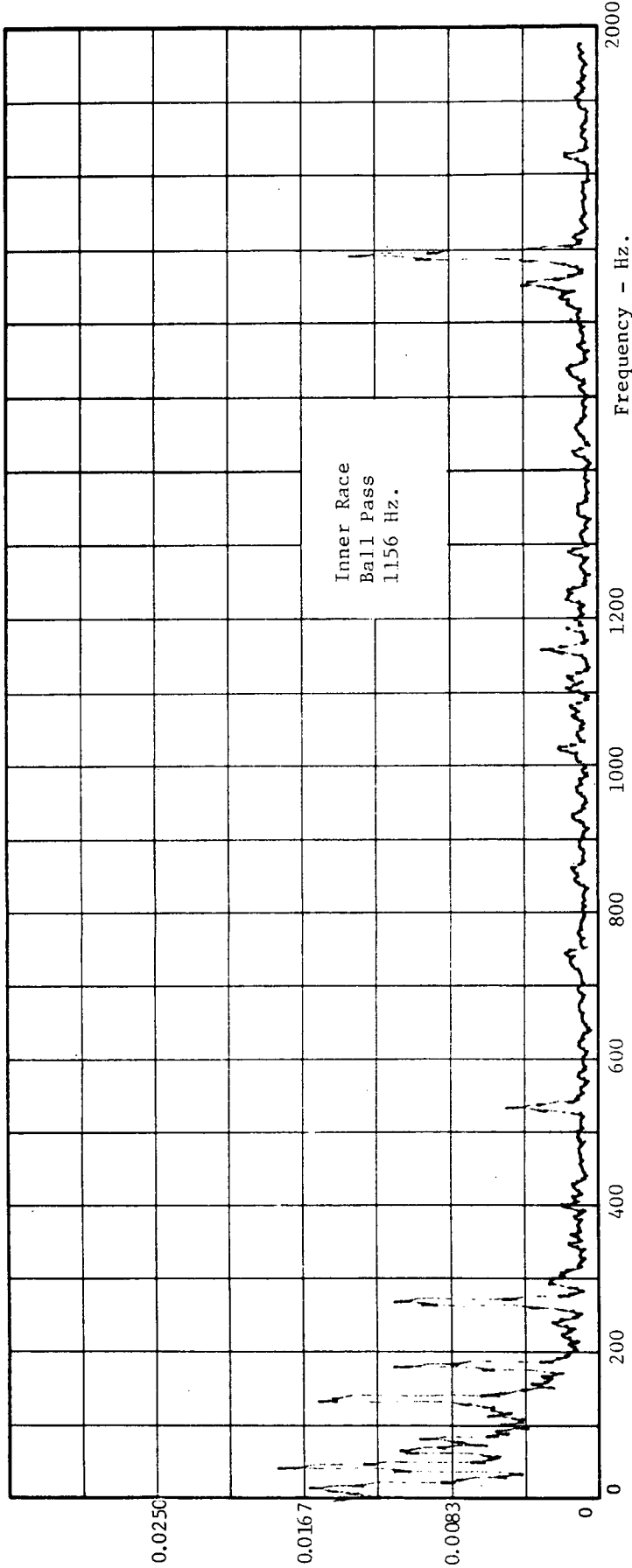


Fig. F-8 Radial Acceleration Spectrum, 250 lb. Thrust, 8000 rpm, Pitted

TEST LOCATION F-2 TAPE NO. 73 JOB \_\_\_\_\_ DATE 10/11/71

TEST CONDITIONS 8000 rpm 1000 lb Thrust Damaged

INPUT: TRANSducer Wilcoxon Acce1 ANALYZER: RANGE-V,RMS 0.1 RECORDER: GAIN 0.5 V/in

CALIBRATOR \_\_\_\_\_ FREQUENCY-HZ 0 - 2 K X-UNITS 0 - 2 K Hz

AMPLIFIER 10 x 10 GAIN x 10 Y-UNITS \_\_\_\_\_

TAPE CHANNEL NO. 5  FM  DIR TIME AVERAGE 32 BY RFB

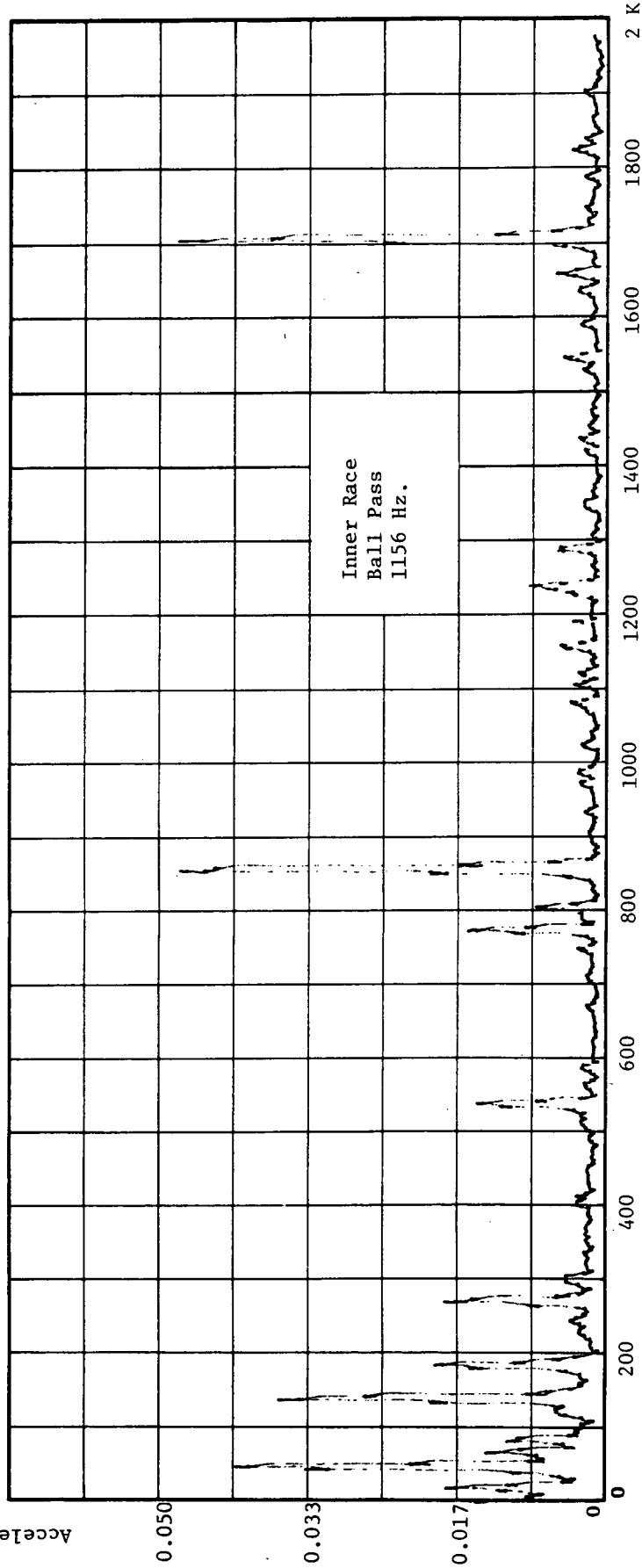


Fig. F-9 Radial Acceleration Spectrum, 1000 lb. Thrust, 8000 rpm, Pitted

TEST LOCATION B-3 TAPE NO. 68 JOB 3/3/71  
 TEST CONDITIONS 8000 rpm 250 lb. Thrust Undamaged  
 INPUT: ANALYZER: RANGE-V,RMS 0.316  
 TRANSDUCER Wilcoxon Accel. FREQUENCY-HZ 0 - 20 K x 4  
 CALIBRATOR 10 MV/G x 100 GAIN x 1  
 AMPLIFIER 2  FM  DIR TIME AVERAGE 64  
 TAPE CHANNEL NO. 2 BY RFB

REORDER: GAIN 0.1 V/in  
 X-UNITS 0.80 K  
 Y-UNITS Peak G's

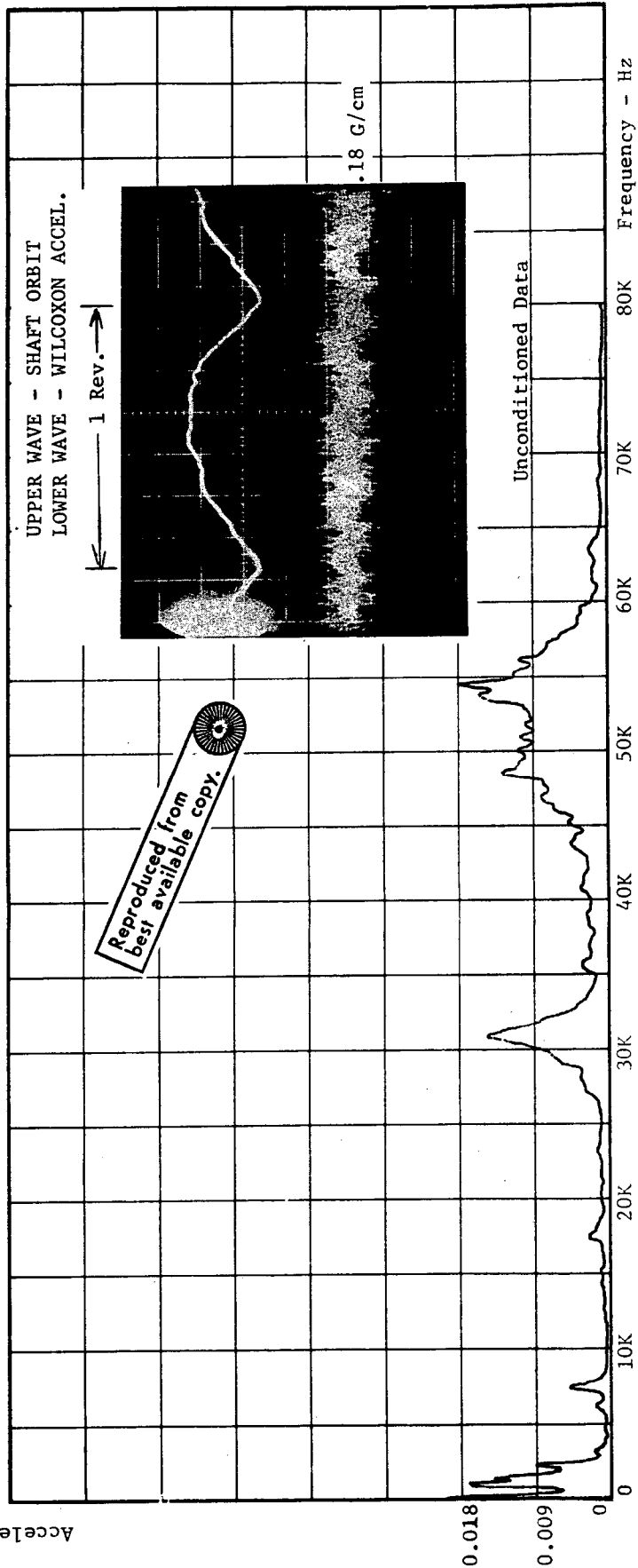


Fig. F-10 Radial Acceleration Spectrum, 250 lb. Thrust, 8000 rpm, Undamaged

TEST LOCATION C-3 TAPE NO. 68 JOB \_\_\_\_\_ DATE 3/3/71  
 TEST CONDITIONS 8000 rpm 1000 lb Thrust Undamaged  
 INPUT: \_\_\_\_\_  
 TRANSDUCER Wilcoxon Accel. ANALYZER: \_\_\_\_\_  
 CALIBRATOR 10 MV/G x 100 RANGE-V.RMS 0.316  
 AMPLIFIER \_\_\_\_\_ FREQUENCY-HZ 0 - 20 K x 4  
 TAPE CHANNEL NO. 2  FM  DIR GAIN x 1 TIME AVERAGE 64  
 RECORDED: \_\_\_\_\_  
 GAIN 0.1 V/in  
 X-UNITS 0 - 80 K Hz  
 Y-UNITS Peak G's  
 BY RFB

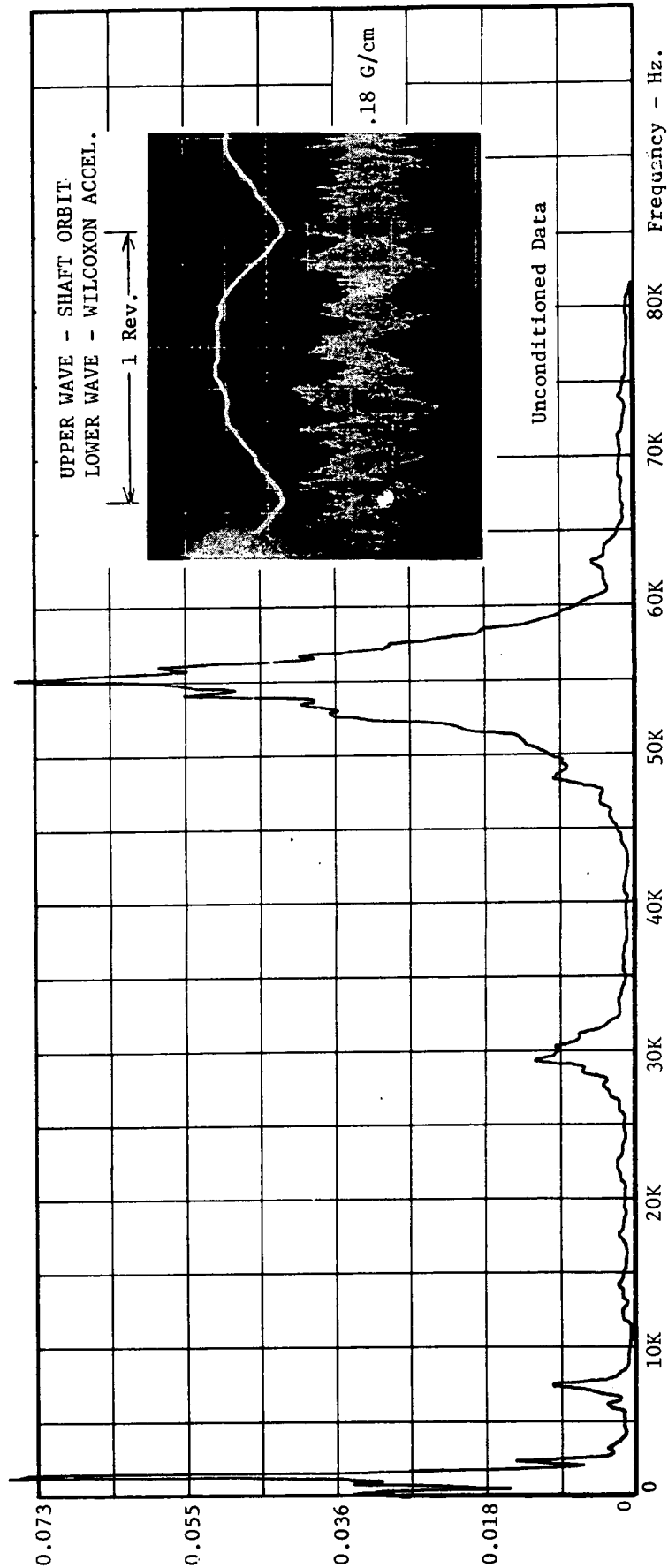


Fig. F-11 Radial Acceleration Spectrum, 1000 lb. Thrust, 8000 rpm, Undamaged

Acceleration G's Peak

TEST LOCATION A-2 TAPE NO. 68 JOB \_\_\_\_\_ DATE 10/11/71  
TEST CONDITIONS 50 lb Thrust 8000 rpm Undamaged  
INPUT: \_\_\_\_\_ ANALYZER: \_\_\_\_\_ RECORDER: \_\_\_\_\_  
TRANSDUCER Wilcoxon Accl. RANGE-V,RMS 0 - 1 GAIN 1.0 V/in  
CALIBRATOR \_\_\_\_\_ FREQUENCY-HZ 0 - 2 K X-UNITS 0 - 2 K Hz  
AMPLIFIER 10 x 500 GAIN x 1 Y-UNITS \_\_\_\_\_  
TAPE CHANNEL NO. 5  FM  DIR TIME AVERAGE 32 BY RFB

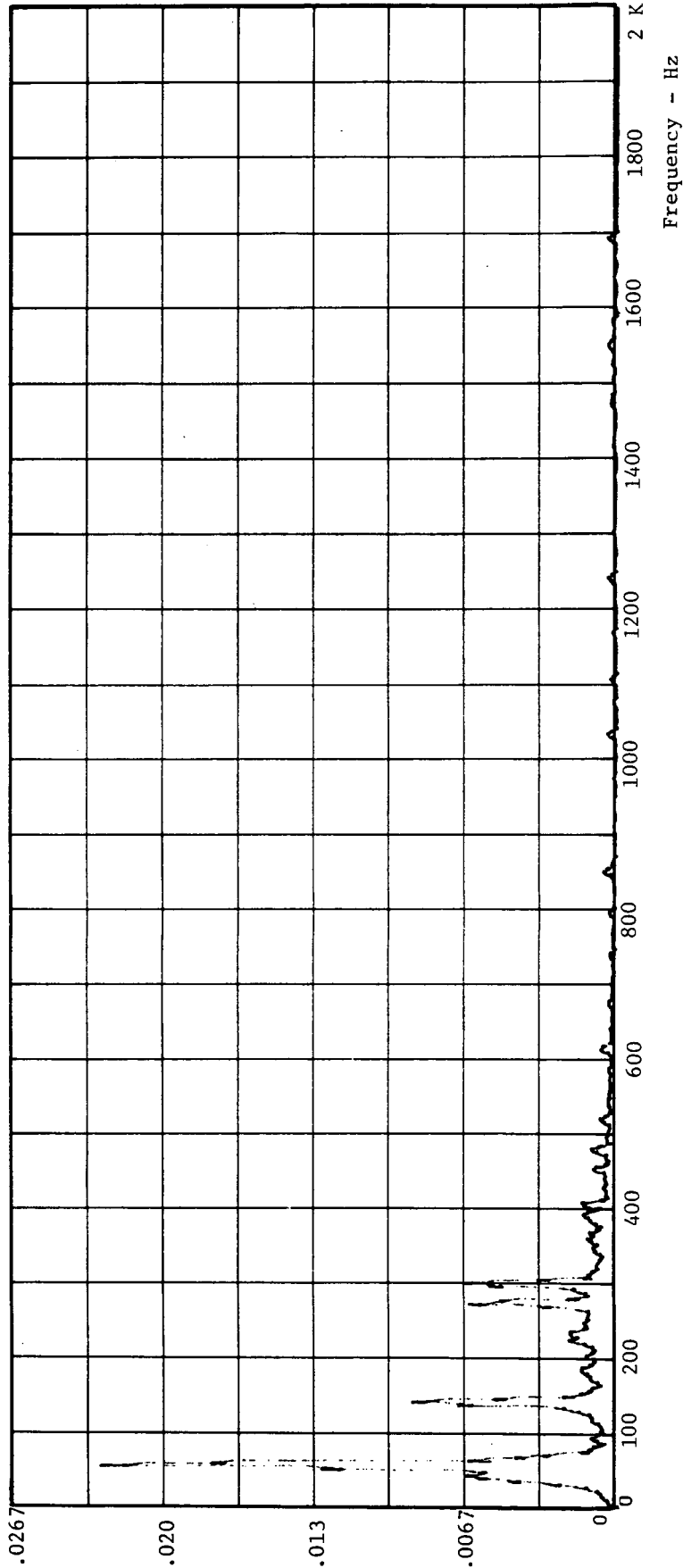


Fig. F-12 Radial Acceleration Spectrum, 50 lb. Thrust, 8000 rpm, Undamaged

Acceleration G's Peak

TEST LOCATION B-2 TAPE NO. 68 JOB \_\_\_\_\_ DATE 10/11/71  
TEST CONDITIONS 250 lb. Thrust 8000 rpm Undamaged  
INPUT: ANALYZER: REORDER:  
TRANSDUCER Wilcoxon Acceleration RANGE V.RMS 0.1 GAIN 1.0  
CALIBRATOR 10 x 100 FREQUENCY:HZ 0 - 2 K X-UNITS 0 - 2K Hz  
AMPLIFIER \_\_\_\_\_ GAIN x 1 Y-UNITS \_\_\_\_\_  
TAPE CHANNEL NO. \_\_\_\_\_  FM  DIR TIME AVERAGE 32 BY RFB

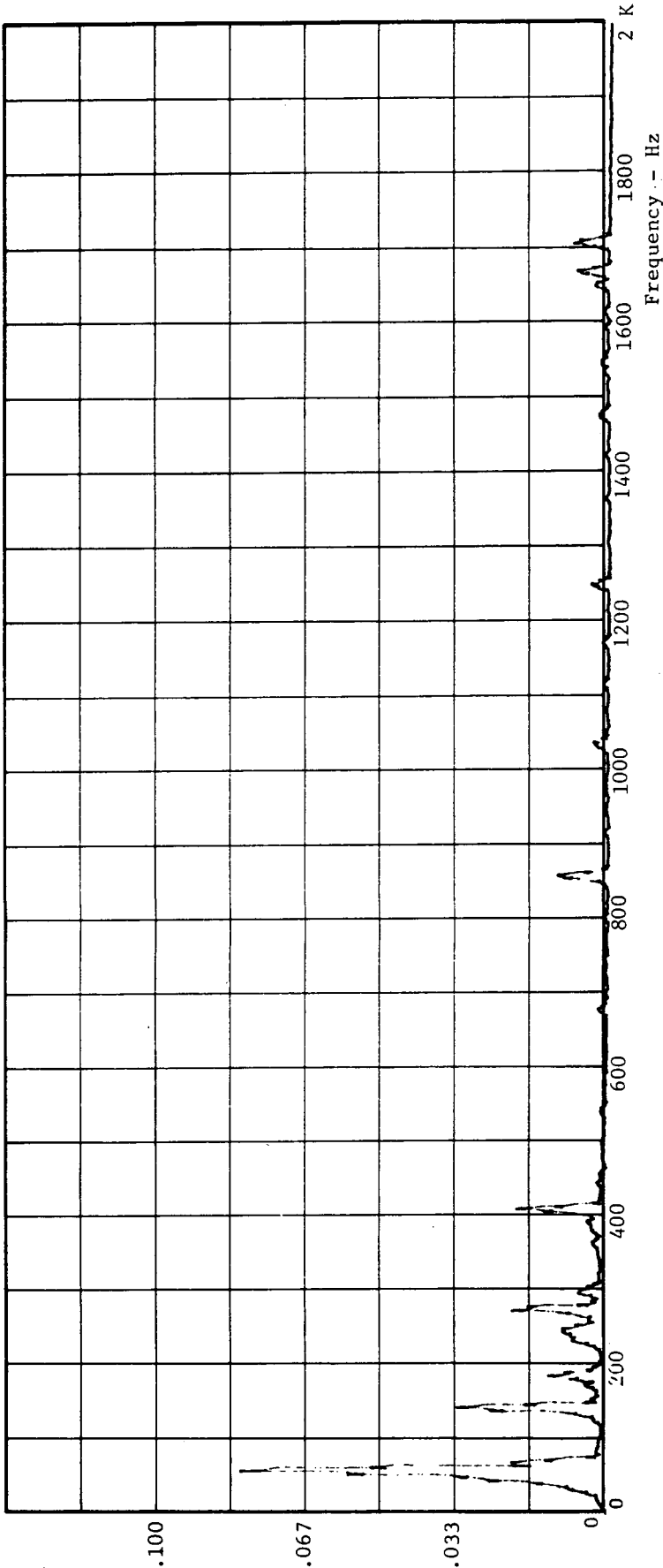


Fig. F-13 Radial Acceleration Spectrum, 250 lb. Thrust, 8000 rpm, Undamaged

TEST LOCATION C-2 TAPE NO. 68 JOB \_\_\_\_\_ DATE 10/11/71  
 TEST CONDITIONS 1000 lb Thrust 8000 rpm Undamaged  
 INPUT: \_\_\_\_\_ ANALYZER: \_\_\_\_\_  
 TRANSDUCER Wilcoxon Accel. RANGE-V,RMS 0.1 RECORDER: \_\_\_\_\_  
 CALIBRATOR \_\_\_\_\_ FREQUENCY-HZ 0 2 K Hz GAIN 1.0 V/in  
 AMPLIFIER 10 x 100 GAIN x 1 X-UNITS 0 - 2 K Hz  
 TAPE CHANNEL NO. 5  FM  DIR TIME AVERAGE 32 Y-UNITS \_\_\_\_\_  
 BY RFB

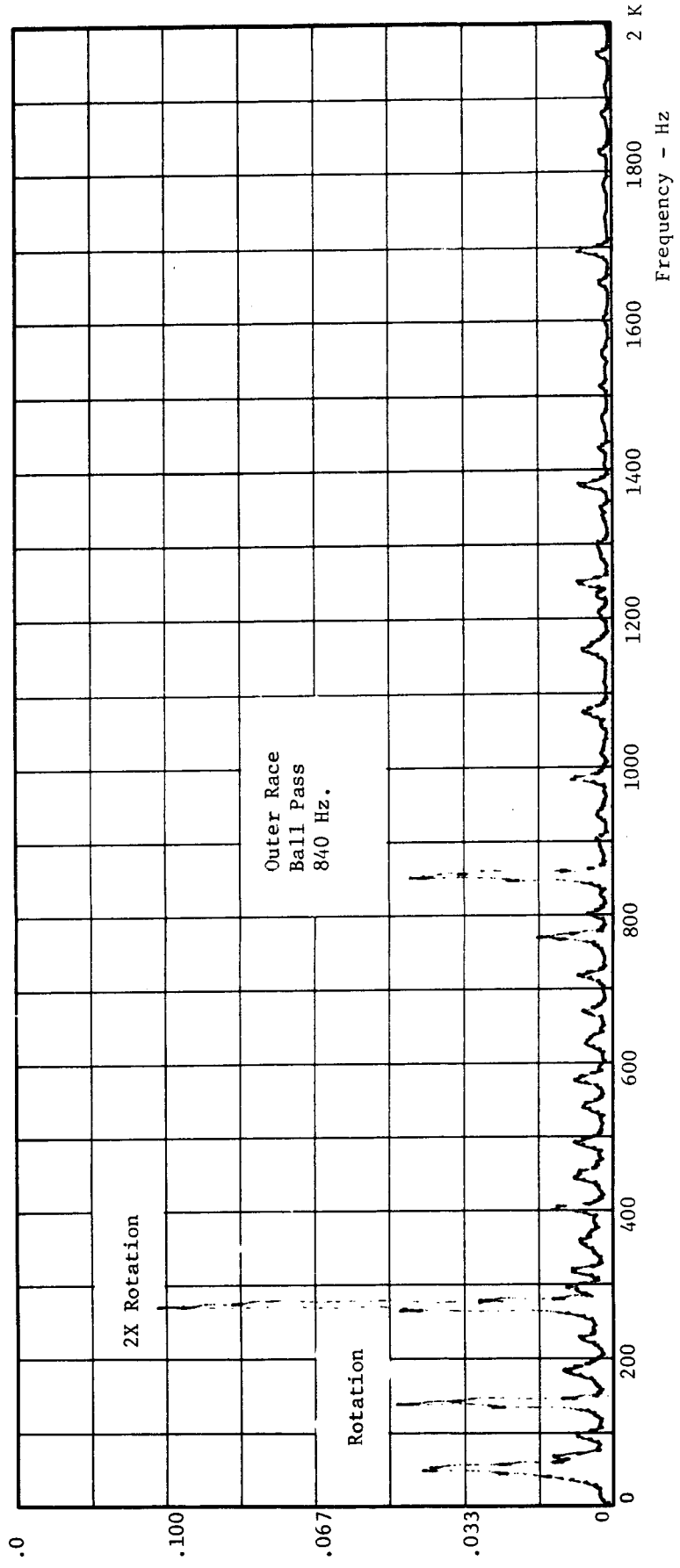


Fig. F-14 Radial Acceleration Spectrum, 1000 lb. Thrust, 8000 rpm, Undamaged

TEST LOCATION A-3 TAPE NO. 69 JOB          DATE 3/3/71

TEST CONDITIONS 6000 rpm 50 lb Thrust Pitted

INPUT: TRANSUCER Wilcoxon Accel. ANALYZER: RANGE-V,RMS 0.316 RECORDER: GAIN 0.1 V/in

CALIBRATOR          FREQUENCY-HZ 0 - 20 K x 4 X-UNITS 0 - 80 K Hz

AMPLIFIER 10 MV/G x 20 GAIN x 1 Y-UNITS Peak G's

TAPE CHANNEL NO. 2  FM  DIR TIME AVERAGE 64 BY RFB

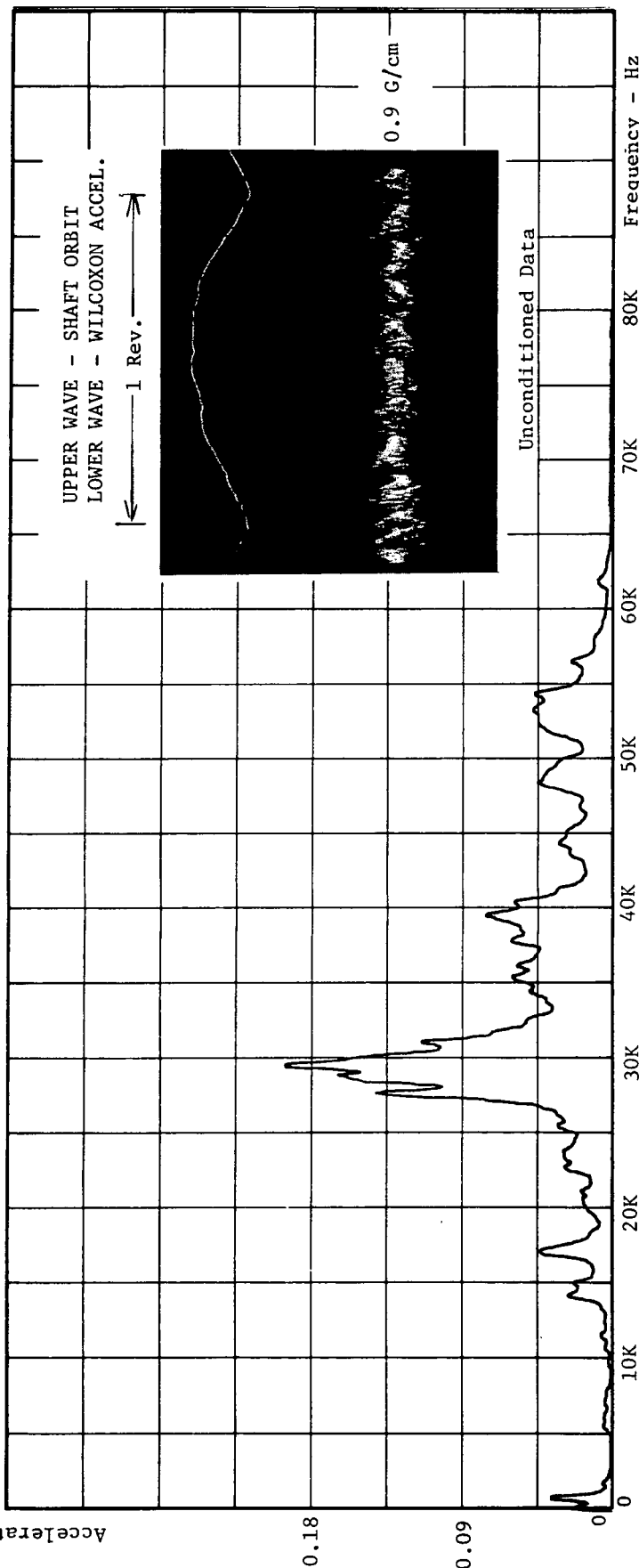


Fig. F-15 Radial Acceleration Spectrum, 50 lb. Thrust, 6000 rpm, Pitted

TEST LOCATION D-3 TAPE NO. 73 JOB \_\_\_\_\_ DATE 3/3/71  
 TEST CONDITIONS 6000 rpm 250 lb Thrust Pitted  
 INPUT: ANALYZER: \_\_\_\_\_  
 TRANSDUCER Wilcoxon Accl. RANGE V.RMS 0.316  
 CALIBRATOR \_\_\_\_\_ FREQUENCY-HZ 0 - 20 K x 4  
 AMPLIFIER 10 MV/G x 20 GAIN x 1  
 TAPE CHANNEL NO. 2  FM  DIR TIME AVERAGE 64  
 RECORDED: \_\_\_\_\_  
 GAIN 0.1 V/in  
 X-UNITS 0 - 80 K  
 Y-UNITS Peak G's  
 BY RFB

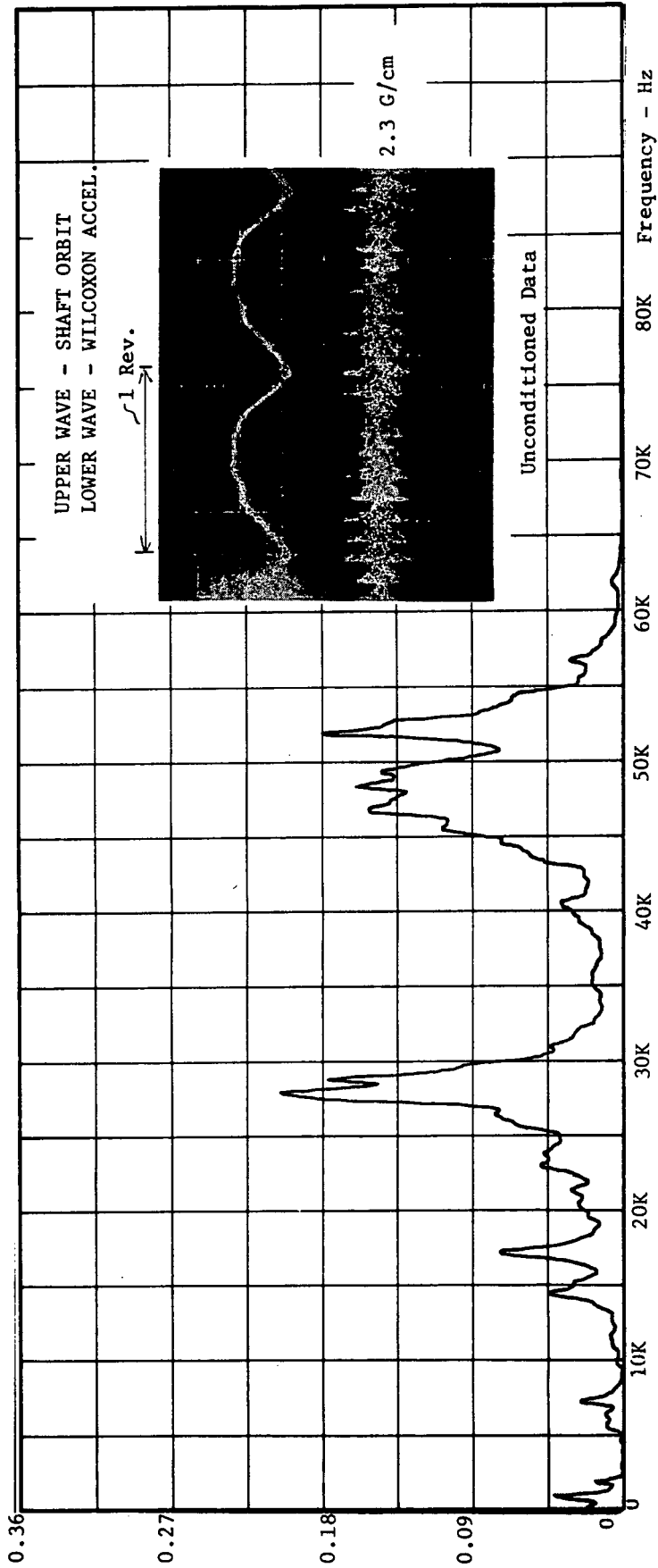


Fig. F-16 Radial Acceleration Spectrum, 250 lb. Thrust, 6000 rpm, Pitted

TEST LOCATION E-3 TAPE NO. 73 JOB          DATE 3/3/71

TEST CONDITIONS 6000 rpm 1000 lb Thrust Pitted

INPUT: TRANSUCER Wilcoxon Accel. ANALYZER: RANGE-V,RMS 0.316 RECORDER: GAIN 0.1 V/in

CALIBRATOR 10 MV/G x 10 FREQUENCY-HZ 0 - 20 K x 4 X-UNITS 0 - 80 K Hz

AMPLIFIER          GAIN x 1 Y-UNITS Peak G's

TAPE CHANNEL NO. 2  FM  DIR TIME AVERAGE 64 BY RFB

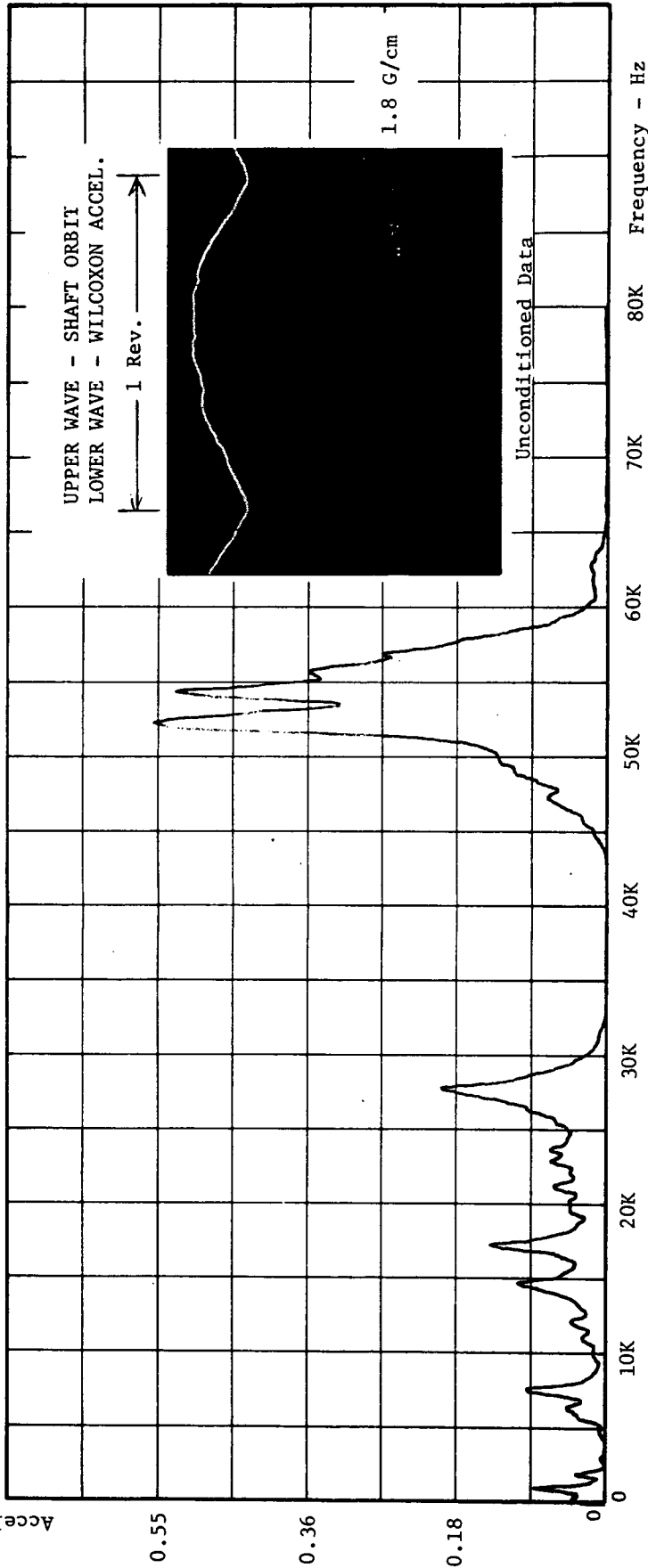


Fig. F-17 Radial Acceleration Spectrum, 1000 lb. Thrust, 6000 rpm, Pitted

TEST LOCATION A-2      TAPE NO. 69      DATE 10/11/71  
 TEST CONDITIONS 6000 rpm 50 lb Thrust      Damaged      JOB \_\_\_\_\_  
 INPUT: \_\_\_\_\_  
 TRANSDUCER Wilcoxon Accl.      ANALYZER: \_\_\_\_\_  
 RANGE-V,RMS 0.1  
 CALIBRATOR 10 x 20      FREQUENCY-HZ 0 - 2 K  
 AMPLIFIER \_\_\_\_\_      GAIN x 10  
 X-UNITS 0 - 2 K Hz  
 Y-UNITS \_\_\_\_\_  
 TAPE CHANNEL NO. 5       FM       DIR      TIME AVERAGE 32  
 BY RFB

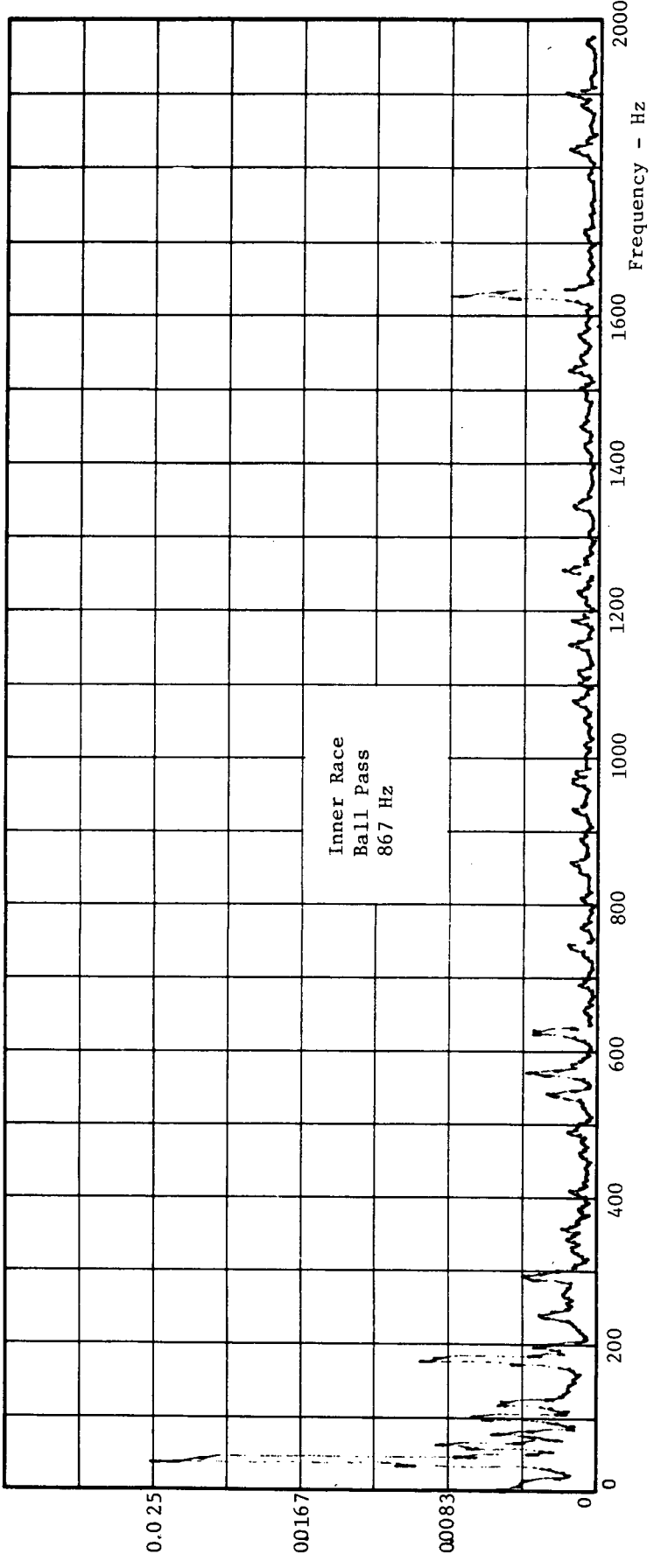


Fig. F-18 Radial Acceleration Spectrum, 50 lb. Thrust, 6000 rpm, Pitted

TEST LOCATION E-3 TAPE NO. 68 JOB Undamaged DATE 3/31/71

TEST CONDITIONS 6000 rpm 50 lb Thrust

INPUT: TRANSDUCER Wilcoxon Accel. ANALYZER: RANGE-V,RMS 0.316 RECORDER: GAIN 0.1 V/in

CALIBRATOR 10 MV/G x 200 FREQUENCY-HZ 0 - 20 K x 4 X-UNITS 0 - 80 K Hz

AMPLIFIER 10 MV/G x 200 GAIN x 1 Y-UNITS Peak G's

TAPE CHANNEL NO. 2  FM  DIR TIME AVERAGE 64 BY RFB

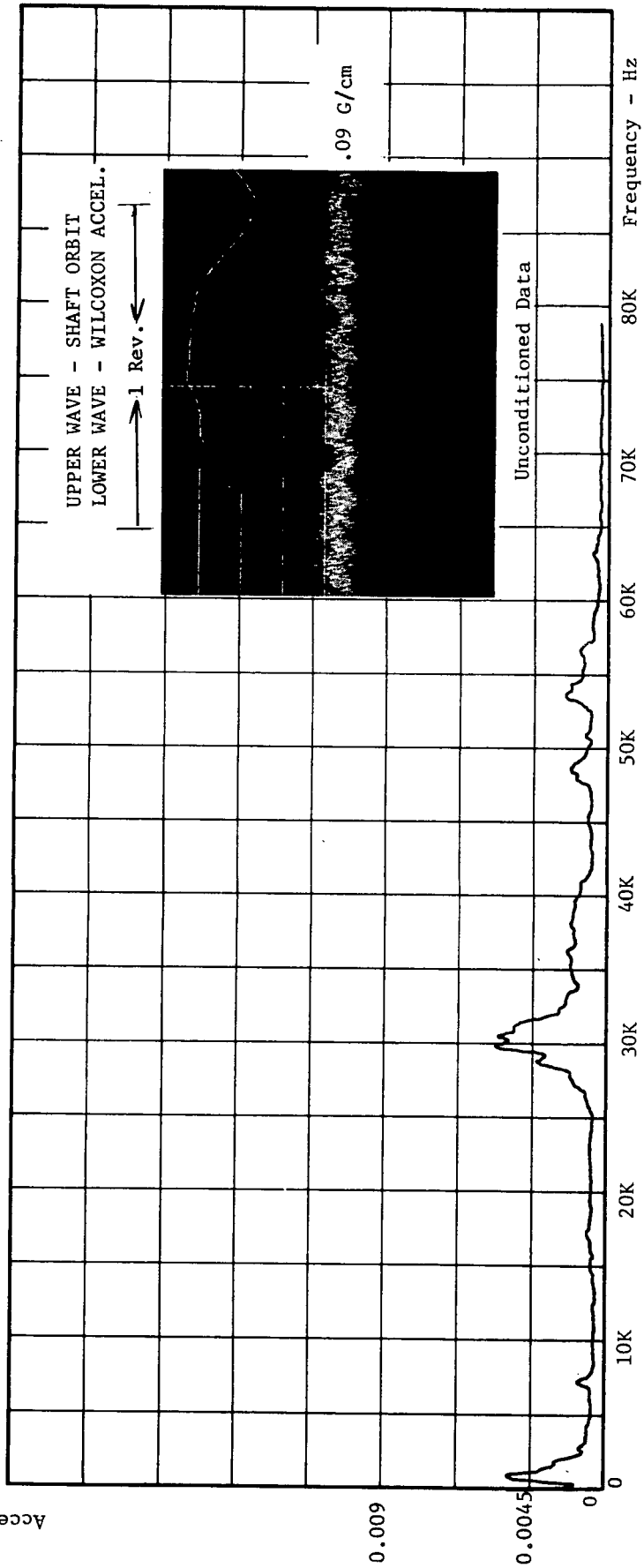


Fig. F-19 Radial Acceleration Spectrum, 50 lb. Thrust, 6000 rpm, Undamaged

TEST LOCATION E-2 TAPE NO. 68 JOB          DATE 10/11/71  
 TEST CONDITIONS 50 lb Thrust 6000 rpm Undamaged  
 INPUT:          ANALYZER:          RECORDER:           
 TRANSDUCER Willcoxon Accel. RANGE-V,RMS 0.1 GAIN 0.5 V/in  
 CALIBRATOR          FREQUENCY-HZ 0 - 2 K X-UNITS 0 - 2 K Hz  
 AMPLIFIER 10 x 200 GAIN x 1 Y-UNITS           
 TAPE CHANNEL NO. 5  FM  DIR TIME AVERAGE 32 BY RFB

Acceleration G's Peak

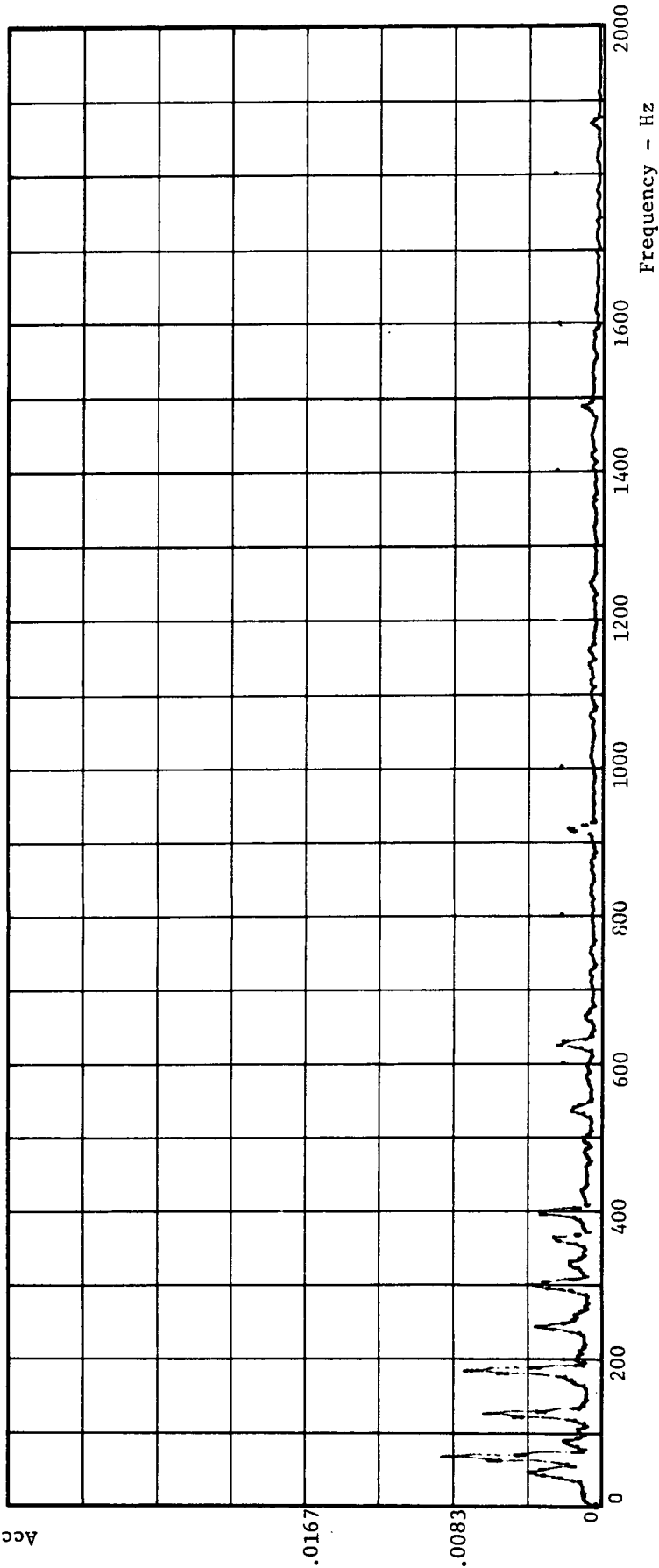


Fig. F-20 Radial Acceleration Spectrum, 50 lb. Thrust, 6000 rpm, Undamaged

TEST LOCATION A-3 TAPE NO. 68 JOB \_\_\_\_\_ DATE 2/23/71

TEST CONDITIONS 8000 rpm 50 lb Before

INPUT: \_\_\_\_\_

TRANSDUCER Wilcoxon - Fault Det. ANALYZER: \_\_\_\_\_

CALIBRATOR \_\_\_\_\_ RANGE V.RMS 1.0

AMPLIFIER 10 MV/G x 100 x .58 FREQUENCY-HZ 0 - 2 K GAIN x 1 X-UNITS 0 - 2 K Y-UNITS \_\_\_\_\_

TAPE CHANNEL NO. 2  FM  DIR TIME AVERAGE no BY RFB

RECORDER: \_\_\_\_\_

GAIN 0.2 V/in

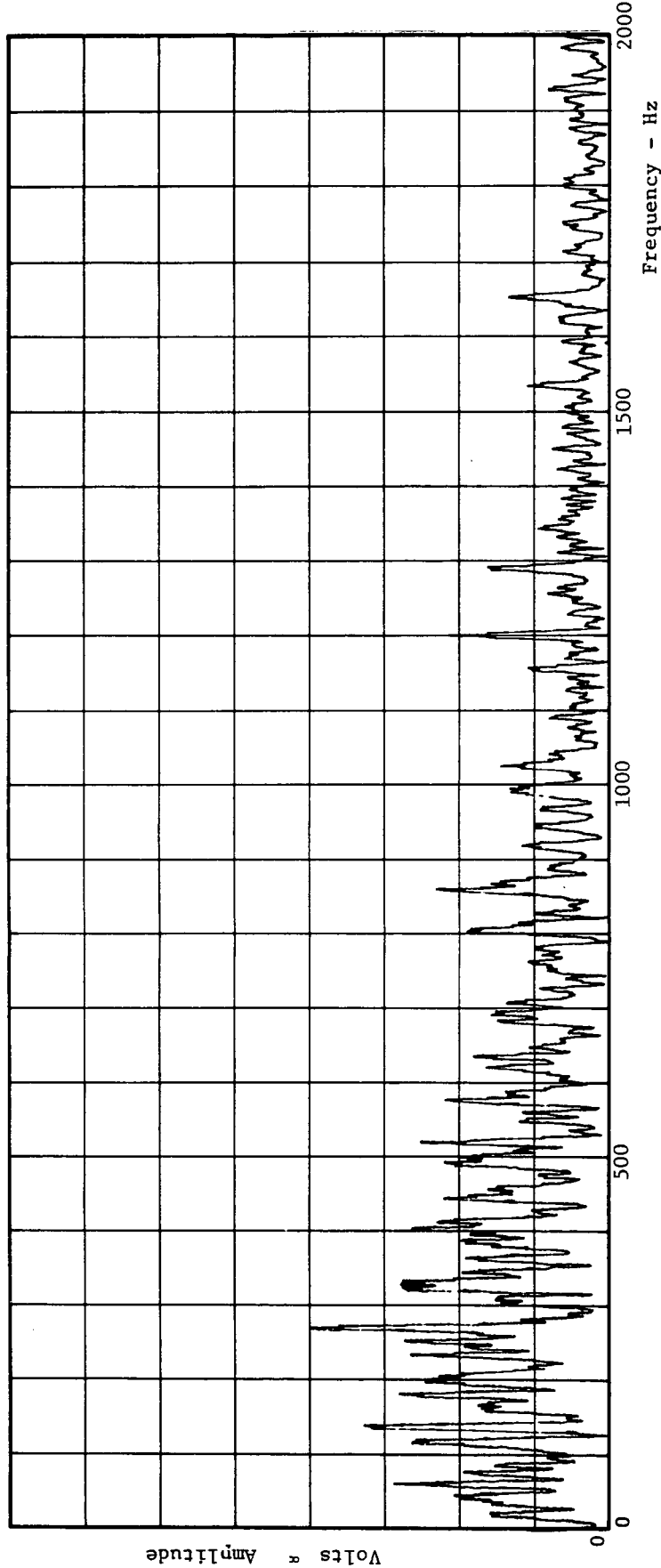


Fig. F-21 Fault Detector Frequency Spectrum, 50 lb. Thrust, 8000 rpm, New Bearing

TEST LOCATION B-3 TAPE NO. 69 JOB \_\_\_\_\_ DATE 2/23/71  
 TEST CONDITIONS 8000 rpm 50 lb Damaged  
 INPUT: \_\_\_\_\_  
 TRANSDUCER Wilcoxon - Fault Det.  
 CALIBRATOR \_\_\_\_\_  
 ANALYZER: RANGE-V,RMS 10 V RECORDER: GAIN 0.2 V/in  
 FREQUENCY-HZ 0 - 2 K X-UNITS 0 - 2 K Hz  
 AMPLIFIER 10 MV/G x 20 GAIN x 1 Y-UNITS \_\_\_\_\_  
 TAPE CHANNEL NO. 2  FM  DIR TIME AVERAGE no BY RFB

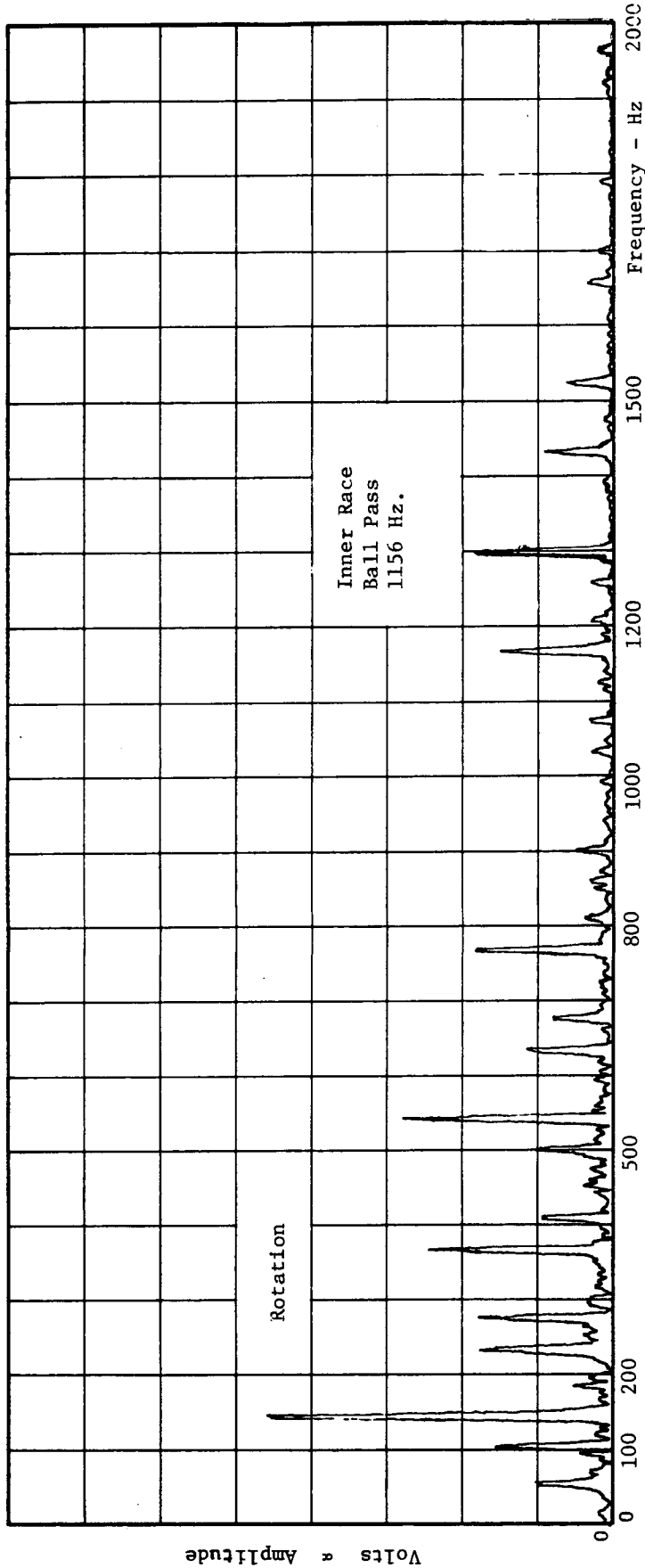


Fig. F-22 Fault Detector Frequency Spectrum, 50 lb. Thrust, 8000 rpm, Pitted

TEST LOCATION E-3 TAPE NO. 68 JOB \_\_\_\_\_ DATE 2/23/71

TEST CONDITIONS 6000 rpm 50 lb Before Fault

INPUT: ANALYZER: RTA

TRANSDUCER Wilcoxon - Fault Det. RANGE V.RMS 1.0 RECORDER: GAIN 0.2

CALIBRATOR \_\_\_\_\_ FREQUENCY-HZ 0 - 2 K X-UNITS 0 - 2 K

AMPLIFIER 10 MV/G x 200 GAIN x 1 Y-UNITS \_\_\_\_\_

TAPE CHANNEL NO. 2  FM  DIR  TIME AVERAGE no BY RFB

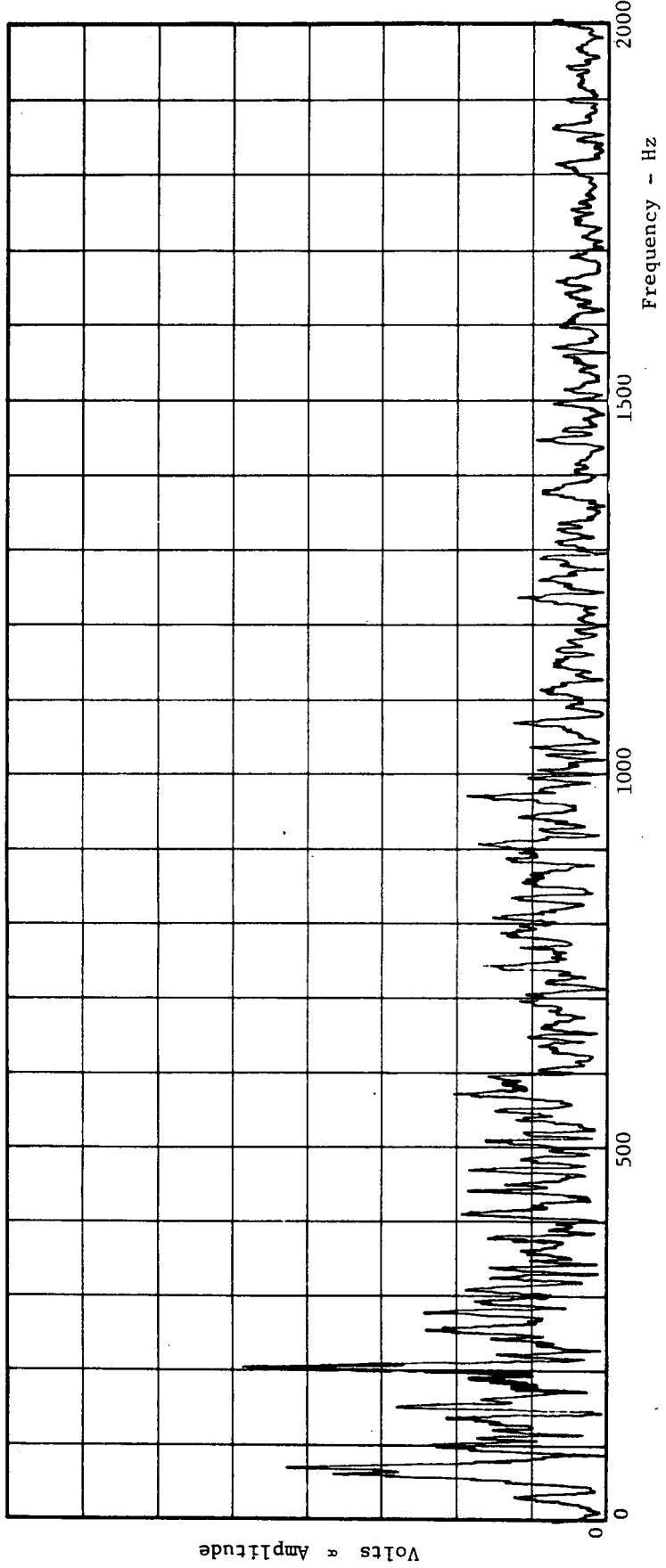


Fig. F-23 Fault Detector Frequency Spectrum, 50 lb. Thrust, 6000 rpm, New Bearing, Undamaged

TEST LOCATION A-3 TAPE NO. 65 JOB \_\_\_\_\_ DATE 2/23/71  
 TEST CONDITIONS 6000 rpm 50 lb Damaged  
 INPUT: \_\_\_\_\_ ANALYZER: RTA RECORDER: \_\_\_\_\_  
 TRANSducer Wilcoxon - Fault Det. RANGE-V,RMS 10 V GAIN 0.2 V/in  
 CALIBRATOR \_\_\_\_\_ FREQUENCY-HZ 0 - 2 K X-UNITS 0 - 2 K  
 AMPLIFIER 10 MV/G x 20 GAIN x 1 Y-UNITS \_\_\_\_\_  
 TAPE CHANNEL NO. 2  FM  DIR TIME AVERAGE no BY RFB

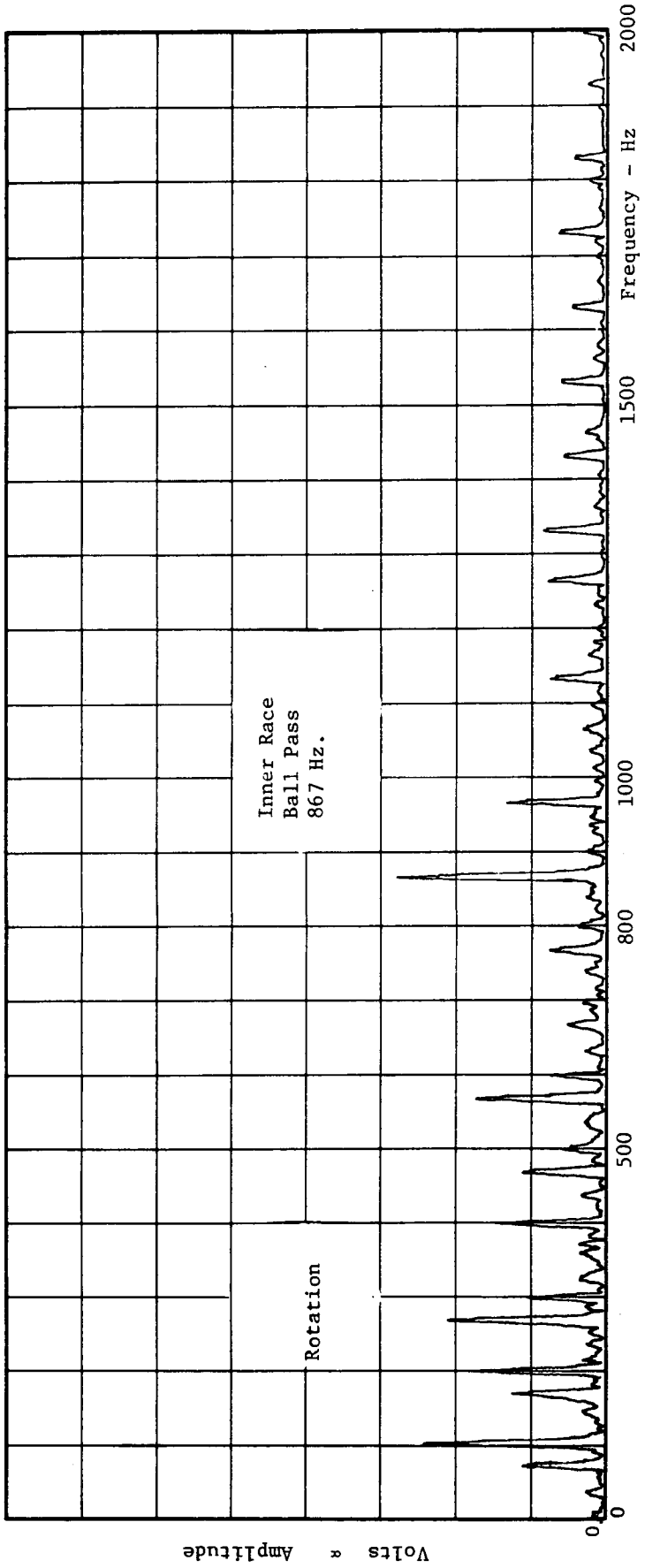


Fig. F-24 Fault Detector Frequency Spectrum, 50 lb. Thrust, 6000 rpm, Pitted

TEST LOCATION C-3 TAPE NO. 69 JOB \_\_\_\_\_ DATE 10/27/71

TEST CONDITIONS 8000 rpm 250 lb Thrust Damaged

INPUT: ANALYZER: \_\_\_\_\_

TRANSDUCER Wilcoxon/Fault Det. RANGE-V,RMS 10.0 RECORDER: \_\_\_\_\_

CALIBRATOR \_\_\_\_\_ FREQUENCY-HZ 0 - 2 K GAIN 0.2 V/in

AMPLIFIER x 20 GAIN x 1 X-UNITS 0 - 2 K Hz Y-UNITS \_\_\_\_\_

TAPE CHANNEL NO. 2  FM  DIR TIME AVERAGE no BY RFB

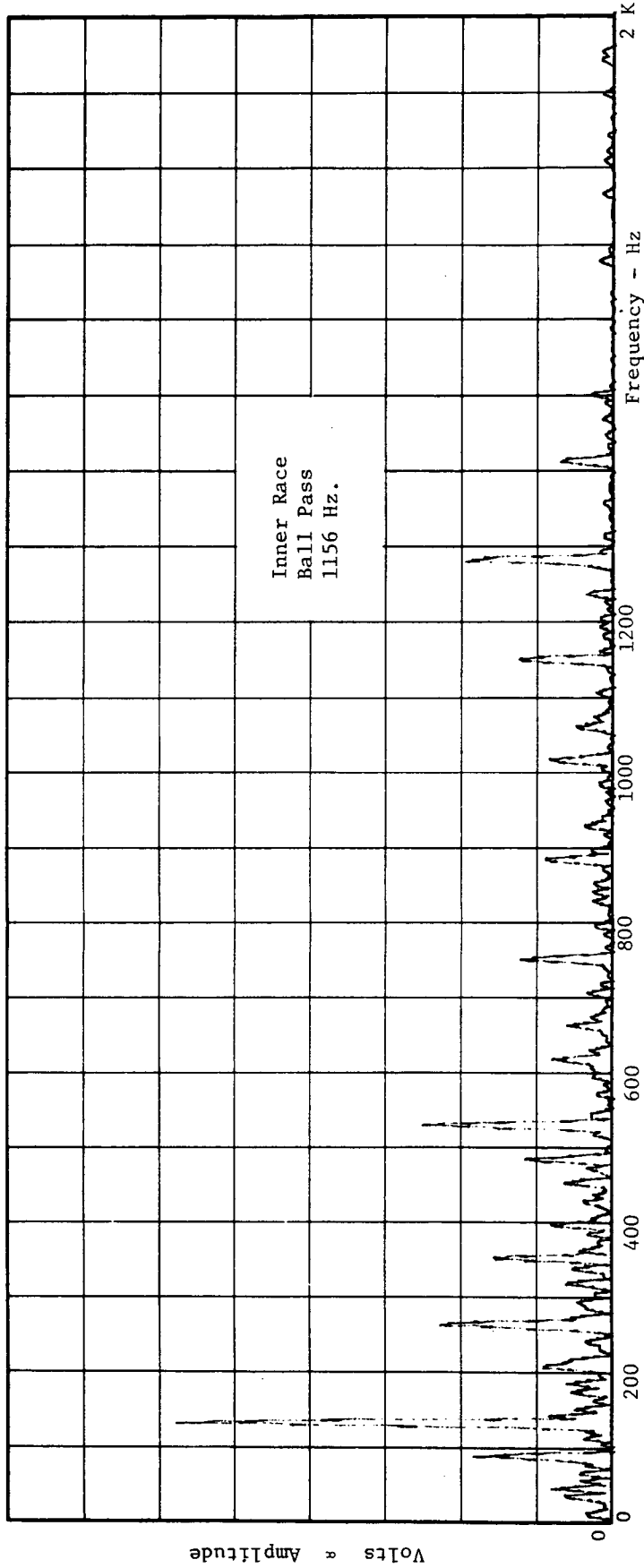


Fig. F-25 Fault Detector Frequency Spectrum, 250 lb. Thrust, 8000 rpm, Pitted



APPENDIX G  
TEST EQUIPMENT

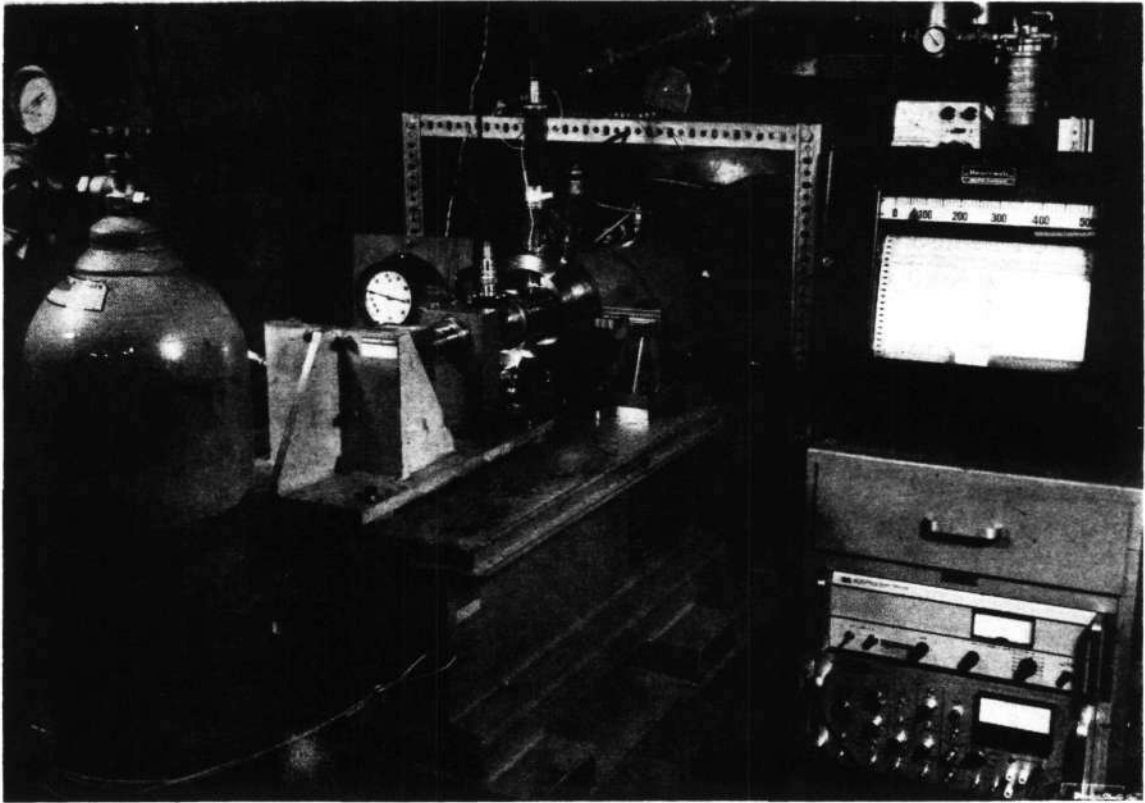


Fig. G-1 Ball Bearing Test Stand with NASA Test Bearing and Instrumentation - Cell 62

Reproduced from  
best available copy. 

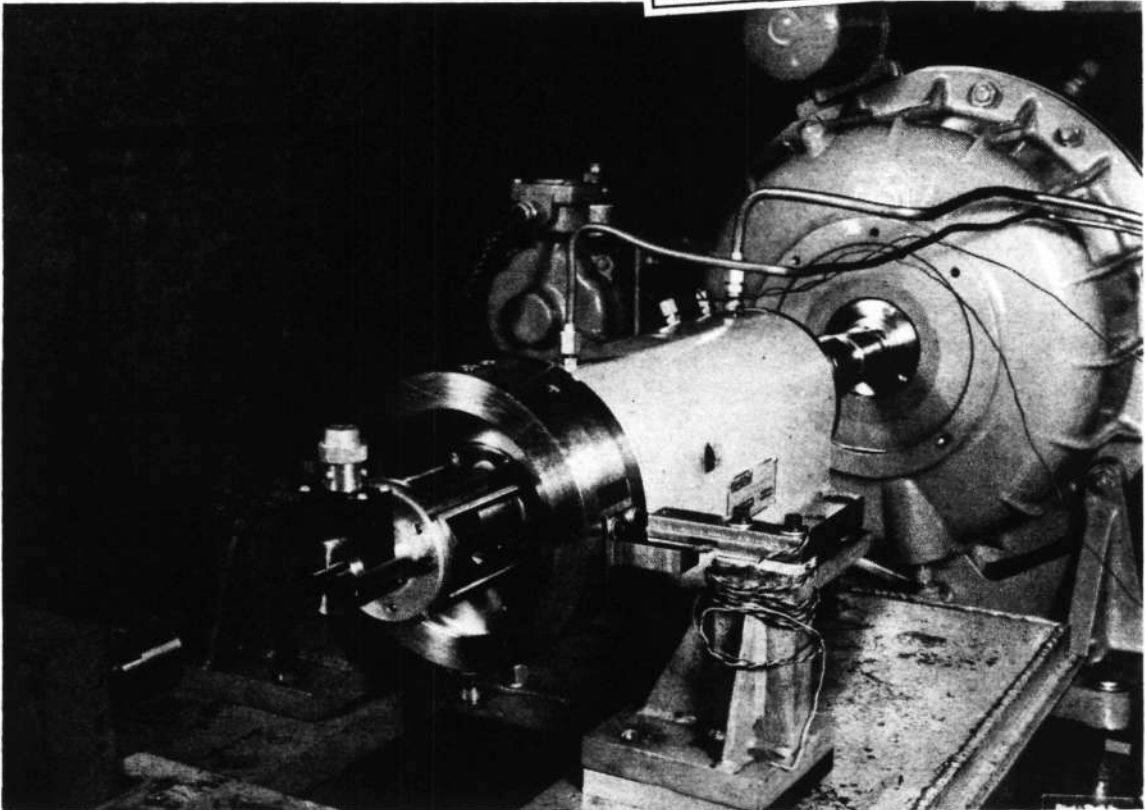


Fig. G-2 NASA Test Bearing Housing with Thrust Load Cell and Torque Arms shown

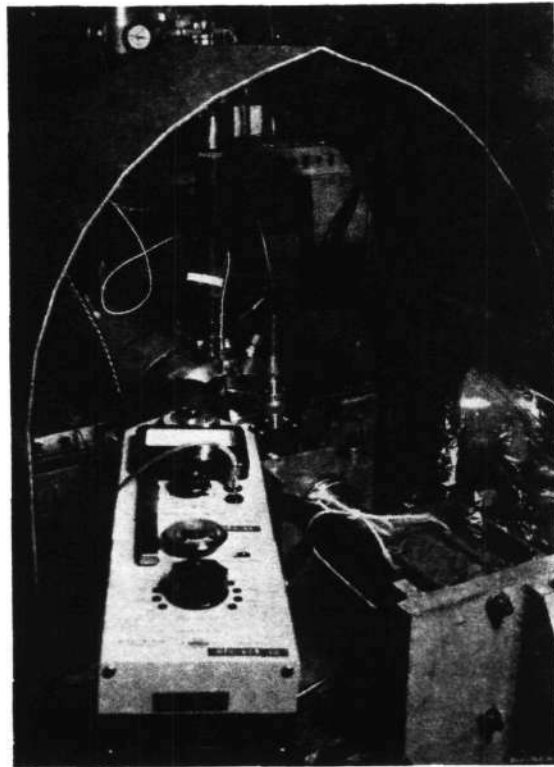


Fig. G-3 NASA Test Setup with B&K Sound Level Meter and Strobe Light in Foreground

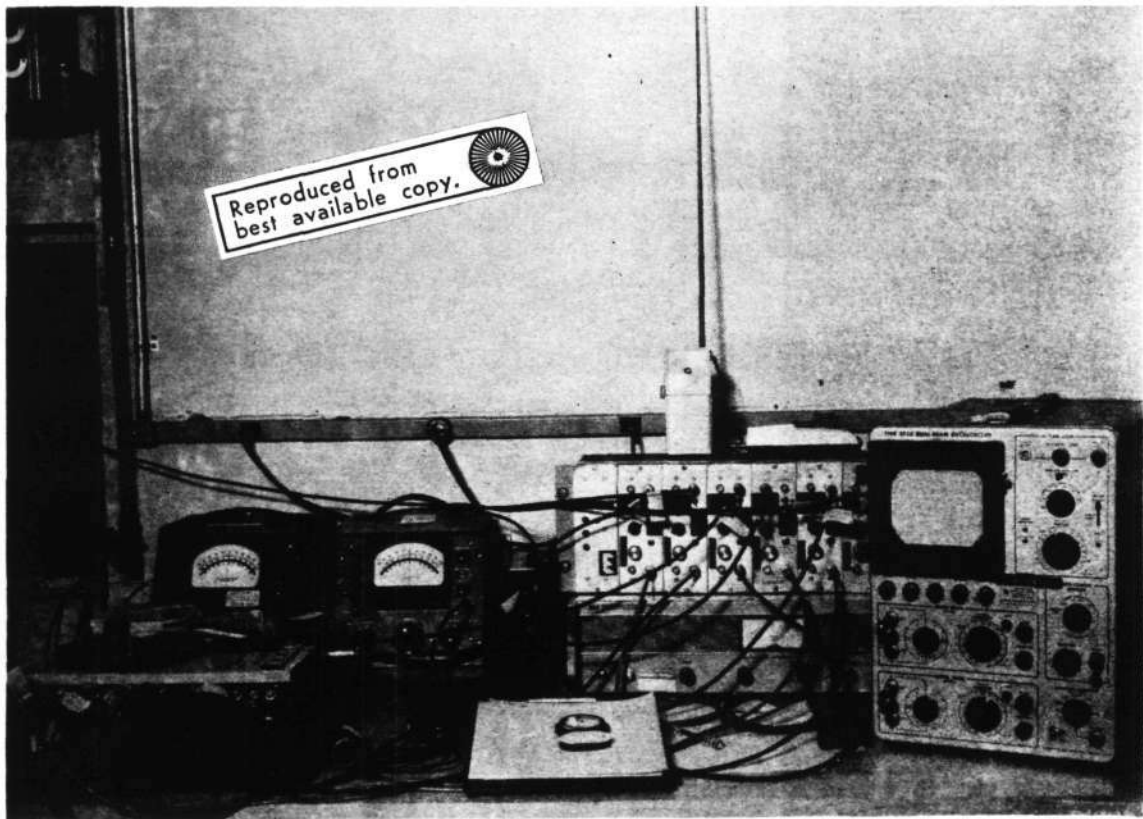


Fig. G-4 Tape Recorder, Amplifiers, Power Supply, Oscilloscope and Other Related Equipment used during NASA Tests

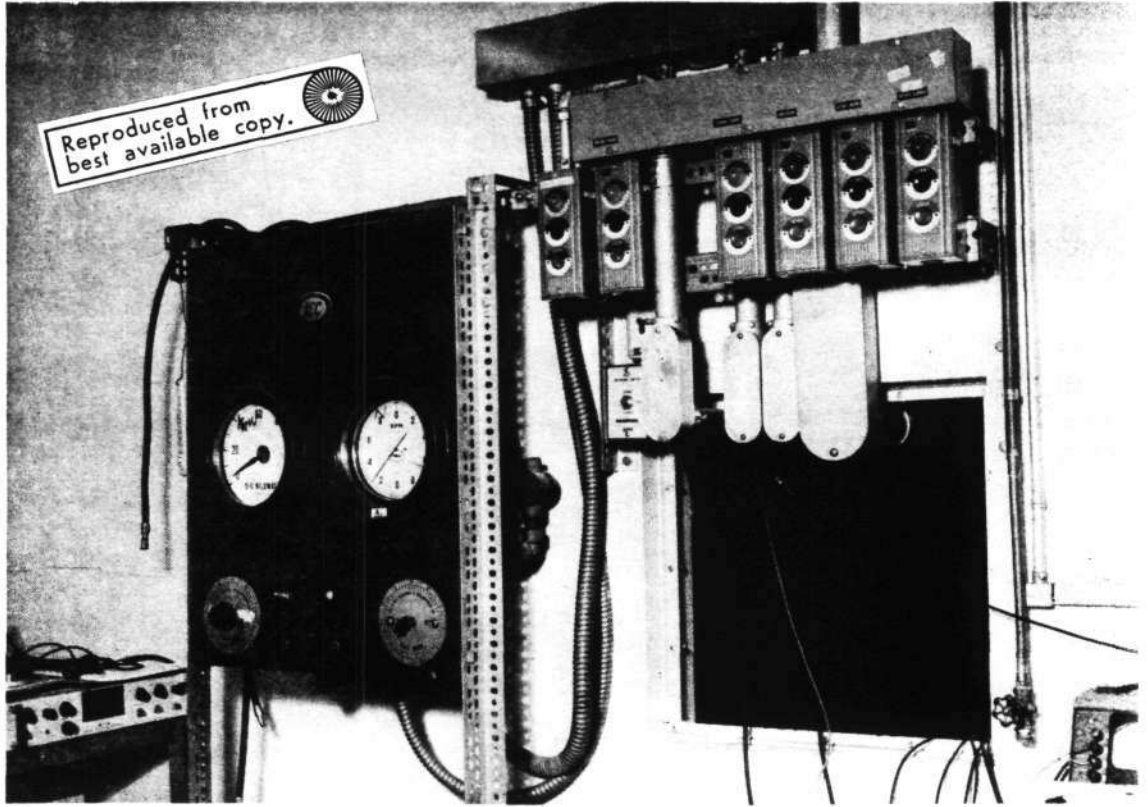
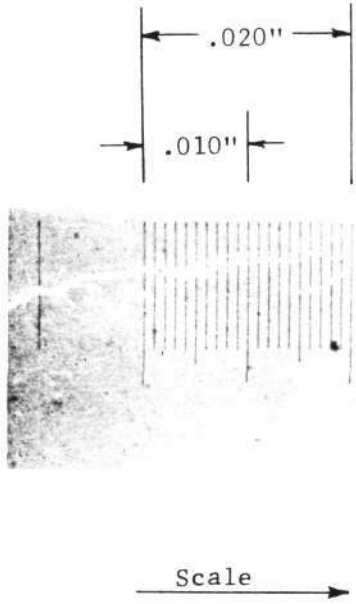
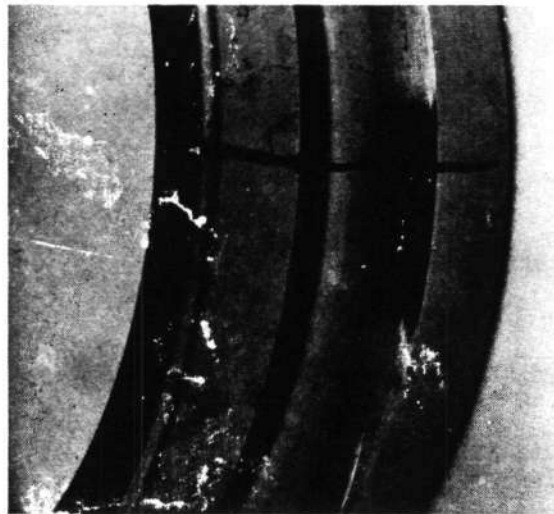


Fig. G-5 Control Panel for Variable Speed Spindle Drive and Main Lubrication System used for NASA Tests

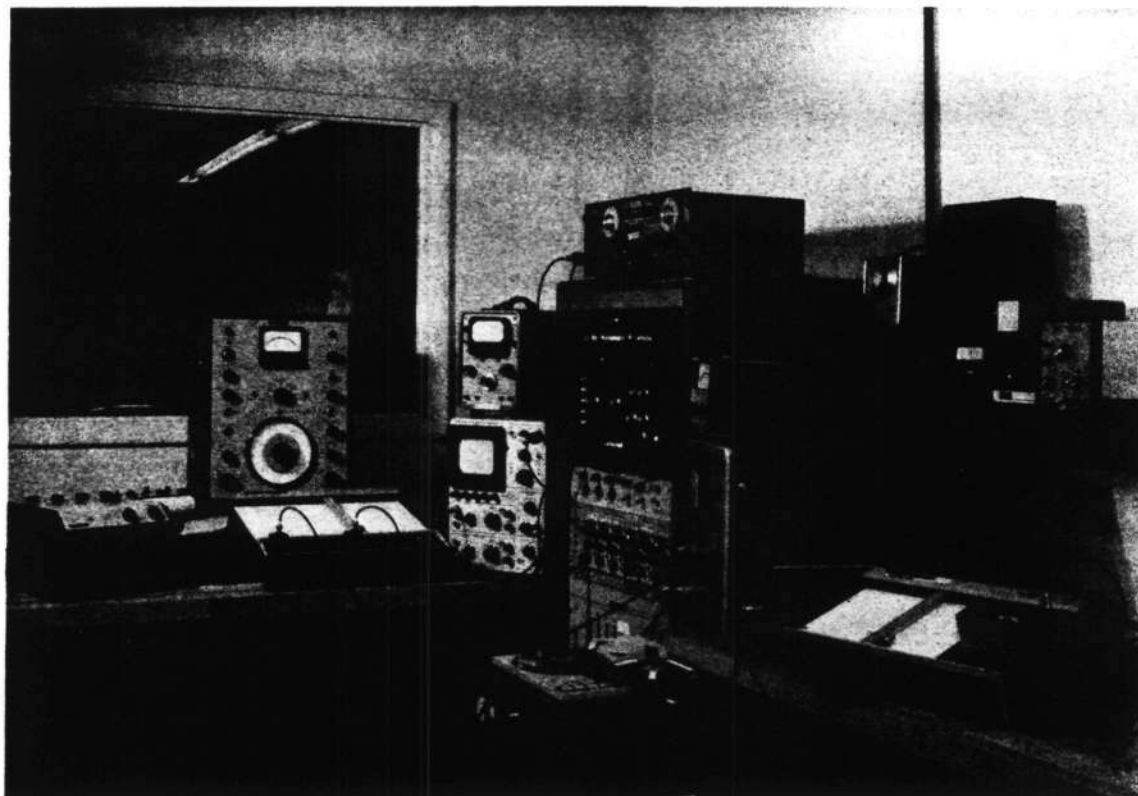


Reproduced from  
best available copy.



Scale 3X

Fig. G-6 Transverse Flaw Acid-Etched Across Raceway of Inner Race. Enlarged Detail Shows 0.012 inch wide by 0.0012 inch deep Fault



Reproduced from  
best available copy. 

Fig. G-7 Photographs of Data Reduction Center Including Real Time Analyzer